PHASE II

for the

POOLED FUND STUDY
SPR-3(22)

DEVELOPMENT OF HYDRAULIC COMPUTER MODELS TO ANALYZE TIDAL AND COASTAL STREAM HYDRAULIC CONDITIONS AT HIGHWAY STRUCTURES

Ayres Associates, Inc.
P.O. Box 270460
Fort Collins, Colorado 80527
(970) 223-5556, FAX (970) 223-5578

Edge & Associates, Inc.
4911 Bay Oaks Court
College Station, Texas 77845

AYRES ASSOCIATES

1. Report No. FHWA-SC-97-04	2. Government Accession No.	3. Recipient's Catalog No.

4. Title and Subtitle	5. Report Date
Development of Hydraulic Computer Models to Analyze Tidal and Coastal Stream Hydraulic Conditions at Highway Structures, Phase II Report	December 1997
	6. Performing Organization Code

7. Author(s)	8. Performing Organization Report No.
L.W. Zevenbergen, E.V. Richardson, B.L. Edge, P.F. Lagasse, J.S. Fisher	

9. Performing Organization Name and Address	10. Work Unit No. (TRAIS)
Ayres Associates 3665 JFK Parkway Building 2, Suite 300 Fort Collins, Colorado 80525 Edge & Associates, Inc. 4911 Bay Oaks Court College Station, Texas 77845	
	11. Contract, Grant, or Study No. Pooled Fund Study SPR03(22)

12. Sponsoring Agency Name and Address	13. Type of Report and Period Covered
South Carolina Department of Transportation P.O. Box 191 Columbia, South Carolina 29202	Final Phase II Report
	14. Sponsoring Agency Code

15. Supplementary Notes

Project Manager, Mr. William H. Hulbert
Technical Advisory Panel: W.L. Hulbert, Chairman, South Carolina DOT; Mr. Michael E. Hogan, Connecticut DOT; Mr. Shawn McLemore, Florida DOT; Mr. Sammy Teal, Georgia DOT; Mr. Mark Murrant, Louisiana DOT; Mr. Michael H. Wight, Maine DOT; Mr. Andy Kosicki, Maryland DOT; Mr. Bobby Whitaker, Mississippi DOT; Mr. Harry Capers, New Jersey DOT; Mr. Steve Georgopoulos, New York DOT; Mr. Archie L. Hankins, North Carolina DOT; Mr. Mark Hammond, South Carolina DOT; Mr. Terry Swygart, South Carolina DOT; Mr. Jack S. Harrell, Virginia DOT; and Mr. Johnny Morris, FHWA.

16. Abstract

Highway structures are subjected to stream instability and foundation scour resulting from dynamic flow conditions caused by tides, currents, storm surges, and upland runoff. The first phase of this study, which was completed in September, 1994, focused on three tasks; (1) compiling a database of literature on tidal processes and computer models, (2) evaluating which computer models are best suited for complex tidal hydrodynamic investigations for bridge structure hydraulic analyses, and (3) evaluating sources and methodologies for determining ocean tide and storm surge characteristics. The computer models selected for tidal bridge hydraulic applications were UNET, a 1-dimensional model and FESWMS, a 2-dimensional model. This phase of the study (Phase II) focused on (1) making useful modifications to the selected models (2) testing the models and developing case studies, (3) developing methods for storm surge hydrograph prediction along the east and gulf coasts and Chesapeake Bay, (4) developing a Users Manual on the models and methodologies and (5) providing training and technical support to the Pooled Fund States. In addition to the Users Manual, the computer models, user interface software, spreadsheets, utility software, data, and computer viewable versions of the manuals were compiled on CD-ROM which is available to the Pooled Fund States. Recommendations for a third phase of this project include further training and support, updates to the manuals and methods, further model enhancement and testing, compiling additional information on tides and hurricane characteristics, wind and wave research and developing guidance and procedures for incorporating upland runoff with storm surges.

17. Key Words	18. Distribution Statement
Computer models, Tidal hydraulics, Storm surge, Bridges, Scour	

19. Security Classif. (of this report)	20. Security Classif. (of this page)	21. No. of Pages	22. Price
Unclassified	Unclassified		

PHASE II

for the

POOLED FUND STUDY
SPR-3(22)

DEVELOPMENT OF HYDRAULIC COMPUTER MODELS TO ANALYZE TIDAL AND COASTAL STREAM HYDRAULIC CONDITIONS AT HIGHWAY STRUCTURES

FINAL REPORT

Submitted to

South Carolina Department of Transportation
P.O. Box 191
Columbia, South Carolina 29202

AYRES ASSOCIATES
P.O. Box 270460
Fort Collins, Colorado 80527
(970) 223-5556, FAX (970) 223-5578

and

Edge & Associates, Inc.

4911 Bay Oaks Court
College Station, Texas 77845

Ayres Job Number 34-0231.00

December 1997

S-CAR12.TXT

TABLE OF CONTENTS

LIST OF FIGURES

LIST OF TABLES

ACKNOWLEDGMENTS

This work was sponsored by the Connecticut Department of Transportation (DOT), Florida DOT, Georgia DOT, Louisiana DOT, Maine DOT, Maryland DOT, Mississippi DOT, New Jersey DOT, New York DOT, North Carolina DOT, South Carolina DOT, and Virginia DOT in cooperation with the Federal Highway Administration (FHWA). The South Carolina DOT was the contracting agency and Mr. William H. Hulbert, Hydraulic Engineer, for the South Carolina DOT, was Technical Project Manager and Mr. Richard L. Stewart, Research and Materials Engineer was Contracting Officer. A Technical Advisory Panel (TAP) composed of a member from each of the Pooled Fund States and the FHWA advised, guided, and reviewed the research. Members of the TAP were Mr. Michael E. Hogan, Connecticut DOT; Mr. Shawn McLemore, Florida DOT; Mr. Sammy Teal, Georgia DOT; Mr. Mark Murrant, Louisiana DOT; Mr. Michael H. Wight, Maine DOT; Mr. Andy Kosicki, Maryland DOT; Mr. Bobby Whitaker, Mississippi DOT; Mr. Harry Capers, New Jersey DOT; Mr. Steve Georgopoulos, New York DOT; Mr. Archie L. Hankins, North Carolina DOT; Mr. William H. Hulbert, South Carolina DOT, Chairman; Mr. Mark Hammond, South Carolina DOT; Mr. Terry Swygart, South Carolina DOT; Mr. Jack S. Harrell, Virginia DOT; and Mr. Johnny Morris, FHWA. Special acknowledgment is made for the help that the members of the TAP provided to the project.

The research reported herein was performed under Pooled Fund Study SPR-3(22) by Ayres Associates, Fort Collins, Colorado and Edge & Associates, Inc., (EAI), College Station, Texas. Dr. Everett V. Richardson, Ayres Associates Senior Associate, served as Principal Investigator and Dr. Billy L. Edge, EAI President, served as Co-Principal Investigator. They were assisted by Dr. Peter F. Lagasse, Dr. Lyle W. Zevenbergen, Mr. John Hunt, and Mr. Morgan Byars of Ayres Associates, and Dr. John S. Fisher of EAI.

The research team benefited greatly by working on tidal hydraulics and scour projects for various Pooled Fund States during this project. The Research Team thanks Florida DOT and Georgia DOT for allowing the use of two of these projects as case studies in the Users Manual.

DISCLAIMER

EXECUTIVE SUMMARY

Tidal waterways are subjected to dynamic flow conditions caused by astronomical tides, ocean currents, storm surges and watershed runoff. Highway structures and encroachments are subjected to stream instability and foundation scour resulting from these dynamic and often extreme flow conditions. Simplified methods have been used extensively to analyze the hydrologic and hydraulic conditions in tidal waterways for bridge hydraulic and scour analyses. The simplified methods are useful and reasonable for many applications, however, computer hydrodynamic modeling is the most accurate method for determining the hydraulic conditions that cause scour at tidally affected bridge crossings.

In the first phase of this study (completed in September, 1994) more accurate techniques for determining hurricane storm surge hydrographs were investigated and several computer models were recommended for tidal hydraulic applications. In this phase of the study, the UNET 1-dimensional and FESWMS 2-dimensional hydrodynamic computer models were selected from the list of recommended models. The focus of this phase included (1) enhancing the selected computer models, (2) testing and developing case studies for the selected models, (3) developing methods for computing storm surge hydrographs, (4) writing a Users Manual on tidal hydraulic modeling for bridge applications to supplement the existing model users manuals and (5) providing training and technical support to the Pooled Fund States.

The primary enhancement to UNET was the inclusion of metric computation capabilities. The work was performed by the model developer as a subcontract to this project. The work was performed on U.S. Army Corps of Engineers version 3.0 of UNET. This version is available from the Research Team for metric simulations. The next Corps of Engineers distribution version of UNET (version 4.0) will incorporate the metric computation capabilities developed in this study.

FESWMS enhancements were performed as part of the ongoing software development supported by FHWA. The primary advance in the use of FESWMS has been the FHWA supported development of the graphical user interface called Surface Water Modeling System (SMS). This user interface is used to develop model networks, run control, variable assignment and output analysis for FESWMS.

In addition to the UNET and FESWMS enhancements and SMS development performed by others, the Research Team has developed utility programs for scour calculations using the output from these programs. The Research Team has also developed an interim procedure to analyze submerged deck bridge hydraulics (pressure flow) because of difficulties with the FESWMS pressure flow computation routine. The Research Team has also been actively Beta testing UNET, FESWMS and SMS.

Through direct testing and the use of UNET and FESWMS on tidal bridge hydraulic projects, the Research Team has been able to test these programs for a wide range of conditions and applications. Case studies were developed for each of these models from projects performed for Pooled Fund States. These case studies were incorporated into the Users Manual developed as part of this study.

Another contribution of this study is in the development of methods for predicting storm surge hydrographs. The synthetic hydrograph is computed from the peak storm surge elevation and the hurricane characteristics of radius of maximum winds and forward speed. Guidance is provided on selecting the appropriate values of the hurricane characteristics. Peak storm surge elevations for 50-, 100-, and 500-year storm surges were also developed as part of this study for numerous locations along the east and gulf coasts and within Chesapeake Bay.

The primary product of this study is a Users Manual for Tidal Hydraulic Modeling for Bridges. The Users Manual is intended to supplement the UNET and FESWMS users manuals. The Users Manual contains recommendations on which model is most appropriate for various conditions including when the simplified methods are applicable. The storm surge hydrology methods and procedures are also contained in the Users Manual along with chapters on the use of UNET and FESWMS for tidal applications. The Users Manual contains several appendices including charts of hurricane properties, predictions of storm surge elevations, maps of the locations of the storm surge predictions, UNET and FESWMS case studies, and the interim methodology for bridge pressure flow computations with FESWMS.

In addition to the Users Manual, the computer models, user interface software, spread-sheets, utility software, data, and computer viewable versions of the manuals were compiled on CD-ROM which is available to the Pooled Fund States.

The following tasks are recommended for a third phase of this project: (1) further training and support, (2) updates to the manuals and methods, (3) further model enhancement and testing, (4) compiling additional information on tides and hurricane characteristics, (5) wind and wave research and (6) developing procedures for incorporating upland runoff with storm surges.

1. INTRODUCTION

This report details the progress of Phase II of the Pooled Fund Study. The research objective of the Pooled Fund Study is to develop, analyze, and advance the methods of computing stream instability and scour at highway encroachments in tidal waters. Present methods are often very conservative and may be inappropriate for complex or large scale tidal waterways. Historically, computer models which efficiently simulate hydraulics, have not been developed for use by highway hydraulic engineers to analyze highway encroachments in tidal waters. Phase I of the project (Ayres Associates 1994) identified and evaluated existing models for use by hydraulic engineers to analyze highway encroachments in tidal waters. The evaluation was limited to public domain models, which are in current use and actively supported. Models best suited for tidal hydrodynamic investigations were selected through a process of elimination based on model capabilities and the desired criteria developed by the Technical Advisory Panel (TAP). UNET and FESWMS-2DH were recommended for use by the states for determining the hydraulic variables used in scour computations.

The objectives of Phase II of the Pooled Fund Study were to continue research and development of the selected models and present findings to the states. The tasks for Phase II of the Pooled Fund Study have been completed as outlined below:

1. Present the current models and methods to the states for use on their current projects.

2. Make required enhancements and corrections to UNET and FESWMS-2DH.

3. Develop methods for tide and storm surge hydrograph estimation.

4. Test the models with real applications and test the new model enhancements.

5. Develop a tidal modeling Users Manual and present a training course for state personnel on UNET, FESWMS-2DH and determining storm surge hydrographs.

6. Make final modifications to the models, training documents, and user guides based on comments from the states.

7. Prepare a Final Report detailing the results of Phase II work.

1.1 Report Organization

This report details the methodologies and findings of the overall Phase II efforts. In addition to this report, a Users Manual and software for tidal bridge hydraulic modeling were developed.

Chapter 2 provides a description of the contents of the Users Manual, "Tidal Hydraulic Modeling for Bridges" (Zevenbergen et al. 1997). This Users Manual is the primary product of this research effort. It contains guidance on developing storm tide boundary conditions, and developing UNET and FESWMS tidal models.

Chapter 3 presents several methods for developing storm tide hydrographs, compares these methods and provides information on selecting the most appropriate method. Chapter 4 details the findings of the model testing performed on UNET and FESWMS, and Chapter 5 contains recommendations for future work.

1.2 Overview of Tidal Hydraulic Modeling

The following steps are recommended for hydraulic modeling of bridges in waterways affected by daily tides and hurricane storm surges.

1. Determine the type of modeling that is most appropriate given the waterway and crossing characteristics. As discussed in Chapter 3 of the Users Manual, methods ranging from tidal prism to dynamic modeling (UNET or FESWMS-2DH) may be applicable.

2. Determine the applicable tidal and storm surge hydrographs for the downstream stage boundary conditions.

3. Determine whether upland runoff should be included as an upstream flow hydrograph and whether the upland runoff should be low flow or flood conditions.

4. Perform a site visit to asses channel conditions, floodplain land use, existing encroachments and structures.

5. Assess existing bathymetric and topographic data for accuracy and aerial extent to determine whether additional survey is needed.

6. Assess existing tide data to determine whether additional data is necessary for calibration and validation purposes.

7. For UNET or FESWMS-2DH dynamic modeling, perform calibration and validation using daily tides.

8. Perform appropriate storm surge modeling for bridge hydraulic design and scour calculations.

2. DESCRIPTION OF THE USERS MANUAL

2.1 Purpose

The Users Manual (Zevenbergen et al. 1997) is the primary product of the Pooled Fund Project. The project was initiated in recognition of the need for more sophisticated approaches to determine hydraulic conditions at bridges in tidal waterways. The Users Manual provides guidance on improved methods for determining hurricane storm tide hydrographs and on the use of computer models that are well suited for complex bridge hydraulic applications in tidal waterways.

HEC-18 (Richardson and Davis 1995) contains several simplified methods for tidal hydraulic analysis. These methods are applicable to many bridge crossings in tidal waterways. As part of the Pooled Fund Study, two computer models were selected for more advanced tidal hydraulic analyses; these are the UNET 1-dimensional model (HEC 1996) and the FESWMS-2DH 2-dimensional model (Froehlich 1996). These models are capable of accurate hydraulic simulation of the situations where simplified methods yield unacceptably conservative results or are inapplicable due to flow complexity. The Users Manual supplements the users manuals associated with UNET and FESWMS by providing specific guidance on using these models in tidal waterways.

The tidal hydrology portion of the manual includes estimates of tidal peak surge elevations for 100- and 500- year hurricanes for the East and Gulf coasts and an atlas of historic hurricane storm surges. An equation is presented for estimating the shape of storm surge hydrographs, and recommendations are given on combining storm surges and daily tide hydrographs. Guidance is also presented on combining upland runoff with storm tide conditions.

Using the methods and models presented in the Users Manual, better predictions of bridge hydraulics and scour in tidal waterways will result. In many cases, the simplified tidal hydraulic methods of HEC-18 will continue to be acceptable; however, where the simplified methods yield overly conservative results, use of the recommended computer models will provide more realistic predictions of hydraulic properties and scour.

2.2 Users Manual Organization

Chapter 1 of the Users Manual provides background information on the Pooled Fund Study and on the contents of the Users Manual.

Chapter 2 of the Users Manual contains the storm surge hydrology results of the study. The chapter presents equations for estimating astronomical tides and storm surge hydrographs and describes the use of spreadsheets for computing these hydrographs. Also referenced are files containing storm surge predictions and an atlas of historic hurricanes grouped by location along the east and gulf coastlines and Chesapeake Bay. Preliminary guidance is also presented on the combined simulation of upland runoff with hurricane storm surges.

Chapter 3 of the Users Manual is a review of the available methods for tidal waterway hydraulic analyses, from the simple methods presented in HEC-18 to the complex dynamic modeling presented in the manual. Based on the geomorphic characteristics of the waterway, recommendations are made on the selection of the most appropriate method.

Chapter 4 of the Users Manual presents guidance for application of UNET to tidal hydraulic analyses. This chapter supplements the UNET manual (HEC 1996) and the HEC-DSS manual (HEC 1995). HEC-DSS is a hydrologic data storage system used by UNET. The chapter includes guidance on the geometric input, model upstream and downstream limits, boundary condition input, trouble shooting, output analysis and performing scour calculations from UNET results. Appendix D of the Users Manual is a case study which applies UNET to the Trout River estuary in Jacksonville, Florida.

Chapter 5 of the Users Manual presents guidance for application of FESWMS to tidal hydraulic analyses. This chapter supplements the FESWMS-2DH manual (Froehlich 1996) and the SMS (BYU 1997) manual. SMS is a pre- and post-processing program developed for FESWMS. The chapter includes guidance on geometric input, model upstream and downstream limits, boundary condition input, trouble shooting, output analysis and performing scour calculations from FESWMS results. Appendix F of the Users Manual is a case study which applies FESWMS to the Altamaha River Sound near Darien, Georgia.

Chapter 6 of the Users Manual contains the references used in the manual.

The Users Manual contains five appendices. Appendix A contains plots of the statistical distribution of hurricane forward speed and radius of maximum wind along the east and gulf coasts. Appendix B contains predictions of hurricane 100- and 500-year peak surge elevations for selected locations along the east and gulf coasts and Chesapeake Bay. Appendix C contains maps showing the site locations presented in Appendix B. Appendices D and F are the UNET and FESWMS case studies. Appendix E is an interim procedure for including bridge pressure flow hydraulics using FESWMS.

Another product of this study is a CD-ROM disk containing the UNET model, FESWMS model, associated input and utility programs, an atlas of historic storm surges for the locations referenced in Appendices B and C, the Users Manual in computer viewable format, tutorial and case study files, and other useful software and information.

3. METHODOLOGY FOR DETERMINING HURRICANE STORM SURGE HYDROGRAPHS

3.1 Abstract

Determination of the appropriate design for protection against bridge scour depends significantly upon the design velocities at the project site. In estuaries with large influences by tides or storm surges, the velocity is controlled by the dynamic change in water level. These changes at the ocean boundary together with the upland runoff drive the hydrodynamics of the system. Because the ocean water surface is a function of the characteristics of storm surges, the velocity is similarly affected. Thus, in order to determine the velocity at the proposed project site, a simulation of the hydrodynamics is required using the ocean storm surge as the driving boundary condition. A problem arises, however, in defining an appropriate method to correctly describe the ocean boundary. This chapter describes three methods for determining the boundary conditions based upon historical and stochastic representations of tropical storms (hurricanes) at the ocean boundary of a particular estuary. Each of the three methods is applied to the Indian River estuary in Delaware. Information is provided to help develop storm surge hydrographs for each of the estuaries in the states represented by the Pooled Fund Project.

3.2 Introduction

Bridge crossings in tidal waters are subjected to foundation scour resulting from sediment transport processes and stream instability. Computer hydrodynamic modeling is the most reliable method for predicting the currents at affected bridge substructure elements. These models require storm surge data and usually an extensive set of simulations in order to generate accurate results. The objective of this chapter is to provide a simple method for determining design conditions for surge elevation and flood velocity at a proposed site. This method is directed specifically towards facilitating computations of storm induced velocities for each potential site in a coastal area. The key features emphasized are the development of a single design hydrograph which yields the 100- or 200-year flood velocity and the adaptation of a relatively new statistical analysis procedure, the empirical simulation technique (EST), to establish better flood-frequency relationships.

These procedures are compared with a simple stochastic approach which has been developed by the U.S. Army Corps of Engineers (COE) for estimating frequency-indexed currents impacting bridges. The COE method is used to select which events to simulate and determine how the results should be analyzed. It was originally applied to estimate probability-exceedance curves at Brunswick Harbor, Georgia (Cialone, Butler, and Amein 1993).

The Indian River Inlet and the two adjacent bays in Delaware are used as an example estuary in this study. The bays are relatively shallow, and two jetties confine the inlet entrance to the Atlantic Ocean. Within the jetties, significant scour has occurred at an existing bridge, causing the placement of stone for bridge pier protection. The tide range at the site is classified as meso-tidal. The U.S. Army Corps of Engineers (COE) obtained the bathymetric data used in the model.

3.3 Data Requirements

The process of determining velocity in a tidal waterway involves the acquisition of surge and tide values and tropical storm parameters in order to determine the storm surge hydrograph shape that will be used as input to the hydrodynamic model of the waterway. The most important factor in storm modeling is the intensity of the hurricane, which is directly related to its central pressure P_o. The pressure at a distance r from the storm center can be expressed as:

$$P_r = P_o + (P_r - P_o)e^{-(R/r)} \tag{3.1}$$

where R is the radius at which the windspeed is greatest.

Since surge intensity varies with central pressure deficit, the hypothetical time evolution of surge plus tide height can be given as:

$$S_{tot}(t) = S_p\left(1 - e^{-|D/t|}\right) + H_t(t) \tag{3.2}$$

where

$D = R/f$ = storm duration
R = radius of maximum wind
f = forward speed
t = time
H_t = height of daily tide
S_p = the known storm surge height
S_{tot} = Storm tide (combined surge and astronomical tide)

3.3.1 Various Sources for Available Data

Three principal models are available to predict storm surge elevations; SURGE, SLOSH, and ADCIRC-2DDI. The Federal Emergency Management Agency (FEMA) uses SURGE to estimate the peak storm tide elevation, S_{tot} (surge and tide, S_p+H_t), and depth-averaged velocities, based on frequency of occurrence (10-, 50-, 100-, 500-year return period). The National Oceanographic and Atmospheric Administration (NOAA) uses SLOSH to compute the peak storm tide elevation, S_{tot} , based on hurricane severity (Hurricane Class 1 through 5). The Corps of Engineers (COE) uses ADCIRC-2DDI to simulate historic hurricanes.

The COE Surge Database (Scheffner, et al. 1994) contains hydrographs for 134 actual hurricanes over 104 years, and is therefore not linked to a specific design storm or return period. The hydrodynamic storm surge simulator used for the COE study was the finite element based model, ADCIRC-2DDI. Storm surge elevations were recorded at 686 coastal (later referenced as WIS stations) and near coastal stations (later referenced as ADCIRC stations). The 340 Atlantic and Gulf WIS stations are located at every 0.25 degrees of latitude and longitude along the coastline in water depth averaging between 10 and 20 meters. There are 346 ADCIRC stations, located on a perpendicular line joining the shore to the nearest WIS stations. All storm events in the study were simulated without tides and are relative to mean sea level (msl). Therefore, peak values do not reflect the

stage of the astronomical tide at the time of historical occurrence, but reflect the surge height (S_p). Thus, peak values have to be combined with different tidal phases in order to yield proper results. This database is referenced as the ADCIRC report.

Neither the FEMA nor the NOAA results include the computed storm surge hydrographs. However, ADCIRC data do include storm surge hydrographs. The ADCIRC data can, therefore, be used instead of the theoretical shape given by Equation 3.2. Comparison of these hydrographs is discussed later in this chapter.

Tropical storm data (*R, f*) can be obtained from NOAA technical report NWS-38 (National Weather Service 1987). This report compiles a probability distribution of the radius of maximum wind *R* and the forward speed (*f*), identified with a given percentile of occurrence. Five discrete probability levels (percent) were chosen for *R*(5, 16-2/3, 50, 83-1/3, 95), and six for *f* (5, 20, 40, 60, 80, 95). Relating *R* and *f* to return periods is currently under investigation at the US Army Corps of Engineers Waterways Experiment Station (WES). Also, the 1987 NOAA report includes actual historical values of *R* and *f* for the 85 year period, 1900-1984.

Other site specific data include bathymetry, friction and transition loss coefficients, as well as local winds, which may play an important part in the simulation of storm impacts. Tide data may be obtained either from the current NOAA Tide Tables or from available public domain computer programs.

3.3.2 Comparison Among Different Sources

As noted previously, there are three primary sources for the determination of offshore water level conditions for the input storm surge hydrograph. All of the available data do not always agree and the user should be aware of the limitations of each data source. For example, the ADCIRC data set is typically for nearshore stations. These stations may not be in the mouth of the estuary or even in shallow water. In addition, the results from SURGE and SLOSH are based upon different models, are produced for different objectives, and do not always agree closely. In Florida, a separate set of hurricane storm surge predictions have been made for the purpose of their coastal construction control line program. In general, these predictions have been validated with recorded tropical storm surges. The user is cautioned to be careful when using a database to know its limitations, whether it has been validated, and to what degree conservatism has been built into the methodology.

3.4 Bays and River Inlets

3.4.1 Study Locations and Closest ADCIRC Stations

Specific bays and river mouths for each state have been identified where storm surge hydrographs may be needed. For each site, the name and location, as well as the closest ADCIRC station has been identified. The distance between the entrance channel and the closest ADCIRC station was also computed. A summary of these locations is presented in **Appendix A**. Detailed shoreline maps showing the inlets and the closest ADCIRC stations and their individual station numbers are presented in **Appendix B**. **Table 3.1** presents an example listing for the State of South Carolina. As shown in the table, the Little River Inlet is located at 33.8428 degrees of Latitude North and 78.5469 degrees of Longitude West. The closest ADCIRC Station is number 411, at 1.4 km, and this inlet is shown on map No. 4 (named "South Carolina - 4").

Table 3.1. Bays and River Inlets for South Carolina.							
Bay or River Inlet	Map No.	Latitude	Longitude	ADCIRC Number	ADCIRC Latitude	ADCIRC Longitude	Difference (km)
SOUTH CAROLINA							
Calibogue Sound	1	32.0994	80.8339	419	31.8840	80.8993	24.7
Port Royal Sound	1	32.2350	80.6444	418	32.1763	80.6573	6.6
St. Helena Sound	1	32.4347	80.3786	417	32.3213	80.4070	12.9
North Edisto River	1	32.5433	80.1892	416	32.5602	80.0836	10.1
Stono Inlet	1	32.6253	79.9778	416	32.5602	80.0836	12.3
Lighthouse Inlet	1	32.6919	79.8825	416	32.5602	80.0836	23.8
Charleston Harbor	1	32.7417	79.8514	415	32.8333	79.6351	22.6
Breach Inlet	1	32.7700	79.8089	415	32.8333	79.6351	17.7
Bulls Bay	1	32.9539	79.5136	415	32.8333	79.6351	17.5
North Santee Bay	1	33.1272	79.2372	414	33.1063	79.2282	2.5
Winyah Bay	1	33.1972	79.1725	413	33.2599	79.1448	7.4
North Inlet	2	33.3256	79.1564	413	33.2599	79.1448	7.4
Pawleys Inlet	2	33.3975	79.1347	413	33.2599	79.1448	15.3
Midway Inlet	2	33.4486	79.1028	413	33.2599	79.1448	21.3
Murrells Inlet	3	33.5258	79.0311	412	33.6097	78.9153	14.2
Hog Inlet	4	33.8342	78.6003	411	33.8316	78.5398	5.6
Little River Inlet	4	33.8428	78.5469	411	33.8316	78.5398	1.4

3.4.2 Storm Surge Hydrographs

Storm surge hydrographs from the COE Surge Database (HURDAT) have been identified for ADCIRC stations of interest. A compact computer disc has been prepared that contains, for each ADCIRC station, the storm surge hydrographs for all storm events at that station. The disk includes 50 hours before and after the peak, with an increment of 15 minutes, as well as headers summarizing the storm HURDAT number and maximum surge value for each storm. Included in **Appendix C** is an example file for ADCIRC station No. 388, the closest station to Indian River Inlet.

No ADCIRC stations are currently provided for the Gulf Coast. Only the closest WIS stations are available. Once these stations become available, the program described in **Appendix C** could be used to read the ADCIRC formatted data and prepare files as described above.

For each nearshore WIS station and the closest WIS station in the Gulf of Mexico, all hydrographs wee analyzed to determine the maximum value for each storm. The maximum values and the duration of the data base, 108 years, ere used to develop an extreme probability distribution. The actual distribution chosen was either a Fisher-Tippett or Weibel depending upon the best fit. The distribution was then used to estimate the maximum storm surge for the 50-, 100-, and 500-year storms. The ACES (WES 1992; Leenknecht et al. 1992) software provided by the Waterways Experiment Station - Coastal and Hydraulics Laboratory was used to determine the proper distribution.

No ADCIRC stations were provided for Chesapeake Bay. At the request of Maryland and Virginia DOT's, approximately 20 stations were identified as points of interest. Based upon further review, a total of 39 stations was chosen to provide storm surge results for both Chesapeake Bay and for the outer coast of the "Eastern Shore." The specific locations and the numbering of the stations are shown in the data and Maps in **Appendices A** and **B.** More detail on the identification of the calculations for the surge data in Chesapeake Bay is given in **Appendix E.**

3.5 Methodologies

In this section, three different methods to determine the velocity-frequency relationship are systematically evaluated. The COE method was developed as an application to the Amein dynamic implicit estuary model. The Empirical Simulation Technique (EST) method was an outgrowth of the incorporation of risk analysis in coastal studies by the Corps of Engineers. The Single Design Hydrograph (SDH) was developed to simplify the considerable computations required by the COE and EST methods, for the cases in which such extensive computations are unwarranted. The analysis presented below shows that the SDH should be applicable to nearly all cases.

3.5.1 Corps of Engineers Method

The procedure utilized by the Corps of Engineers (COE) is based upon developing a set of storm parameters (radius of maximum winds, *R*, and forward speed, *f*) combined with tidal possibilities, in order to approximate the full range of conditions that may occur at a site. A complete description of the method is given by Cialone, Butler and Amein (1993). The initial step is to select values for *R* and *f* which represent maximum and minimum storm duration *D*, determined by dividing estimates of the maximum and minimum *R* by the minimum and maximum *f*, respectively. A more conservative estimate could be made by selecting more extreme values for *R* and *f*, but this would require more simulations.

Four tidal possibilities are considered: high tide, mid-falling tide, low tide and mid-rising tide. It is assumed that the time of landfall is completely independent of the tidal position. The peak combined storm surge and tide value (S_{tot}) is computed from either the NOAA or FEMA database, or the storm surge (S_p) is obtained from the COE database. Equation 3.2 is used to determine the hydrograph shape, and the hydrodynamic model is run for the two durations combined with four tide positions, which results in eight storm-plus-tide events for each return period. Finally, for each storm-tide combination, the hydrodynamic estuary model is used to compute the velocity at specified locations (nodes) for statistical analysis. The eight peak flood and ebb velocities obtained from the model are ranked from one to eight and the cumulative probability is then given by the Gumbel distribution:

$$P(X \le X_r) = \frac{r}{(n+1)} \qquad (3.3)$$

where: r = the data rank such that $r = 1$ corresponds to the smallest response
n = number of observations (response) = 8 in this case

Thus, $P = r/9$ is the probability associated with the appropriate ranked velocity. The results are then used to develop a velocity-frequency relationship.

The drawback of the COE method is in the evaluation of the storm duration ($D=R/f$). Taking extreme values of R and f may lead to very high storm durations (above 6 hours). **Figure 3.1** shows actual duration for 59 east coast and 75 gulf coast hurricanes. For the data shown in Figure 3.1, the mean for all measured tropical storms on the Atlantic and Gulf coasts is around 2 hours, and most values are between 1 and 3 hours. Therefore, by using extreme values of R and f, the COE method may be inaccurate in the sense that it may yield values that are not representative of typical conditions that occur at a site.

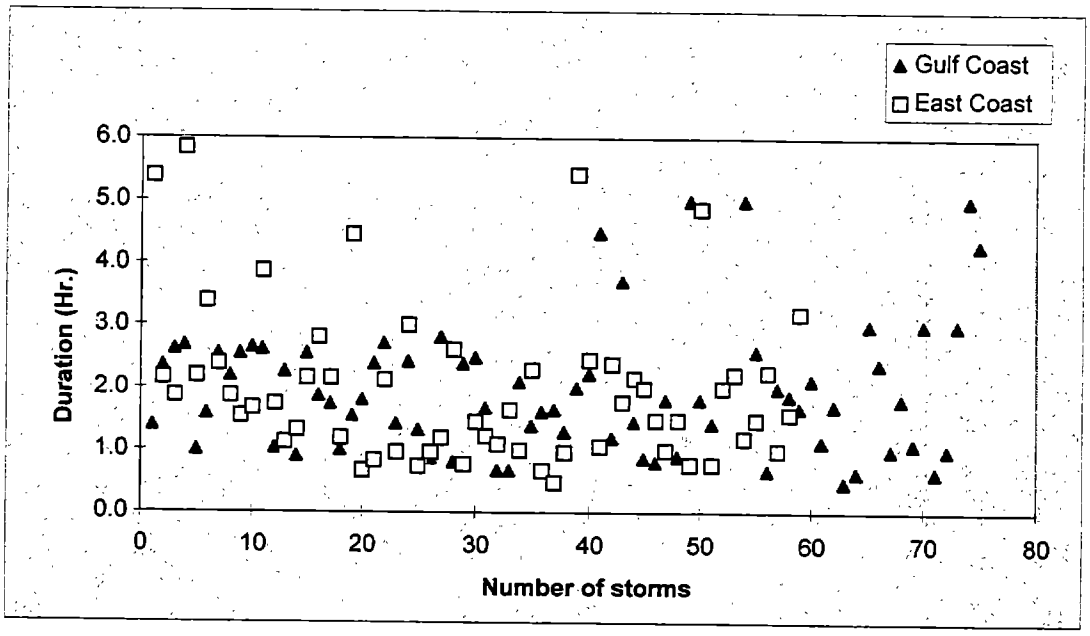

Figure 3.1. Storm duration (R/f) for the East and Gulf Coasts during the 85-year period, 1900-1984.

3.5.2 Empirical Simulation Technique

The Empirical Simulation Technique (EST) method is derived from a probabilistic approach and it was previously used for computing surge-frequency relationships (Grace 1994). The primary goal of the EST is to resample and interpolate a historical data base, in order to generate a larger set of data, statistically similar to the historical data. The EST is a statistical procedure designed to develop joint-probability relationships among the various parameters of a multi-parameter system. In the EST method, the following steps are performed:

1. Establish a database of the input and response parameters associated with historical events at the station of interest. In this application, the input parameters are the storm and surge parameters. The response parameters are the results of the simulations, particularly the peak flood and ebb velocities at the nodes of interest. These responses are computed with the hydrodynamic estuary model, using as input either hydrographs obtained with Equation 3.2 or the historical hydrographs available from ADCIRC.

2. Expand the historical data by slightly perturbing the events. This will produce a training dataset. This phase should include high return-period events.

3. The EST program then performs N simulations of a T-year sequence.

4. For each year, random numbers between 0.0 and 1.0 determine the number of storms (n) specified to occur that year, based on a Poisson distribution (cumulative probability of occurrence), given by:

$$P(s, \lambda) = \frac{\lambda^s e^{-\lambda}}{s!} \qquad (3.4)$$

where: s = number of storms per year
λ = number of events / record length in years
$P(s, \lambda)$ = the probability of experiencing s storms per year.

For the Indian River, the data set consists of 15 storms over 104 years (λ = 0.144 storms/year); thus, the probability of no hurricanes occurring in a year is P(0) = 0.8657, and the probability of one hurricane occurring is P(1) = 0.1248 (from the Poisson probability distribution). Therefore, if the random number is < 0.8657, no storms are simulated this year. If the random number is between 0.8657 and (0.8657+0.1248), one storm is simulated, and so on.

5. For a random selection of the n storms (n determined above) from the training set population, a random number selection from 0.0 to 1.0 determines input and responses by way of the nearest neighbor interpolation technique (Borgman, et al. 1992). This technique is explained below:

   Let V_j be the selected storm vector (composed of the storm parameters) and U_k $(k=1, K,$ chosen) the K nearest storm vectors (from Euclidean distance, weighting the components according to judged importance), then the new simulated event is:

$$W = V_j + \sum_{k=1}^{K} 2(N_k-0.5)\,(U_k-V_j) \qquad (3.5)$$

   where N_k are K independent uniform random numbers on the interval [0, 1.0] generated by the computer. Therefore, $2(N_K-0.5)$ varies on the segment [-1,1].

6. According to the distance between the new simulated storm W and the storms of the neighborhood (V_j and U_k), the corresponding response variables (surge) at each of the neighbors are weighted, and yield a new simulated surge value.

7. Go back to step one for the second year of the simulation.

The EST procedure ultimately results in N repetitions of T years each of simulated event responses. The EST is not simply a technique consisting of resampling of historical events, but rather it is an approach intended to simulate the vector distribution contained in the training set population. As described above, the EST method selects a sample storm based on a random number selection between 0 to 1 and then performs a random walk from the selected event to the nearest neighbor vector. The walk is based on independent uniform random numbers between [-1,1] and has the effect of simulating responses which are not identical but are similar to the historical events.

The calculation of a frequency of occurrence relationship for the responses can then be performed. First, an empirical estimate of the cumulative probability distribution function for the response is given by the Gumbel equation. Next, the cumulative probability for a n-year return event is given by:

$$F(n) = 1 - \left(\frac{1}{n}\right) \qquad (3.6)$$

where: *F(n)* is the cumulative probability of occurrence for an event with a recurrence interval of n-years.

The frequency of occurrence relationship of the response is obtained by linearly interpolating a response from Equation 3.3 which corresponds to the probability distribution function associated with a return period specified in Equation 3.6.

3.5.3 Single Design Hydrograph

The single design hydrograph, SDH, is a method that produces a single hydrograph based on Equation 3.2. It is developed from (a) historic storm surges with an elevation equal to that of the FEMA, NOAA or ADCIRC prediction (for each stage of interest), (b) a duration equal to the average value of the historical durations at the site considered, and (c) these data are combined with a mid-rising tide. This tidal phase was seen to be the most appropriate to get consistent and conservative hydrodynamic results compatible with the other methods. The advantage of this method is that it only requires one simulation with the hydrodynamic estuary model for each return period of interest.

3.5.4 Comparison Among Different Hydrographs

It is interesting to compare the hydrograph shape obtained from Equation 3.2 with the historical storm surges from the ADCIRC model. **Figure 3.2** shows storm surge hydrographs at ADCIRC Station 388, near Indian River, for the four highest storm surges at this station.

3.6 Application: Indian River Model

3.6.1 Indian River Estuary

Indian River Bay is located on the southeast coast of Delaware, (see **Figure 3.3**). Indian River Bay and Rehoboth Bay connect to the Atlantic Ocean through Indian River Inlet. The inlet is spanned by a bridge on State Highway 14. The bridge is supported by two piers, and the inlet is extended seaward by jetties. The narrowest part of the inlet is approximately 500 feet wide and over 1,200 feet long. Depths in the inlet average 40 feet, but exceed 80 feet in places. Hydrographic survey data for the inlet and the two bays were collected in 1988 by the Coastal Engineering Research Center (CERC) and the Philadelphia District of the Corps of Engineers (Cialone 1994). These data were used to develop the finite element grid for the RMA-2V (TABS software) model. RMA-2V is a two-dimensional, depth-averaged, free surface, finite element model for solving hydrodynamic problems (Thomas and McAnally 1990). The finite element mesh, shown in **Figure 3.4** (generated using the FastTABS software), consists of 797 elements and 2,160 nodes. The model was set up using three areas where Manning's n and eddy viscosity could be independently specified. These areas are offshore of the inlet, the inlet, and the two bays. A 30-hour simulation period (15 hours before and 15 hours after the peak storm surge) was used in all cases, with 30-minute time steps. Figure 3.4 also shows the nodes in the inlet for which the results were collected.

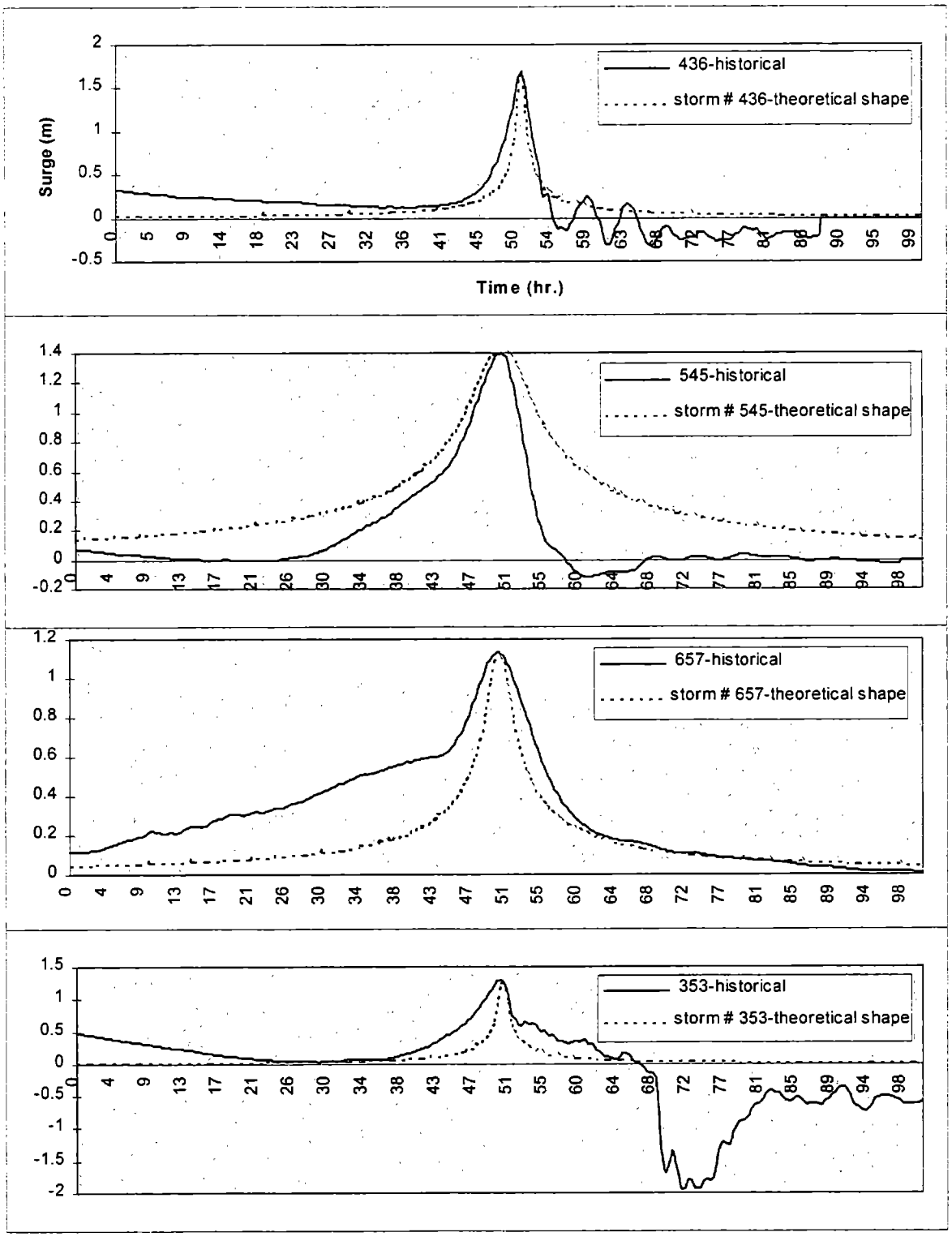

Figure 3.2. Comparison between the historical and theoretical hydrographs for the four highest storms at ADCIRC Station 388 near the entrance to Indian River Inlet.

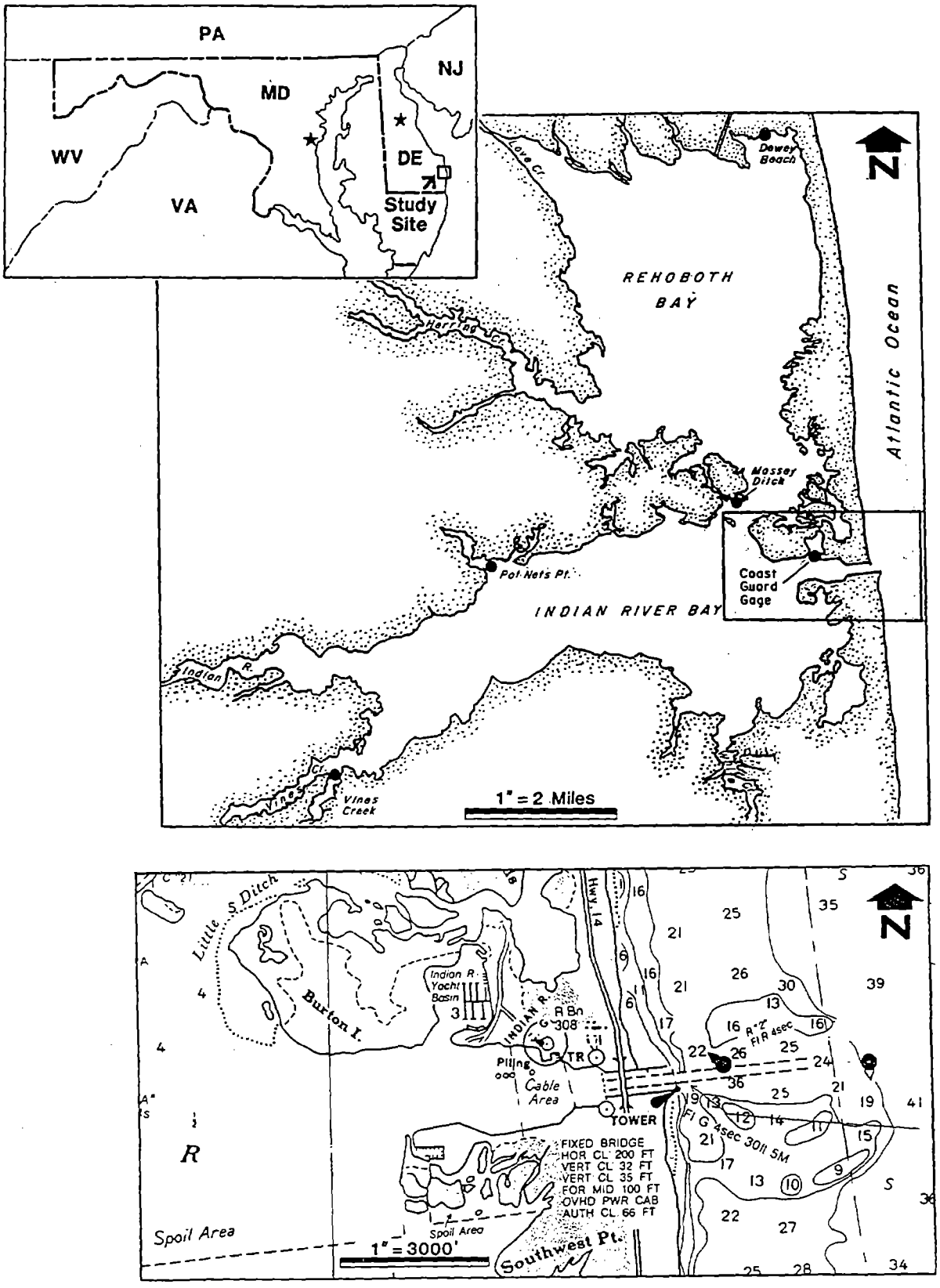

Figure 3.3. Indian River site map.

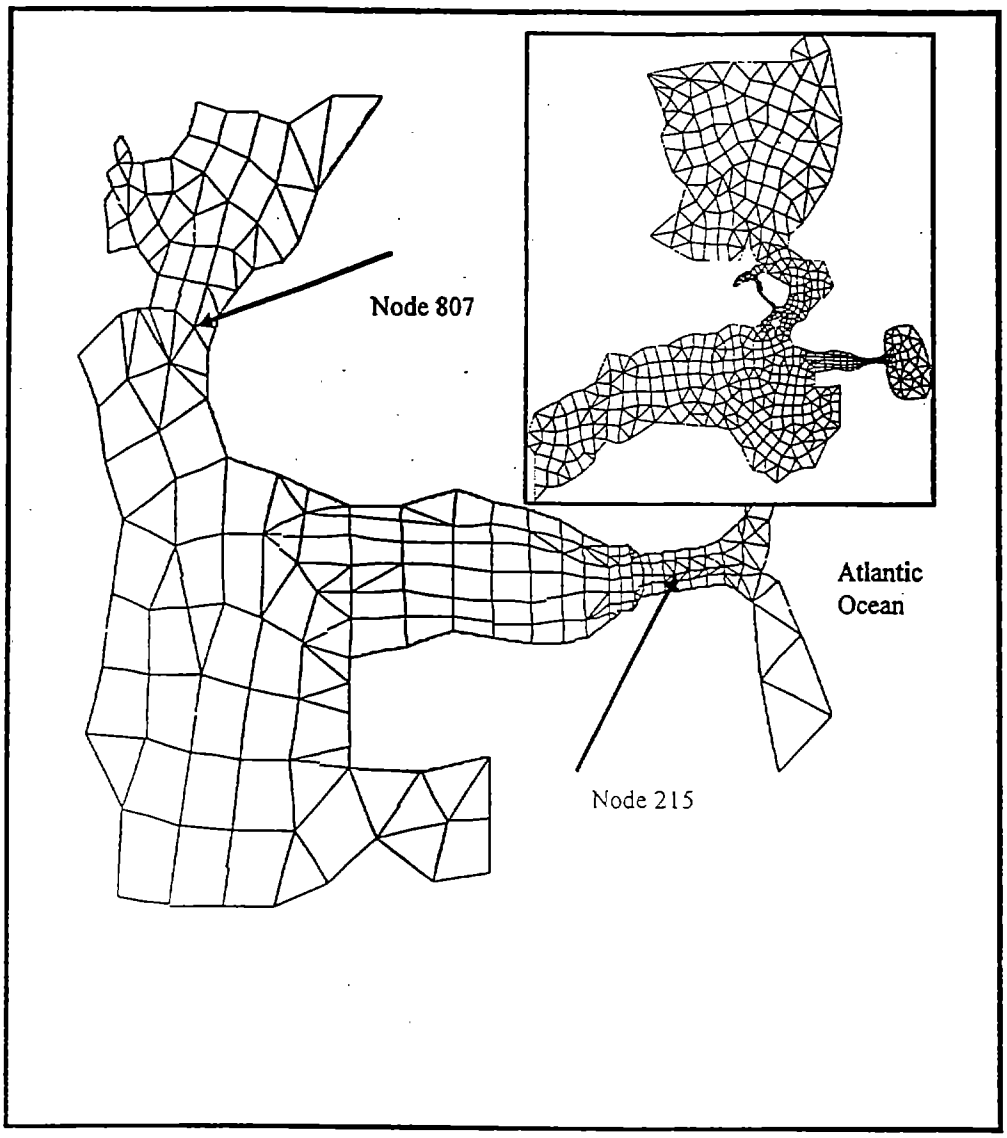

Figure 3.4. Indian River 2-dimensional model finite element mesh.

The following procedures were used to collect storm data for the study site. The closest ADCIRC station to Indian River was station 388, just a few miles from the ideal input point. A total of 18 storm events were identified from the ADCIRC report which impacted station 388 for the 104 year period, 1886 through 1989. However, 3 storms had to be removed from the set because tropical storm parameters were not available from the NOAA report NWS 38. This NOAA report lists parameters for the 85-year period, 1900-84. (We will assume for the rest of this study that the historical database is 104 years long.) The 15 remaining events are shown in **Table 3.2**. For example, Hurricane Camille (HURDAT No. 672), that occurred during August 1969, had a radius of maximum winds of 8 nautical miles, a forward speed of 16 knots, a duration of 0.5 hours (8/16), and a resulting surge of 0.6 m. (Note that the metric units are as presented in the NOAA report.)

Surge-frequency data were determined with the ACES program using the values in Table 3.2, and they are presented in **Table 3.3**.

Table 3.2. Tropical Events Impacting Station 388 off the Indian River (from Scheffner et al. 1994 and National Weather Service 1987).

HURDAT Storm No.	Given Name	Date (m/d/yr)	Surge (ft)/(m)	Radius of Maximum. Winds R (nm)	Forward Speed f (kts)	Duration d = R/f (hr)
327	not named	8/17/1933	3.3/1.0	39	18	2.2
332	not named	9/8/1933	3.6/1.1	40	9	4.4
353	not named	8/29/1935	4.3/1.3	6	9	0.7
370	not named	9/8/1936	3.3/1.0	34	16	2.1
386	not named	9/10/1938	2.6/0.8	45	47	1.0
436	not named	9/9/1944	5.6/1.7	17	23	0.7
440	not named	10/12/1944	1.3/0.4	29	13	2.2
541	HAZEL	10/5/1954	1.6/0.5	25	26	1.0
545	CONNIE	8/3/1955	4.6/1.4	38	7	5.4
552	IONE	9/10/1955	1.3/0.4	22	9	2.4
597	DONNA	8/29/1960	1.3/0.4	26	26	1.0
657	DORIA	9/8/1967	3.6/1.1	20	9	2.2
672	CAMILLE	8/14/1969	2.0/0.6	8	16	0.5
712	AGNES	6/14/1972	2.0/0.6	20	11	1.8
748	BELLE	8/6/1976	1.0/0.3	25	21	1.2

Table 3.3. Extremal Surge Analysis Based on the Weibull Extreme Probability Distribution.

Return Period (yr)	25	50	100	200	300	400	500
Surge (ft)	3.3	4.3	5.3	6.2	6.7	7.1	7.4
(m)	1.0	1.3	1.6	1.9	2.0	2.2	2.3

3.6.2 Single Design Hydrograph Method

The single design hydrograph (SDH) is a method requiring a minimal set of runs. Design hydrographs are generated based on the procedure described previously, and yields directly the 25-, 50-, 100-, 200- 300-, 400-and 500-year return period velocities, using the 25-, 50-, 100-, 200-, 300-, 400- and 500-year single design hydrographs respectively. Data from Tables 3.2 and 3.3 were used to develop all hydrographs for the SDH method. For example, the surge hydrograph for the 100-year event is computed as follows:

1. The peak surge is equal to that of the 100-year event. Table 3.3 yields 5.3 ft. Another method would be to directly get the 100-year storm surge from the FEMA or NOAA database.

2. The duration is the mean of all storm durations at the site of interest: 1.91 (Table 3.2)

3. The hydrograph is then obtained by using Equation 3.2 combined with the mid-rising tide (the mean tide amplitude at the Indian River site is 1.9 ft).

Figure 3.5 shows the single design hydrograph for the 100-year event.

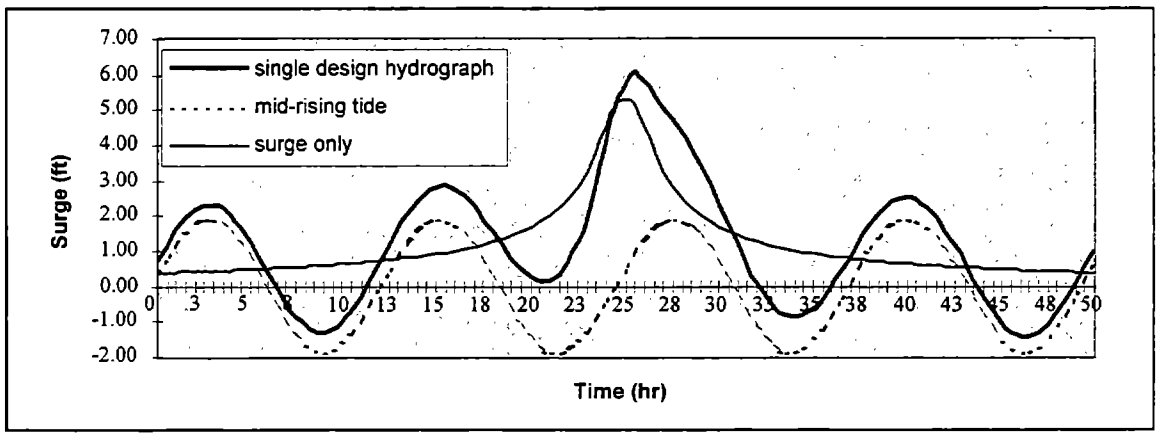

Figure 3.5. Single design hydrograph for the 100-year event.

For the COE and EST methods, four tidal possibilities were selected: high tide, mid-falling tide, low tide and mid-rising tide. The SDH approach uses only one tide condition – mid-rising tide. The NOAA tide table provided the mean tide range at the Indian River as approximately H_t /2= 1.9 feet. More tidal possibilities would yield only a small improvement in accuracy whereas it would require much more simulation time, as shown in Section 3.7.

3.6.3 Empirical Simulation Technique (EST)

As discussed above, the primary element of this procedure is to resample and interpolate a sparse historical database, in order to generate a larger set of data, statistically similar to the historical data.

Previous surge data used in this study include peak surge values that could also have been obtained from either FEMA or NOAA. However, two different sets of hydrographs were developed for the EST method. First, hydrographs were represented by Equation 3.2. This was a conservative procedure when compared to the other two methods. Hydrographs were also directly extracted from the ADCIRC database. Among the 15 storms, storm HURDAT numbers 386, 545 and 748 were not present in the dataset. They were therefore substituted with theoretical shapes. Figure 3.3 shows the difference between the theoretical and the historical hydrographs for the four largest storms at the entrance to Indian River Inlet. The effects of these differences upon the computed velocities are explained later in Section 3.7.

It was first necessary to establish a database of the input and response parameters associated with historical events at the station of interest. In this application, the input parameters are, for each storm event, the radius of maximum winds R, the forward speed f, the central pressure P_o, the distance between the landfall point and the site considered, the direction of propagation, the peak surge and the tide phase. The response parameters are the results of the FastTABS hydrodynamic estuary model simulation; particularly the peak flood and ebb velocities. An example input file to the EST for the first 12 sets of input and response vectors is given in **Table 3.4**. In the first event for storm 327, 1 represents the tidal phase (1,2, 3, and 4 for high tide, mid-falling, low and mid-rising tide, respectively), 158 is the distance in nautical miles between the landfall point and the station (which is at 2,430 nm from the Mexican border), 3.28 feet is the peak surge value at that station, 145 is the angle of propagation in degrees clockwise from North, 966.5 mb is the minimum central pressure, 39 nm is the radius of maximum winds, 18 knots is the forward speed. The response vector is 6.27 ft/s for the peak flood velocity.

Table 3.4. Example EST Input Showing Hurricane Parameters and Maximum Ebb or Flood Velocities.

	HURDAT No.	Tide Condition	Distance (nm)	Peak Surge (ft)/(m)	Azimuth of Storm	P_o (mb)	R (nm)	f (kts)	V (ft/s)/(m/s)
1	327	1	158	3.28/1.00	145	966.5	39	18	6.27/1.91
2	327	2	158	3.28/1.00	145	966.5	39	18	4.40/1.34
3	327	3	158	3.28/1.00	145	966.5	39	18	4.37/1.33
4	327	4	158	3.28/1.00	145	966.5	39	18	5.83/1.78
5	332	1	229	3.61/1.10	220	956.7	40	9	6.06/1.85
6	332	2	229	3.61/1.10	220	956.7	40	9	5.07/1.55
7	332	3	229	3.61/1.10	220	956.7	40	9	4.80/1.46
8	332	4	229	3.61/1.10	220	956.7	40	9	5.46/1.66
9	353	1	1,005	4.27/1.30	130	892.3	6	9	7.70/2.35
10	353	2	1,005	4.27/1.30	130	892.3	6	9	4.12/1.26
11	353	3	1,005	4.27/1.30	130	892.3	6	9	4.46/1.36
12	353	4	1,005	4.27/1.30	130	892.3	6	9	7.39/2.24

The statistical procedure itself consisted of 100 simulations for a 208 year period. This time frame was chosen because it is assumed that the EST method can accurately extrapolate to return periods up to twice the length of the record (104 *2 = 208), and the longer record provides more accurate estimates at all shorter return periods. Because of the high uncertainty of the results, extrapolation of the data in order to yield return periods greater than 200 years is left to the reader.

Appendix D explains how to use the EST software (EST208 and RETUR208) in order to determine the velocity-frequency relationship.

3.6.4 Corps of Engineers Method

The Corps of Engineers method (COE) requires extreme values for the radius of maximum wind and the forward speed that were also obtained from National Weather Service (1987). The 20 and 80 percentile of occurrence for *f* and the 16 2/3 and 83 1/3 percentile of occurrence for the *R* were chosen as shown in (**Figure 3.6**). Therefore, two different values of *D* were computed, D_{max} and D_{min}. **Table 3.5** summarizes the values used in the COE analyses.

Table 3.5. Extreme Values for R and f from National Weather Service (1987).	
R(16 2/3 %) = 23.7 nm	*R*(83 1/3 %) = 42.9 nm
f(20 %) = 10.4 knots	*f*(80 %) = 30.0 knots
D_{max} = 42.9/10.4 = 4.1 hr	D_{min} = 23.7/30.0 = 0.8 hr

Stage values were obtained from Table 3.3. The COE method requires (2 durations * 4 tides * 7 stages) 56 hydrodynamic simulations (compared with 60 for the EST method). Probability tables (**Table 3.6**) present the percent of surge-plus-tide events with velocities at the node which are equal to or less than the values of velocity indicated (for flood and ebb conditions). An example interpretation of these results might be as follows: for a 100-year stage of 5.3 ft, the range of velocities expected are from 5.18 to 8.58 ft/s with the expectation that a current exceeding 6.35 ft/s would occur less than 44 (100-56) percent of the time.

Results of all simulations for the observed nodes are plotted in **Figure 3.7** for the flood and ebb velocities. Values from the EST method were averaged from 100 simulations, and the 80 percent confidence interval was computed. The COE method yields mean velocities at the observed nodes with an 80 percent confidence interval. The SDH method only yields one velocity for each return period, and no confidence interval. Figure 3.7 was obtained using theoretical hydrograph shapes (Equation 3.2) for each method.

Figure 3.8 shows a comparison between the EST procedures using either historical or theoretical data, including 80 percent confidence limits bounding the predictions. The largest difference is for the flood velocity at node 215 in the estuary, where results obtained from the theoretical hydrographs are overestimated. In this case, the velocity with a 200-year return period is 17 percent larger. Also, ebb velocities are under estimated in both cases, giving an error close to 10 percent. Note that the two estimates are bound by two lines representing the 80 percent confidence limits of each.

There are several factors that could explain these discrepancies. First, as shown in Figure 3.2, theoretical hydrographs are symmetrical whereas the historical data are not. Most of the time a negative surge appears after the peak, which tends to increase the negative slope and therefore the resulting ebb velocities. Second, the storm duration (represented by the width of the peak) appears to be in most cases lower in the historical data than in the theoretical data. Therefore, the slope and resulting velocities, especially the flood velocities (positive slope), are lowered. Node 807, inside the bay, shows excellent correlation for the flood velocity, probably due to the damping of the system which responds to the main characteristics of the hydrograph only, as this node is far from the boundary conditions. Lastly, **Figure 3.9** shows results for the COE and the SDH method over 500 years including 80 percent confidence limits for the COE results. As mentioned above, none of the extreme prediction methods should be used to extrapolate data with accuracy above 300 years (three times the length of the historical data of 104 years).

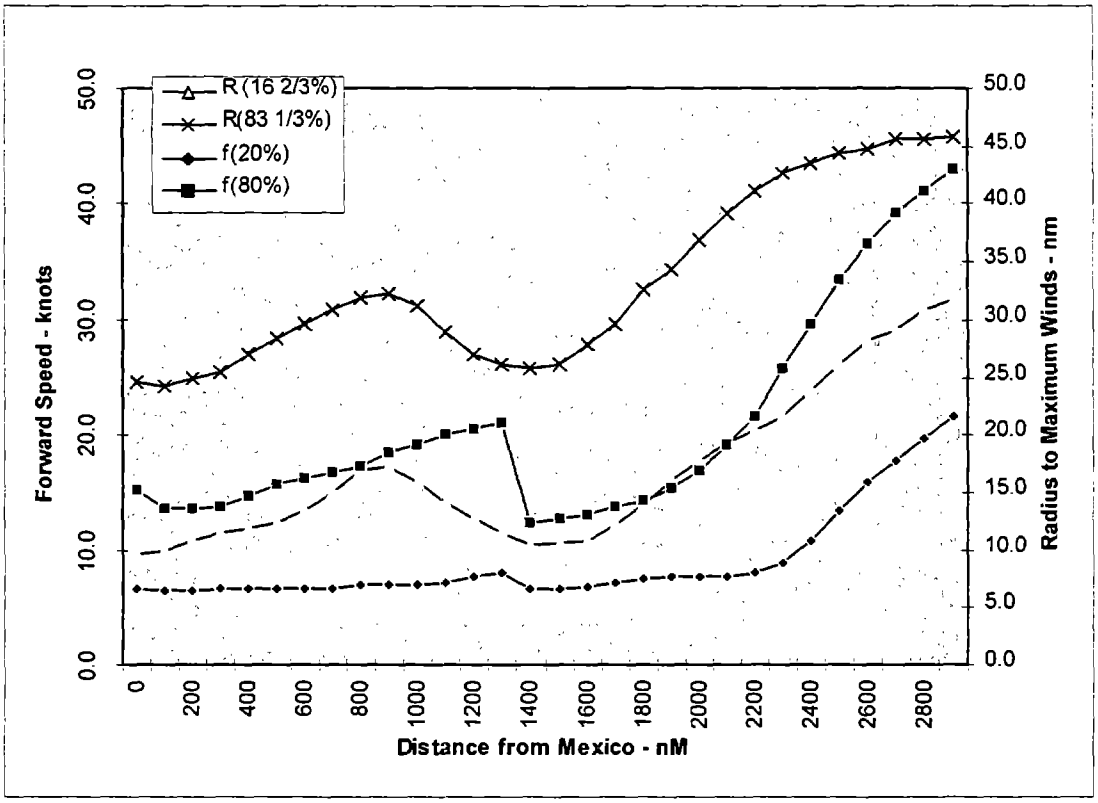

Figure 3.6. Storm parameters (NOAA NWS 38).

Table 3.6. Peak Flood and Ebb Velocities at Node 215 and Exceedance Probabilities at Seven Stages for the COE Method at Indian River.

Rank	Stage 1: 3.3 ft Return Period = 25 Years		
	Flood Velocity (ft/s)/(m/s)	Ebb Velocity (ft/s)/(m/s)	Cumulative Probability (%)
1	3.85/1.17	-4.61/-1.41	11 = 1/9
2	4.10/1.25	-4.66/-1.42	22 = 2/9
3	4.69/1.43	-5.29/-1.61	33 = 3/9
4	4.88/1.49	-5.34/-1.63	44 = 4/9
5	5.35/1.63	-5.76/-1.76	56 = 5/9
6	5.91/1.80	-5.94/-1.81	67 = 6/9
7	6.39/1.95	-5.98/-1.82	78 = 7/9
8	6.62/2.02	-6.11/-1.86	89 = 8/9

Rank	Stage 2: 4.3 ft Return Period = 50 Years			Stage 3: 5.3 ft Return Period = 100 Years		
	Flood Velocity (ft/s)/(m/s)	Ebb Velocity (ft/s)/(m/s)	Cumulative Probability (%)	Flood Velocity (ft/s)/(m/s)	Ebb Velocity (ft/s)/(m/s)	Cumulative Probability
1	3.98/1.21	-4.88/-1.49	11 = 1/9	5.18/1.58	-5.09/-1.55	11
2	4.35/1.33	-4.89/-1.49	22 = 2/9	5.22/1.59	-5.17/-1.58	22
3	4.93/1.50	-5.65/-1.72	33 = 3/9	5.41/1.65	-6.02/-1.83	33
4	5.35/1.63	-5.69/-1.73	44 = 4/9	5.80/1.77	-6.02/-1.83	44
5	5.84/1.78	-6.30/-1.92	56 = 5/9	6.35/1.94	-6.76/-2.06	56
6	6.62/2.02	-6.45/-1.97	67 = 6/9	7.32/2.23	-6.79/-2.07	67
7	7.32/2.23	-6.71/-2.05	78 = 7/9	8.21/2.50	-7.41/-2.26	78
8	7.62/2.32	-6.82/-2.08	89 = 8/9	8.58/2.62	-7.55/-2.30	89

Rank	Stage 4: 6.2 ft Return Period = 200 Years			Stage 5: 6.7 ft Return Period = 300 Years		
	Flood Velocity (ft/s)/(m/s)	Ebb Velocity (ft/s)/(m/s)	Cumulative Probability (%)	Flood Velocity (ft/s)/(m/s)	Ebb Velocity (ft/s)/(m/s)	Cumulative Probability
1	5.40/1.65	-5.26/-1.60	11	5.52/1.68	-5.34/-1.63	11
2	6.25/1.91	-5.42/-1.65	22	6.49/1.98	-5.56/-1.69	22
3	6.26/1.91	-6.28/-1.91	33	6.79/2.07	-6.51/-1.98	33
4	6.31/1.92	-6.34/-1.93	44	6.80/2.07	-6.53/-1.99	44
5	6.83/2.08	-7.09/-2.16	56	7.09/2.16	-7.26/-2.21	56
6	7.93/2.42	-7.11/-2.17	67	8.27/2.52	-7.30/-2.23	67
7	8.99/2.74	-8.02/-2.44	78	9.42/2.87	-8.35/-2.55	78
8	9.40/2.87	-8.22/-2.51	89	9.85/3.00	-8.59/-2.62	89

Rank	Stage 6: 7.1 ft Return Period = 400 Years			Stage 7: 7.4 ft Return Period = 500 Years		
	Flood Velocity (ft/s)/(m/s)	Ebb Velocity (ft/s)/(m/s)	Cumulative Probability	Flood Velocity (ft/s)/(m/s)	Ebb Velocity (ft/s)/(m/s)	Cumulative Probability
1	5.62/1.71	-5.40/-1.65	11	5.69/1.73	-5.46/-1.66	11
2	6.69/2.04	-5.68/-1.73	22	6.83/2.08	-5.76/-1.76	22
3	7.16/2.18	-6.68/-2.04	33	7.43/2.26	-6.79/-2.07	33
4	7.22/2.20	-6.74/-2.05	44	7.44/2.27	-6.92/-2.11	44
5	7.29/2.22	-7.38/-2.25	56	7.54/2.30	-7.47/-2.28	56
6	8.53/2.60	-7.44/-2.27	67	8.72/2.66	-7.55/-2.30	67
7	9.76/2.97	-8.62/-2.63	78	10.01/3.05	-8.80/-2.68	78
8	10.2/3.11	-8.87/-2.70	89	10.46/3.19	-9.09/-2.77	89

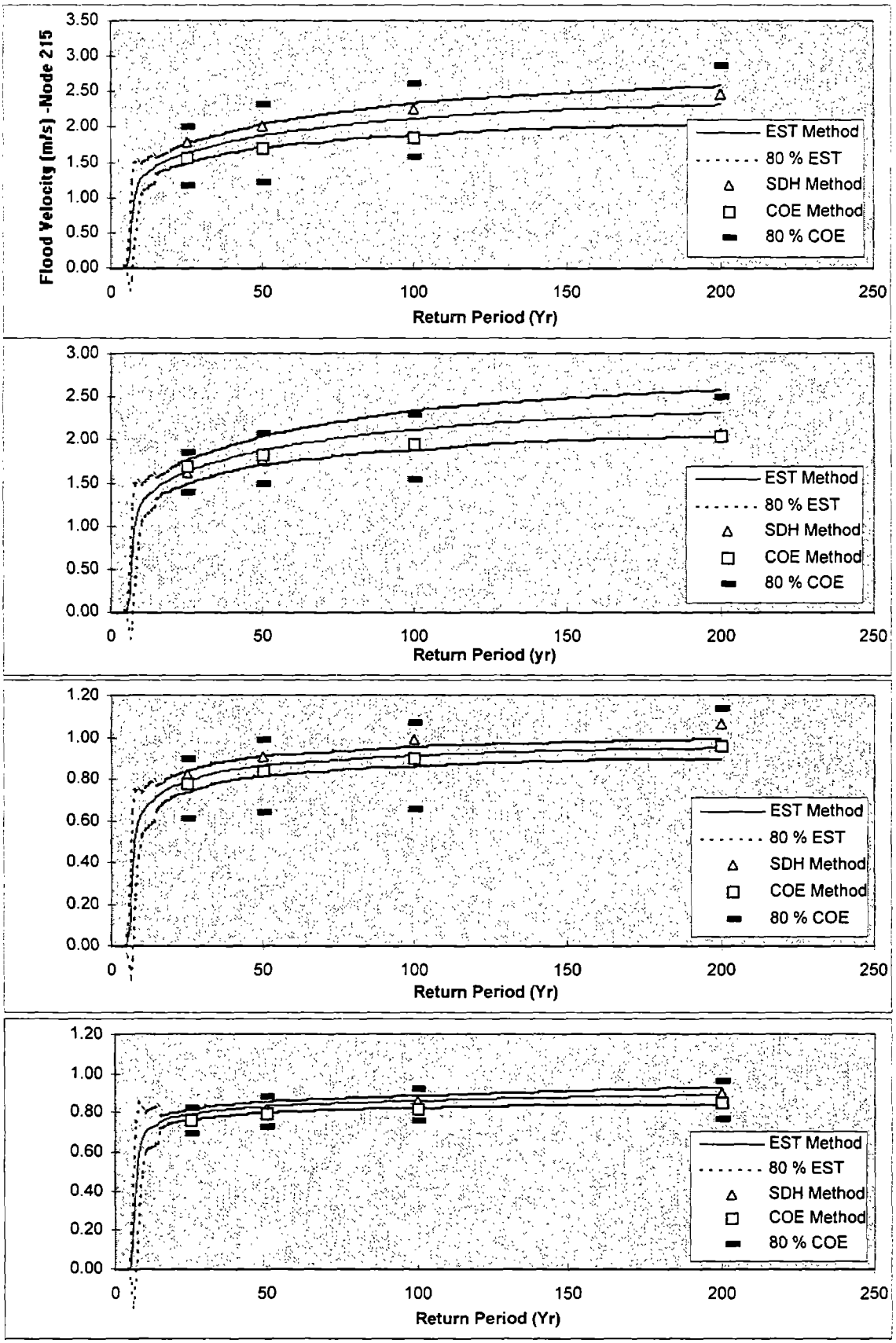

Figure 3.7. Velocity versus return period for all three methods.

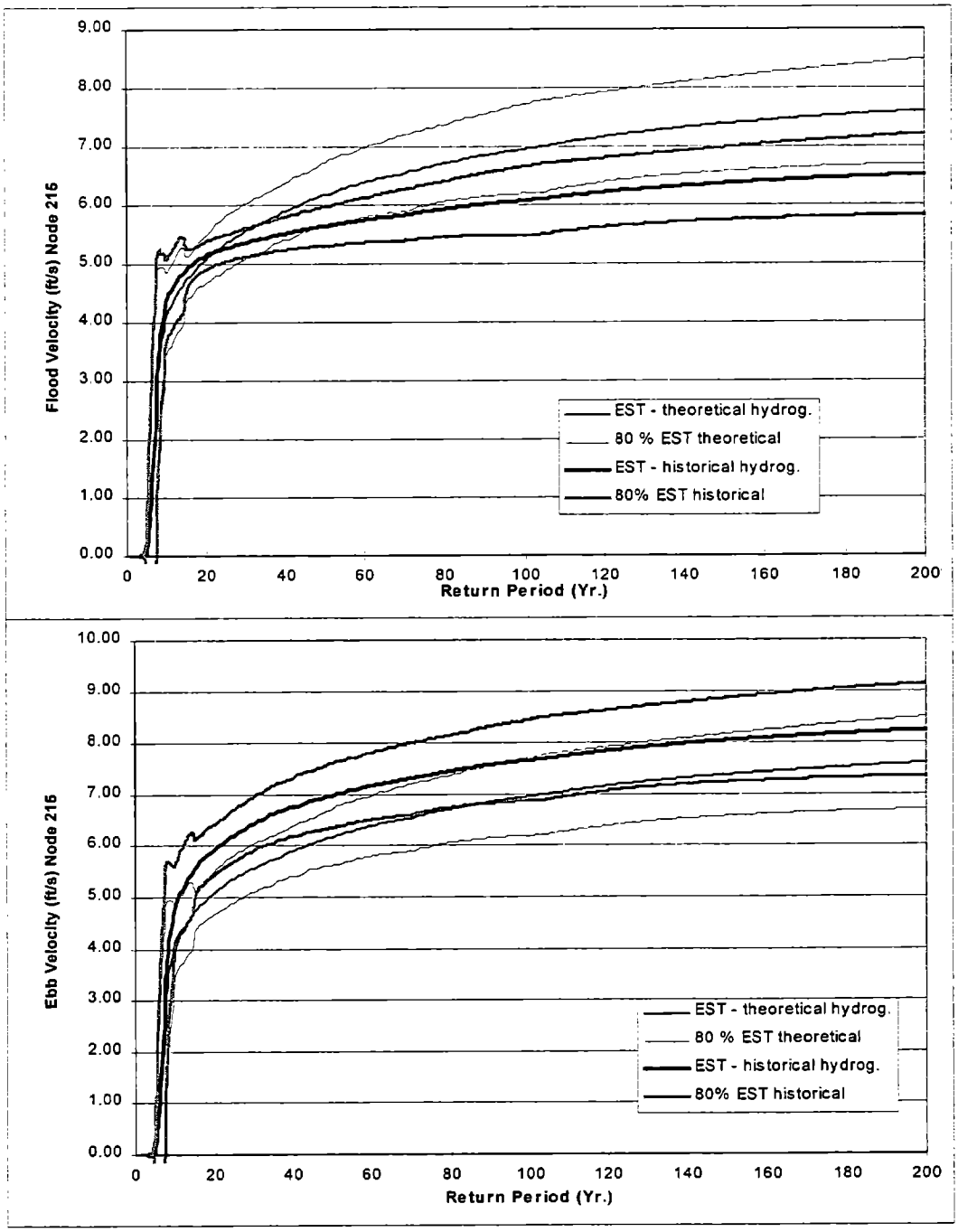

Figure 3.8a. Velocity versus return period - comparison between theoretical and historical hydrograph shape input for the EST at Node 215.

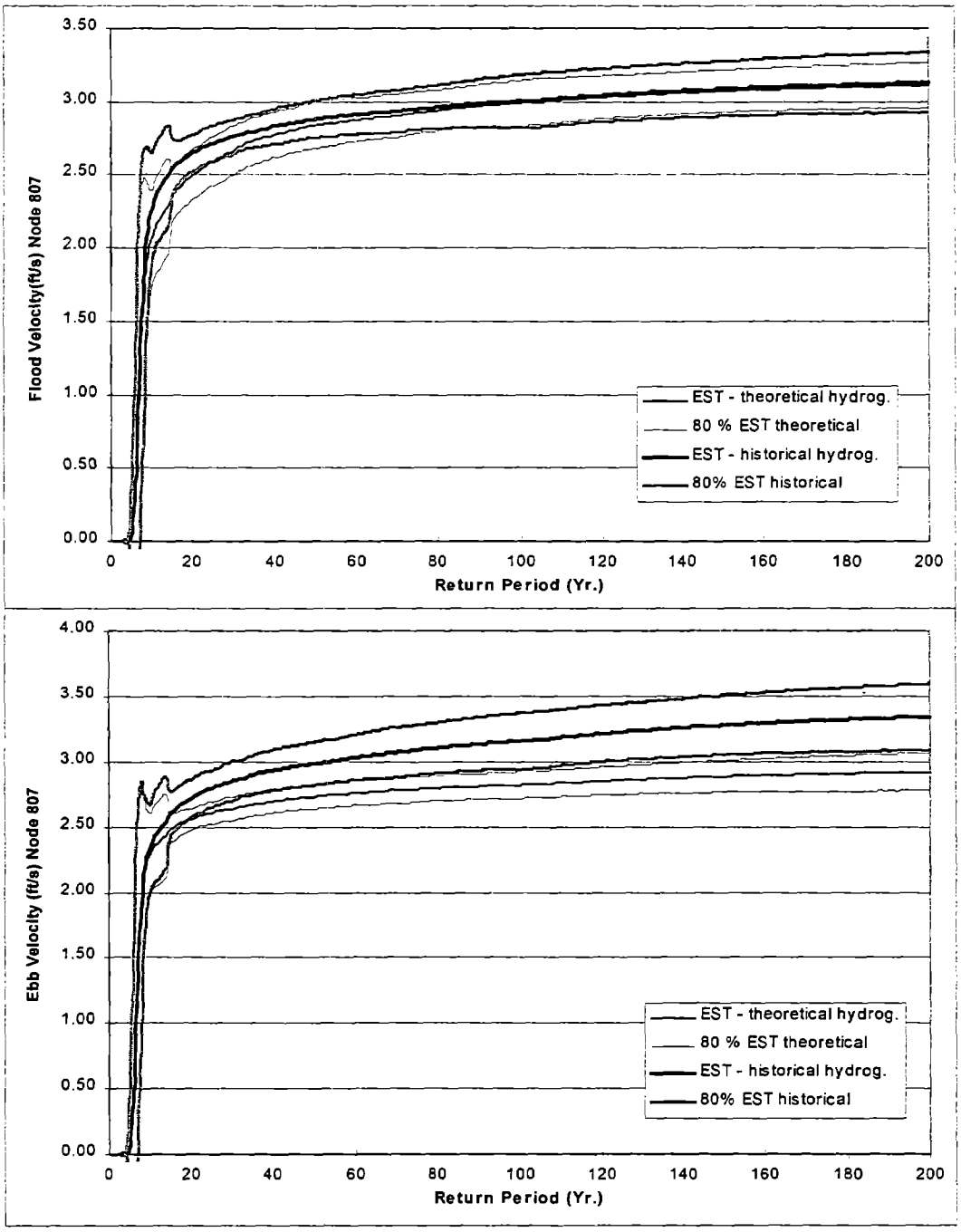

Figure 3.8b. Velocity versus return period - comparison between theoretical and historical hydrograph shape input for the EST at Node 807.

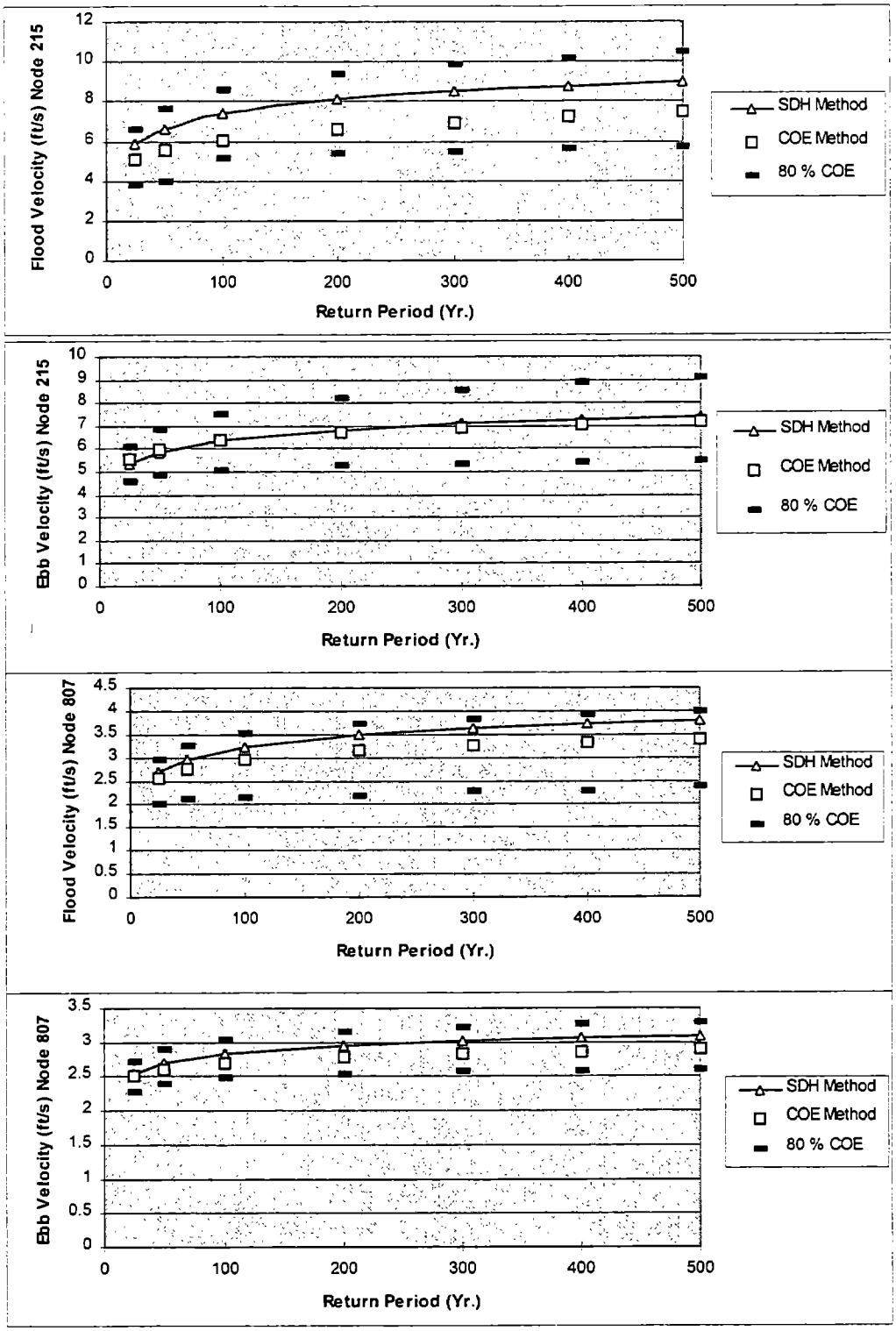

Figure 3.9. Velocity versus return period for SDH and COE over 500 years.

3.7 Probability and Impact of Different Storms

Simulations were also used to investigate whether the impacts of a fast moving storm (short duration) on flood and ebb velocities in a bay are more or less important than that of a slow moving storm (long duration). This was carried out for both the Indian River site and for the a hypothetical model estuary shown in **Figure 3.10**.

3.7.1 Impact of Various Hydrograph Shapes

Various simulations were run to compute the flood velocities for the Hurricane of September 1926 that occurred near Palm Beach, FL. The storm surge hydrographs were obtained with the COE method. This method requires input of the duration of the storm and the mean tide. This latter was easily obtained from the NOAA tide tables. Four different phases were studied: high tide, mid-falling tide, low water and mid-rising tide.

Two different storm durations were chosen for this case: R/f = 1.58 hr (the actual data for that storm) and an extreme value of 4.5 hr.

In the first case, the surge-plus-tide elevation was 11.3 ft (FDNR 1992), and the tide amplitude was 1.4 ft (NOAA tide table for Palm Beach). All simulations were 30 hours long, 15 hours before and after the peak surge, with a 30-minute increment.

From these results the relative importance of the duration of the storm and the phase of the tide could be evaluated. As a general rule, the duration of the storm mainly influences the magnitude of the velocity. This is related to the fact that the duration shapes the hydrograph with regard to the slope, which is responsible for the flood velocity. In this analysis, we are mainly interested in the maximum velocity, and in the duration of that velocity above a particular threshold. The maximum value obviously appears for the shortest storm, because of the slope of the hydrograph. It is also the case that for the shortest storm a threshold value is held the longest. For the duration of 4.5 hr, the peak is almost the same independent of the storm phase, and lasts around 4 hours. For the short storm (1.58 hr), the maximum value is obtained at mid-rising tide, however it is at mid-falling tide that the threshold of 3 ft/s is held the longest (almost 7 hr.)

A simulation was also run adding a flowrate of 165,000 cfs at the east end of the mesh. In this case, the differences observed are in accordance with the estimations: for rising tide, the velocity is constantly decreased, and for falling tide the flowrate adds to the negative velocity.

Other simulations were computed with the same peak surge but with a tide amplitude of 3.4 ft (NOAA tide table for Savannah). As expected, the larger tide increases the hydrograph peak, and results in higher velocities in all cases. Also, the same characteristics as described above were observed.

As a conclusion, the tide phase does not have a major role in the determination of the velocity. For long storm durations, the results are very close regardless of the phase; and for short durations, two tidal possibilities, represented by mid-rising tide and high tide levels, would be sufficient to represent the range of values that may occur.

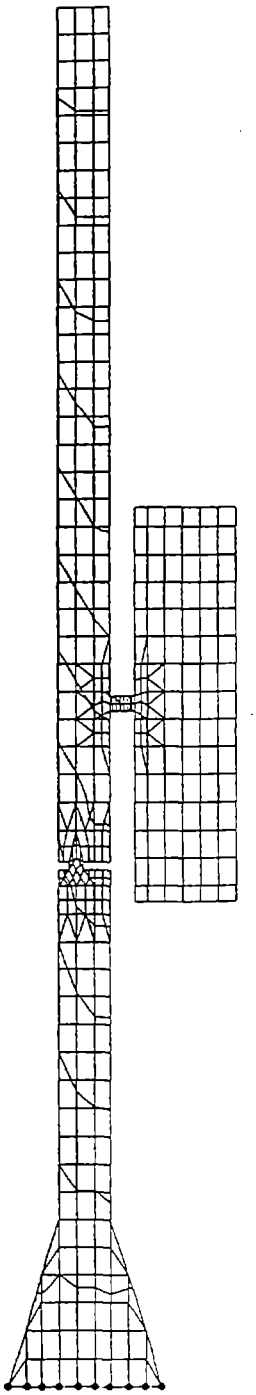

Figure 3.10. Finite element model of the hypothetical case.

Another important observation is that a high peak surge value with a long duration could yield smaller or equal velocities than a smaller peak with a shorter duration. Therefore, the duration has a stronger effect than the peak value.

3.7.2 Tide Influence and Number of Events

As discussed above, for the COE and EST methods, four tidal possibilities were selected: high tide, mid-falling tide, low tide, and mid-rising tide. While more tides might yield greater accuracy, it would require much longer simulation time. In fact, it was noticed that two tides only, high and low, yielded similar results to using four tides. **Figure 3.11** shows a comparison of results obtained from the extremal analysis package of the ACES program (WES 1992; Leenknecht et al. 1992), for the four most important events combined with two or four tides, the eight most important events combined with two or four tides, and all 15 events combined with four tides. It can be clearly seen that running the eight biggest storms yields consistent results with the 15 events simulation, except for low return periods, which was to be expected.

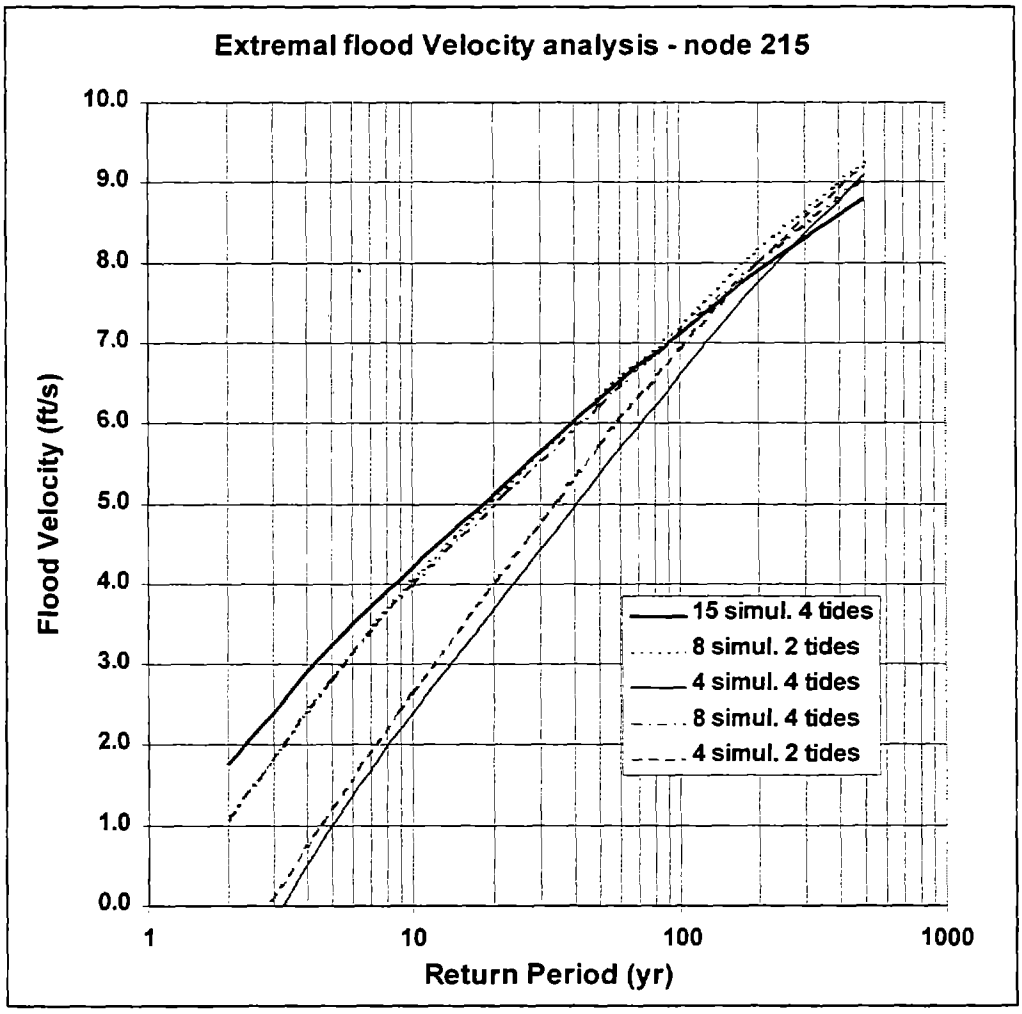

Figure 3.11. Results for the four and eight largest storm events, combined with two or four tides, along with all 15 storm events combined with four tidal possibilities.

Results were obtained as follows. As the storm values picked to run FastTABS were selected over 104 years, and each peak surge value was combined with four different phases of the tide, then the length of record (N-year) used in the ACES extremal analysis package was set to 400 years. This method gave coherent results, opposed to N-year = 100. When running the procedure with two tides, we still use N-year = 400, and combined high and low tide twice.

As can be seen on Figure 3.11, the number of tides can be cut by two without reducing the accuracy significantly. It can also be concluded that fewer tidal possibilities will yield better accuracy than fewer events (the simulation of eight storms combined with two tides gives better results than the simulation of four storms combined with four tides).

As a conclusion, if fewer simulations are desired, the number of tidal possibilities should be reduced rather than the number of events.

3.7.3 Impact of a Fast or Slow Moving Storm on Flood Velocities in the Indian River Model

This section deals with the influence of fast (short duration, usually less than 1.5 hr) or slow (long duration) moving storms on flood velocities. At this point it is interesting to recall that the mean duration of a storm is 2 hours for the East and Gulf Coasts, and that 90 percent of the storms have a duration between .5 and 3 hours (**Figure 3.12**).

In the Indian River case, velocities tend to increase with the surge, but durations influence that trend (**Figure 3.13**). As shown above, it is particularly interesting to note that a high surge with a long duration often yields lower velocities than a lower surge with a shorter duration. Therefore, whether the fast moving storm is more likely to produce as high a storm surge as a slow moving storm is not a major problem because in most cases the fast moving storm will generate the greatest velocities anyway.

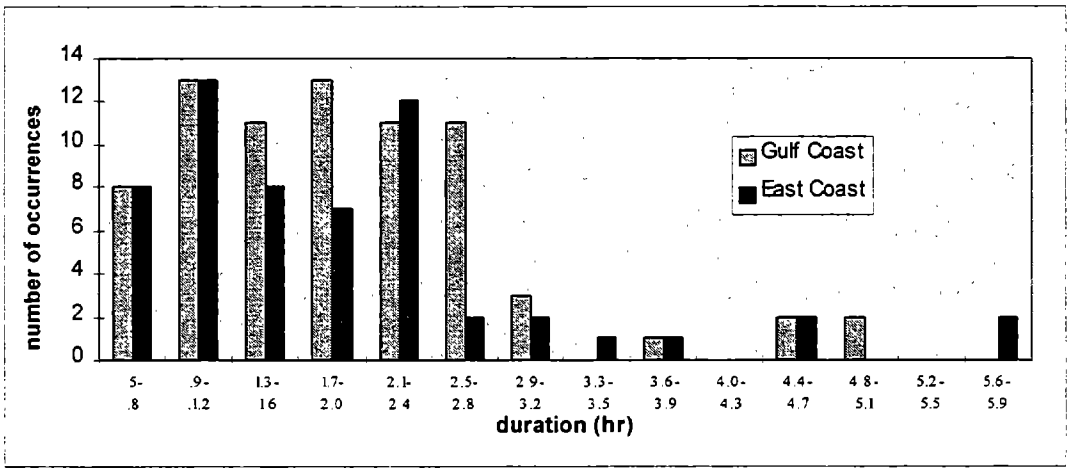

Figure 3.12. Frequency of occurrence of a storm duration (0.4 hour intervals) based on hurricanes occurring during the 85-year period, 1900-1984.

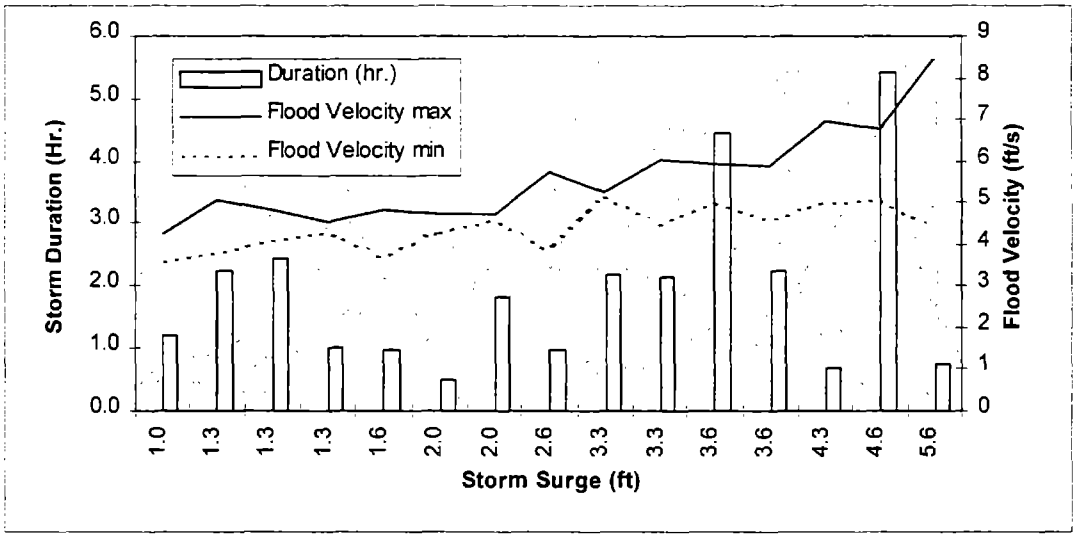

Figure 3.13. Results of the FastTABS simulation in the Indian River at the entrance channel, Node 215.

It is nevertheless difficult to judge the effect of each input parameter (surge and duration), as there are few data and they may be correlated (in the Indian River case, high surges are usually associated with low durations). Also, very long duration storms were associated with high storm surges and yielded low velocity values that have little effect for extremal velocity analysis.

The impact of storm speed cannot be totally defined without also investigating whether a fast moving storm (short duration, causing a rapid rise) is likely to produce as high a storm surge as a slow moving storm. This is related to the frequency of occurrence of high intensity, fast moving and slow moving storms. This issue is addressed in the following section.

3.7.4 Interrelations Among Hurricane Parameters

The most important factor in storm surge modeling is the intensity of the hurricane, which is directly related to its central pressure P_0. Harris (1959) demonstrated that the storm surge height S_p is approximately proportional to the central pressure depression, other factors being constant. This implies that storm surge height is directly related to P_0 because central pressure depression is defined as the difference between P_0 and peripheral pressure (usually near 1013 mb.) Also, the duration depends on the radius of maximum winds R and the forward speed f, as shown in Equation 3.2. Therefore, investigation of the interrelations among the three hurricane parameters P_0, R and f is necessary to fully determine appropriate hurricane characteristics for modeling purposes. NOAA Technical Report NWS 38 (1987) used different methods to test the interrelations among hurricane parameters. The conclusions were as follows:

1. In general, the parameters P_0, *R* and *f* for landfalling hurricanes are mutually independent, although the lack of data north of Chesapeake Bay prevented the determination of meaningful statistic results for that region. The NWS felt that for purposes of storm-surge frequency computations, all parameters should be considered locally independent.

2. It was shown, however, that hurricanes with very large *R's* are generally found to be of moderate or weak intensity (high P_0). Also, extremely intense hurricanes (low P_0) and those with small *R's* tend to occur together (**Figure 3.14**).

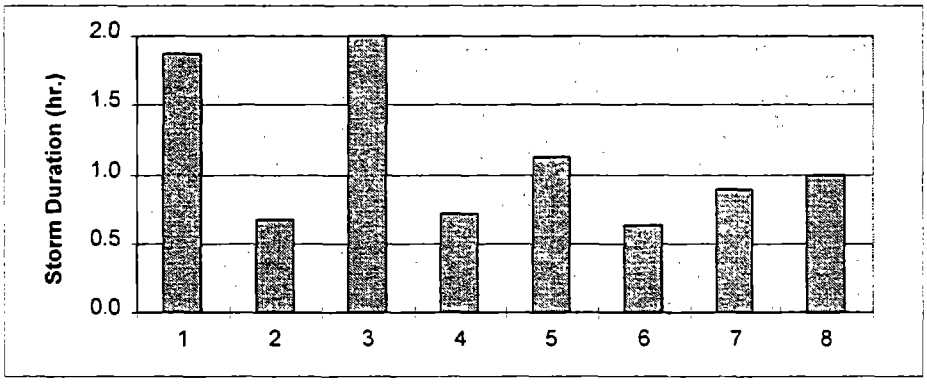

Figure 3.14. For eight severe hurricanes since 1900 (P_0 < 930 mb), small values of R yielded low duration values between 0.6 and 2 hr, most of them being under 1.1 hr.

A direct consequence of these results is that there is not a clear dependence between the duration of a storm and its intensity. However, small *R's* (and therefore small durations, assuming that there is no dependence between *R* and *f*) are usually associated with intense hurricanes and, therefore, high storm surge.

This conclusion should be interpreted narrowly. For any limited area, the NWS argues that even if sufficient data were available, it is likely that the above conclusions might not be true. An application is also seen on Figure 3.13 for the case of the Indian River. Fifteen major hurricanes were reported for which durations are plotted versus the computed surge. The tendency of having small *R* (and small duration) for high surges (above 3 ft) is true for 5 out of 7 cases. Lower surge values also appear to have low durations in this case. Also, the range of durations is wider for high surges, but there is no particular trend associated with this graph. This further confirms the independence of these parameters.

It was also noticed that although the velocity values tend to increase with the surge, the duration greatly affects these results. The highest velocities were obtained for very short durations (0.7 hr) associated with fast moving storms which are associated and with high surges.

As a conclusion, both the hypothetical model estuary and the Indian River examples showed that extremal values happen for fast moving storms, even if the peak surge value was smaller than a slower storm. As a consequence, the probability of occurrence of such

fast moving storms was investigated. Although hurricane parameters P_0, R and f were shown to be generally mutually independent, it appeared that small R's have the tendency to occur with low P_0, and, therefore, the fast moving storms (low duration, small R) are likely to be of high intensity (low P_0). The Indian River example supports these observations. These results have to be interpreted narrowly, however, as local interrelations between hurricane parameters may appear. As a consequence, fast moving storms will generally be the main factor in determining extremal values.

3.8 Conclusions

The objective of this study was to recommend procedures to determine flood velocity-frequency relationships for hurricane storm surges. Three methods have been examined for determining the effect of tropical storms on currents in an estuary:

1. Corps of Engineers (COE)
2. Empirical Simulation Technique (EST)
3. Single Design Hydrograph (SDH)

The same approach could be adopted for extra-tropical storms which have a much higher frequency of occurrence, but with different rise and fall patterns.

The methods were applied to actual data for Indian River, Delaware. The COE method yields a very large confidence interval and requires more simulations in order to reduce the confidence interval. The EST method is probably the most accurate as it recreates and extends the historical data 100 times, thereby accounting for a random tide. The SDH method provides a fast and reasonable estimate of the maximum velocity at the locations of interest. It is recommended that in all but the most complicated cases, the SDH method should be followed and in some cases extended to consider different combinations of peak surge and tide.

4. MODEL TESTING

4.1 FESWMS Testing

Testing was carried out to evaluate the performance of several features of the FESWMS program. The majority of the test cases were run on FESWMS Version 2b, date stamped August 16, 1996. Additional tests were performed using FESWMS Version 2c, date stamped April 19, 1997.

4.1.1 Computation of Pressure Flow at Bridges

Tests with Version 2b

The model was tested for its ability to accurately compute solutions in situations where the low chord of the bridge deck is submerged (pressure flow). Tests were run on four different model cases. For each case several variations were tried. A total of 19 simulations were computed. The four cases are described below:

Case 1: A simple channel with no obstructions, uniform slope and roughness.

Case 2: A compound channel with obstructions on the overbanks, symmetrical about the longitudinal axis.

Case 3: The same as Case 1 but with small, symmetrical obstructions at the two sides.

Case 4: The Sue Creek bridge model from the Surface Water Modeling System (SMS) tutorial files.

A common result seen in all of the pressure flow test cases was a point beyond which further lowering of the pressure ceiling did not increase the water surface upstream of the velocity inside the bridge opening. Also, the continuity performance of the models deteriorated significantly at all locations downstream of the bridge as the ceiling was lowered. Some models had over 30% continuity loss. When continuity was lost at the bridge, it was not regained at any point downstream of the bridge. This point is illustrated by **Figure 4.1**, which shows water surface elevation contours and continuity for one of the Case 4 simulations.

The solutions in Cases 1 and 3 were clearly inaccurate when pressure flow was incorporated. Even though the geometry, ceiling, and boundary conditions for these cases were symmetrical about the longitudinal axis, the simulation results were highly asymmetrical. **Figure 4.2** is a velocity contour plot of Case 1 showing the asymmetry of the solution. This asymmetry indicates a definite numerical problem for these cases. Additionally, the water surface increase caused by the pressure flow was well beyond what should be expected.

Cases 2 and 4 did not exhibit the problem with asymmetry to a significant extent. Furthermore, the water surface increases computed did not appear excessive. The only apparent problems with these cases were the continuity loss and the failure to increase energy loss with decreasing ceiling elevation, which is probably related to the continuity loss. The continuity loss is indicative of a significant numerical problem.

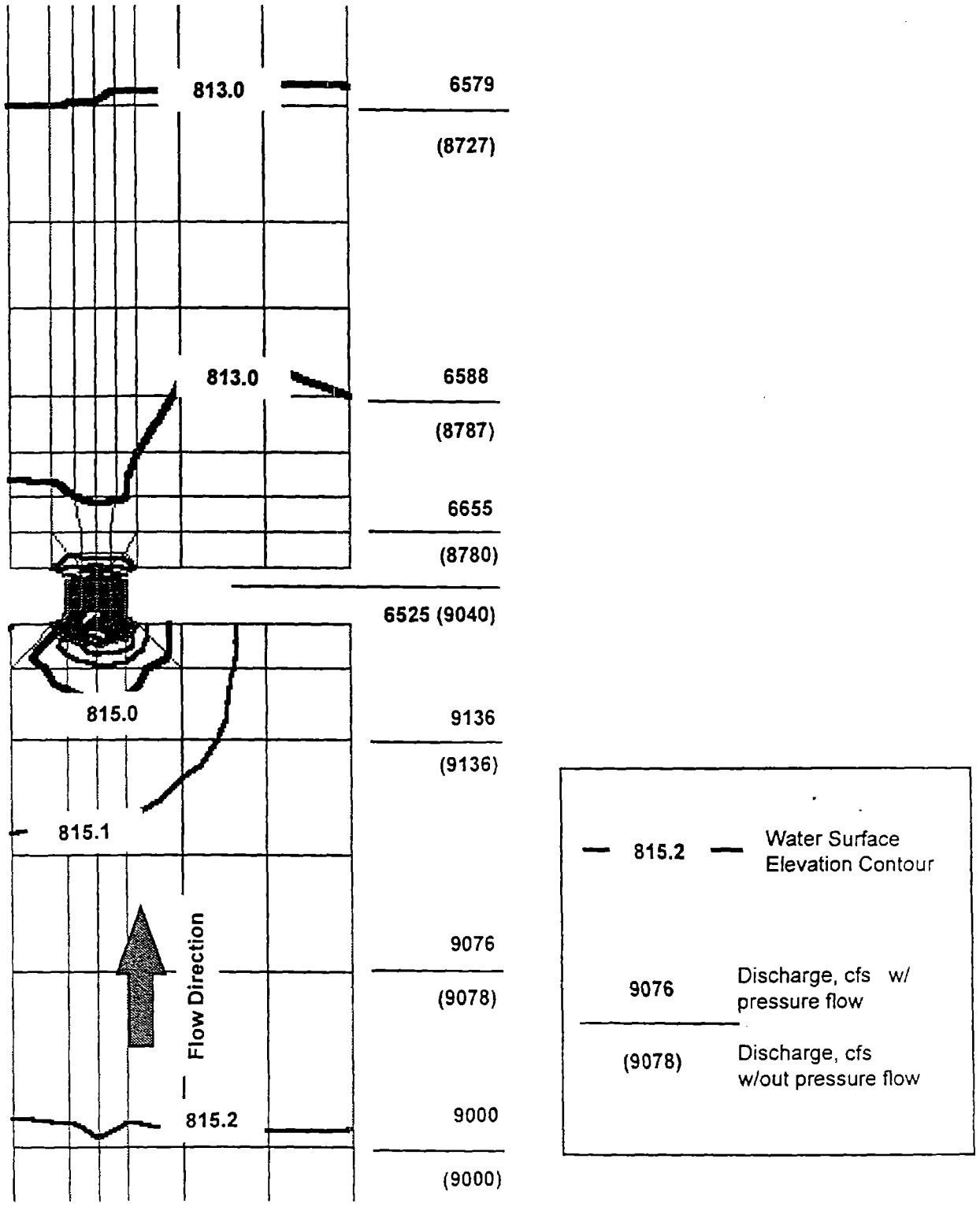

Figure 4.1. Illustration of test Case 4 showing continuity loss.

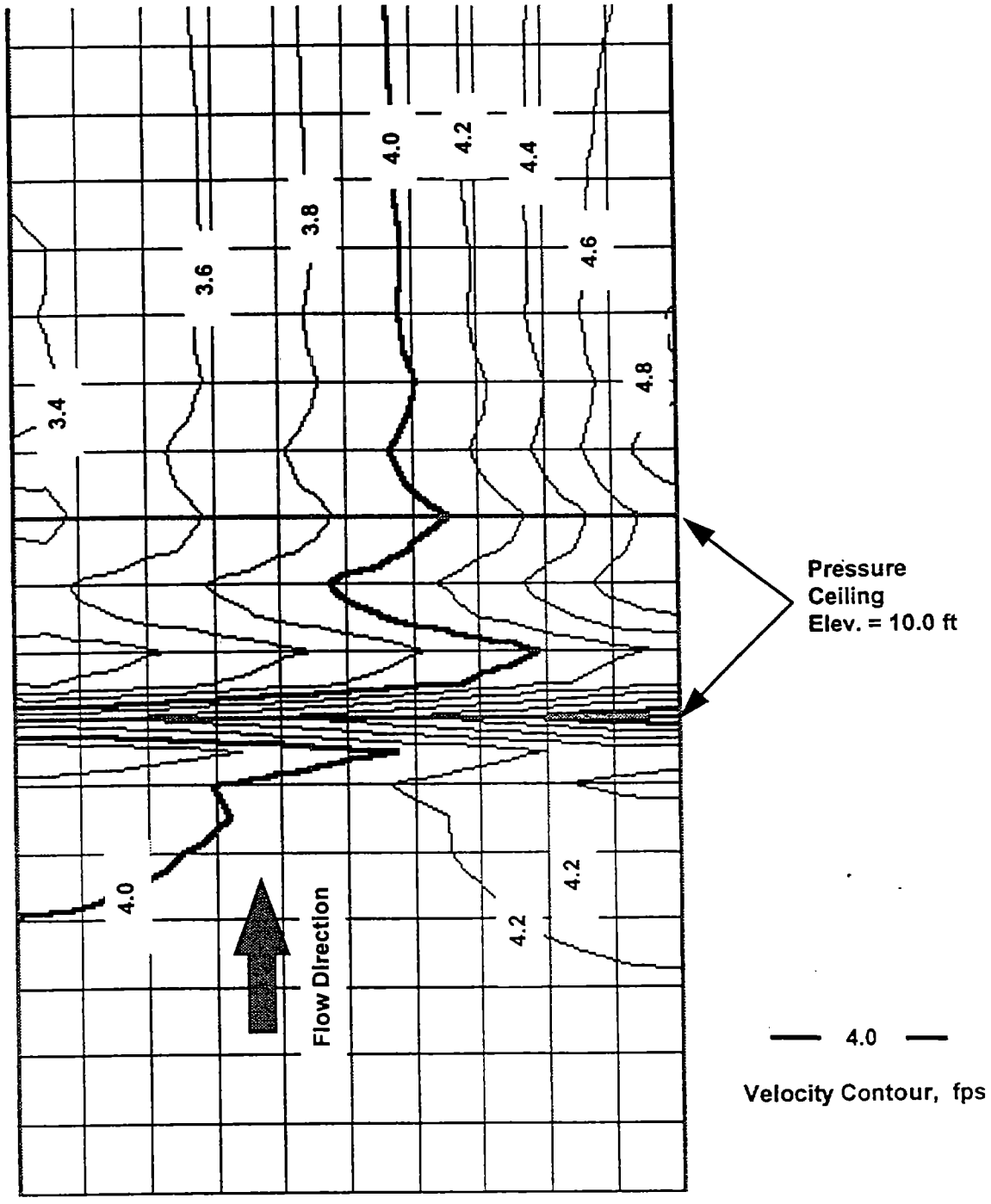

Figure 4.2. Velocity contour plot of Test Case 1 showing asymmetry in solution.

Tests with FESWMS Version 2c

The pressure flow component was tested using the Sue Creek model from the SMS tutorial files. As with the previous testing, the only differences between the test models were the pressure flow ceiling elevations. In each case, all the flow must go through the bridge opening since approach roadway and bridge overtopping were not incorporated into the model. The asymmetry of the solutions with version 2b was not present in version 2c, nor was the significant continuity loss. It is clear, however, that FESWMS Version 2c does not properly account for pressure flow in computing the hydraulics through the bridge. The introduction and lowering of the pressure ceiling causes the water surface elevation upstream of the bridge and the flow velocity within the bridge opening to decrease when they should increase. **Table 4.1** illustrates this point. All of the simulations in the table have a discharge of 9000 cfs and a downstream water surface elevation of 811.0 feet. Node 219 is located in the center of the pressure flow region, and node 107 is about 225 feet upstream from the bridge.

Table 4.1. Pressure Flow Test Results Using FESWMS Version 2c.

Pressure Ceiling Elevation (ft)	Depth at Node 219 (ft)	Velocity at Node 219 (ft/s)	Continuity at Bridge (%)	Unit q at Node 219, cfs/ft	Water Surface Elevation at Node 107 (ft)
no pressure	10.52	12.78	102.9	134.4	812.99
810.00	11.55	11.30	99.4	130.5	812.98
809.75	11.82	10.96	99.2	129.5	812.97
809.00	12.98	9.30	94.9	120.7	812.94

According to the model documentation, the depth computed by FESWMS in pressure flow regions includes pressure head. It appears that this combined depth (flow depth plus pressure head) is being used as the flow depth, resulting in lower velocities in the bridge for pressure flow conditions than for free surface conditions. The decreased velocity results in lower energy loss through the bridge and lower water surfaces upstream of the bridge for pressure flow conditions as compared to identical free surface conditions. This result appears to be identical to FESWMS Version 1.

Recommendations for Submerged Deck Applications

It is not recommended that the pressure flow component of any version of FESWMS through version 2c be used for tidal or riverine bridge hydraulic analyses. As new versions of the model become available, testing should be performed to ensure that appropriate results are produced. In the interim, the methodology presented in the tidal hydraulics users manual (Zevenbergen et al. 1997) should be used. The alternative method uses the depth variable Manning n component to simulate the additional losses produced by a submerged deck.

4.1.2 Dynamic Simulation

The previous FESWMS release, version 2a, was not capable of dynamic simulation. Testing of the dynamic capability of version 2b was done using the Sue Creek network file and modified input data files. The test simulations had time-variant downstream head boundaries to represent tidal fluctuations. The program completed dynamic solutions for each time step on these test models and used the correct downstream head value at each time step.

It is often desirable to begin a simulation with a steady-state solution and then go on to dynamic simulations. Version 2b was not able to perform a steady-state solution prior to dynamic simulations, as it ignored the input request for steady-state iterations. This problem was not evident in version 2c.

4.1.3 Friction Slope Boundary Condition

In many riverine studies, it is convenient to have the model automatically assign the downstream head boundary elevation based on an assumed friction slope at the downstream cross section. This capability is documented in the FESWMS Version 2 user's manual. The feature was tested and found to be inoperative for versions 2b and 2c.

4.1.4 Rating Curve Boundary Condition

Similarly to the friction slope boundary condition, it would be desirable in some studies to have the downstream head assigned automatically by the use of a user-defined rating curve. All attempts to enable this feature in model test cases were unsuccessful for versions 2b and 2c.

4.1.5 Culvert Flow

The performance of the culvert feature of FESWMS was evaluated using several culvert test cases including both inlet-control and outlet-control situations. For each test simulation, the tailwater and headwater elevations were read along with the discharge through the culvert. The results were compared to HY-8 runs reflecting the same culvert configurations and tailwater elevations.

In inlet control situations, FESWMS consistently reported higher culvert discharges than HY-8 for a given headwater elevation. This is because FESWMS uses the following equation for inlet control:

$$Q_c = C_c A_c \sqrt{2g(HW - z_i)} \qquad (4.1)$$

in which

Q_c = the culvert discharge (cfs, m^3/s),
C_c = a discharge coefficient,
A_c = the culvert flow area (ft^2, m^2),
g = the acceleration due to gravity,
HW = the headwater elevation (ft, m), and
z_i = the culvert invert elevation (ft, m).

This is essentially an orifice equation. For this equation to be theoretically correct, it should be the elevation of the centroid of the flow area that is subtracted from **HW** rather than the invert elevation. Furthermore, the inlet control equations used by HY-8 are actually fifth-degree regression curves fit to empirical data for each different type of culvert, not the theoretical weir equation.

In situations where the culvert was in outlet control and the tailwater level was well above critical depth, the results from FESWMS were close to those from HY-8. In outlet-control situations where the tailwater depth was below the culvert's critical depth y_c, FESWMS produced lower headwater elevations for a given discharge than HY-8. This is because HY-8 never uses a downstream control depth less than y_c in outlet control computations. FESWMS uses the tailwater depth as the control, even when it is below y_c, unless the user has defined a minimum tailwater depth in the input.

In one outlet-control case the user-defined tailwater elevation was used to try to force FESWMS to use the same control depth as HY-8. This was expected to result in a solution close to the HY-8 solution. Instead, FESWMS produced an inlet control solution with a much higher discharge for the solved headwater and tailwater. In this case, the model incorrectly used an inlet control solution, when the outlet control solution should have been used.

In a steady state solution incorporating culverts, FESWMS results can be compared with HY-8 to ensure accurate hydraulic computations. The area, hydraulic radius, and loss coefficients can be manipulated to arrive at the correct solution, and the overall simulation will still benefit from the 2-dimensional flow analysis. For dynamic simulations, especially when large culverts are included, the changing area and hydraulic radius cannot be simulated automatically in FESWMS. The only alternative is to stop the simulation, manually change the area and hydraulic radius, and restart the model. This procedure would have to be performed frequently during a model run. It would be difficult, however, to know when to change these parameters, and discontinuities in computed discharge would occur in the solution when these parameters are manually changed.

4.1.6 Weir Flow

All of the test cases for weir flow indicated that the model computes accurate weir flow solutions, according to the method recommended in FHWA Hydraulic Design Series 1 (1978), where weir nodes are used. The only problem identified with weir nodes is that when the submergence is high (meaning that the tailwater depth above the crest of the weir is near the headwater depth) the model has difficulty converging to a solution. In some cases, the model becomes unstable and diverges. In others, the model oscillates about the solution without converging. Both situations can probably be attributed to the steepness of the function used to compute the effect of submergence on the weir flow.

4.1.7 Pier Drag Calculations

The automatic pier drag calculations of FESWMS were checked against manual computations using the following formula:

$$F_d = \frac{1}{2} C_d \rho V^2 A_p \qquad (4.2)$$

in which

F_d = the drag force (lb, N),
C_d = the drag coefficient,
A_p = the projected obstruction area of the pier (ft^2, m^2),
V = the flow velocity at the pier (ft/s, m/s), and
ρ = the density of water (slugs/ft^3, kg/m^3).

The FESWMS results matched the manual calculations well.

4.1.8 Depth-Varied Roughness Coefficients

A series of tests were run on a simple model to test the depth-varied Manning's n feature of FESWMS. These tests indicated the model was varying the n values with depth properly, in correspondence with the user-input specifications.

It was learned from FHWA that a bug had been identified in version 2b of the model related to the variable roughness feature which was being addressed for future versions. The bug was not evident in the test cases performed for this study.

4.1.9 Element Wetting and Drying

Areas of the model that may be submerged for part of the simulation and dry for other parts of the simulation can be identified and either included or excluded from the finite element computations by FESWMS. This feature appears to work for steady state models but results in errors and model termination in dynamic models for FESWMS Versions 2b and 2c. This error does not occur in FESWMS Version 1, which should be used for applications requiring wetting and drying until this feature is corrected.

4.2 UNET Testing

Testing was carried out to evaluate the performance of several features of the UNET program. The test cases were run on an unreleased UNET Version 3.0, date stamped December 13, 1996.

4.2.1 Operation in Metric (SI) Units

The current HEC release version of UNET (version 3.2) is not capable of operation in Standard International (SI) units. As part of this study, Dr. Barkau modified UNET for dual unit computations. Dr. Barkau's current UNET executable, date stamped December 13, 1996, incorporates this functionality. Dr. Barkau tested the metric version using several complex network models. Testing of the metric operation was also performed on the Broward River, Duval County, Florida network model. The computed peak discharge, stage, and velocities were tested for verification of the new methods. The cross section geometry file and boundary conditions files were both converted to SI units. The switch

indicating the desired units is located on the first line of the cross section geometry file as follows:

JC METRIC

Field	Variable	Value	Description
0	ID	JC	Record Identifier
1	UNITS	METRIC	Operation in METRIC Units

The default units in UNET are English, and the JC record is not required for operation in English units.

Test results indicated that the SI units function was operating properly with this latest version of UNET. Values computed using English units were compared with values computed using SI units and negligible differences in the computed values after conversion were observed.

A sensitivity to the upstream inflow hydrograph values using the metric simulation was observed during the model testing. The metric version of UNET became unstable when small values of discharge were used for the upstream flow boundaries. This could be considered a limitation of the model itself, but the corresponding flow values in English units resulted in a stable solution during the English unit simulations.

UNET does not support the use of heterogeneous units in the cross section geometry and boundary conditions files. Both must use a consistent set of units for correct results.

It is anticipated that the next distribution version of UNET (Version 4.0) will contain the capability for metric computations. It is recommended that Version 3.2 be used for English unit simulations, and the modified Version 3.0 be used for SI simulations (available from Research Team) until release of Version 4.0.

4.2.2 Standard Weir Submergence Relationships

The use of standard weir submergence relationships was incorporated in UNET by the Corps of Engineers between Phase I and Phase II of this study.

4.2.3 Output of Velocity and Other Variables to HEC-DSS

The current release versions of UNET (version 3.0 and 3.2) allow the output of velocity to HEC-DSS. Velocity output is partitioned into channel velocity, floodplain or overbank velocity and average cross section velocity. In addition, maximum flow, stage, and velocity profiles for each reach can be output to DSS.

5. RECOMMENDATIONS FOR FUTURE WORK

This section suggests topics for potential future work on tidal hydraulic modeling for bridge hydraulics. It includes a wide variety of support and further research topics which would provide improved modeling capabilities and techniques to the Pooled Fund States.

5.1 Training Courses

Additional training courses should be available to the Pooled Fund States to train the staff hydraulic engineers and to provide training for consultants. The training courses should be tailored to the individual states' needs. A number of options would be possible including an overview course in tidal hydraulic modeling or 1-D and 2-D modeling courses, with each course including storm tide hydrology lessons. Given the range of material covered in the Users Manual, it would also be possible to prepare a variety of short (1/2-day) modules that a state could select to structure a 1-week course to the specific needs of their participants. The courses could be offered directly through the pooled fund or, if desired by the Pooled Fund States and approved by the National Highway Institute (NHI), through the NHI. For an NHI course, a Participant Workbook and formal lesson plans would be developed.

5.2 Technical Support and Users Group

Currently, the participants from the first training course can contact the Research Team via E-mail regarding questions on tidal hydraulic modeling. When these questions are answered, the question and the response are distributed to all class participants via E-mail. It is proposed that this "Users Group" be continued and expanded in a future phase.

Additional support for the Pooled Fund States could extend to consultants working on state projects and, potentially, on-site support for state projects.

5.3 Updates to the Users Manual and Software

As the computer models, input software, methods and technology are improved and upgraded, this information needs to be transmitted to the model users at the Pooled Fund States. The Users Manual should be updated through future editions to remain current with the technology.

5.4 Model Testing

As future versions of the computer models are released, it is recommended that they be tested to ensure that the existing features continue to function correctly and that new components perform as expected. It is proposed that one UNET and two FESWMS test cases be produced. The test cases should incorporate the features most likely of use in tidal modeling and as many other features as are reasonable. The test cases should be as simple as possible while still providing a thorough test of the model capabilities. Two FESWMS simulations are recommended because some features should be tested under steady-state conditions and other features under dynamic conditions. Continued Beta testing of SMS should also be performed.

5.5 UNET Model Input Enhancement

The use of COED for UNET could be improved. COED is designed for HEC-2 but is useful for UNET input. The COED help screens could be tailored for UNET to provide variable

descriptions during input. A more ambitious approach would be to incorporate UNET into SMS much as WSPRO is currently being incorporated. This may be worthwhile, but the Corps of Engineers has plans to incorporate UNET into HEC-RAS. It may be best to wait on the HEC-RAS product.

5.6 Wind and Wave Research

Research should be performed to develop wind frequency data for the tidal hydrograph to determine wave height for establishing bridge low chord elevations. Also, including wind stresses, as appropriate, in FESWMS models should be investigated to include the use of onshore, offshore, and along-shore winds.

5.7 Expand Synthetic Storm Surge Hydrograph Methodology

When comparing the synthetic storm surge hydrographs to actual hydrographs, the current methodology appears to work well for the positive surge. Actual hydrographs can also have negative elevations caused by offshore winds. Research should be conducted to develop a method to incorporate the negative elevations into the surge prediction.

5.8 Combining Storm Surges with Daily Tides

Current research is not conclusive on the most appropriate procedure for combining storm surges with daily tides. This topic should be expanded in a future phase.

5.9 Expand Materials on Tides and Hurricanes

This research would be focused on providing additional information on tides, developing tidal hydrographs and on the characteristics of hurricanes. This should include guidance on selecting storm surge values when different sources (FEMA, NOAA, etc.) conflict.

5.10 Upland Runoff Research

The combined probability of an upland runoff event and a storm surge should be investigated. This research could be directed at predicting the frequency of rainfall caused by hurricanes or for predicting runoff directly. The peak runoff rate, the shape of the runoff hydrograph and the lag time should be investigated.

5.11 Operation of Salinity Barriers

Salinity barriers control the movement of brackish water into upland channels during normal tidal conditions. These structures may be ineffective during storm surges. Methods could be developed to include the hydraulic effects of these structures into tidal models.

5.12 Weir Instability in FESWMS

Under conditions of high submergence, the analysis of weirs in FESWMS can become numerically unstable. Additional work could be performed to incorporate modifications in FESWMS or to develop procedures to avoid the problems.

6. REFERENCES

Ayres Associates, 1994. "Development of Hydraulic Computer Models to Analyze Tidal and Coastal Stream Hydraulic Conditions at Highway Structures," Final Report, Phase I HPR552, South Carolina Department of Transportation, Columbia, SC.

Borgman, L.E., 1992. "Empirical Simulation of Future Hurricane Storm Surge Histories as a Tool in Engineering and Economic Analysis," Proceedings of the International Conference on Civil Engineering in the Oceans V, American Society of civil Engineers.

BYU, 1997. "SMS Surface Water Modeling System," Reference Manual, Version 5.0, Brigham Young University - Engineering Computer Graphics Laboratory, Provo, UT.

Cialone, M., 1994. Personal Communication.

Cialone, M., Butler, H. Lee, and Amein, M., 1993. "DYNLET1 Application to Federal Highway Administration Projects." Technical Report CERC-93-xx, U.S. Army Corps of Engineers, Waterways Experiment Station.

Federal Highway Administration, 1978. "Hydraulics of Bridge Waterways," Hydraulic Design Series No. 1, Washington, D.C.

Florida Department of Natural Resources, 1992. "Palm Beach County, Storm Surge Model Study."

Florida Department of Natural Resources, 1991. "Okaloosa County, Storm Surge Model Study".

Froehlich, D.C., 1996. "Finite Element Surface-Water Modeling System: Two-Dimensional Flow in a Horizontal Plane," FESWMS-2DH, Version 2, User's Manual, U.S. Department of Transportation, Federal Highway Administration, Research, Development, and Technology, Turner-Fairbank Highway Research Center, McLean, Virginia.

Grace, Peter J., 1994. "Application of an Empirical Simulation Technique To Lake Okeechobee Storm Surges." Master of Engineering Project, Texas A&M University.

Harris, D.L., 1959. "An interim Hurricane Storm Surge Forecasting Guide," National Hurricane Research Project Report No. 32, Weather Bureau, U.S. Department of Commerce.

HEC, 1995. "HEC-DSS User's Guide and Utility Manuals," User's Manual, Davis, CA: Hydrologic Engineering Center, US Army Corps of Engineers, CPD-45.

HEC, 1996. "UNET --One-dimensional Unsteady Flow Through a Full Network of Open Channels," User's Manual, Davis, CA: Hydrologic Engineering Center, US Army Corps of Engineers, CPD-66 Version 3.1.

Leenknecht, D.A., Szuwalski, A., and Sherlock, A.R., 1992. Automated Coastal Engineering System: User's Guide Version 1.07, CERC, U.S. Army Engineers Waterways Experiment Station, Vicksburg, MS.

National Weather Service, 1987. "Hurricane Climatology for the Atlantic and Gulf Coasts of the United States." NOAA Technical Report NWS 38.

Richardson, E.V. and S.R. Davis, 1995. "Evaluating Scour at Bridges," Third Edition, Hydraulic Engineering Circular No. 18, U.S. Department of Transportation, Federal Highway Administration, Publication No. FHWA-IP-90-017.

Scheffner, N.W., Borgman, L.E., and Mark, D.J., 1993. "Applications of Large Domain Hydrodynamic Models To Generate Frequency-of-Occurrence Relationships," ASCE Estuary and Coastline Modeling Conference, Chicago, IL.

Scheffner N.W., Mark D.J., Blain C.A., Westerink J.J., and Luettich R.A., Jr., 1994. "A Tropical Storm Data Base For The East And Gulf Of Mexico Coasts Of the United States," U.S. Army Corps of Engineers, Coastal Engineering Research Center.

Thomas, W.A., and McAnally, W.H., Jr., 1990. "User's Manual for the Generalized Computer Program System: Open-Channel Flow and Sedimentation, TABS-2," U.S. Army Engineer, Waterways Experiment Station, Vicksburg, MS.

WES, 1992. "Automated Coastal Engineering System ," ACES, Technical Reference by Leenknecht, D.A., Szuwalski, A. and Sherlock, A.R., Vicksburg, MS: Coastal Engineering Research Center, Waterways Experiment Station, CPD-66.

Zevenbergen, L.W., Hunt, J.H., Byars, M.S., Edge, B.L., Richardson, E.V., and Lagasse, P.F., 1997. "Tidal Hydraulic Modeling for Bridges Users Manual," Ayres Associates, Fort Collins, CO.

APPENDIX A
Tidal Waterway and ADCIRC Station Locations

APPENDIX A

State	Waterway Name	Map #	Lat.	Long.	Adcirc #	Adcir lat.	Adcirc long.	Difference (km)	ADCIRC results 50 year (m)	100 year (m)	500 year (m)	Lat.	Long.	WIS #
LOUISIANA														
	Sabine Pass	1	29.6875	93.8306	539	29.6873	93.7569	7.1	3.28	4.20	6.34	N29-41-15	W93-49-50	139
	Calcasieu Pass	1	29.7547	93.3408	537	29.7385	93 2562	8.4	3.33	4.08	5.82	N29-45-17	W93-20-27	141
	Vermilion,West &	2	29.5719	92.0489	532	29.4740	92.0983	11.9	2.32	2.82	3.98	N29-34-19	W92-2-56	146
	East Cote Blanche Bay	2	29.3642	91.6022	530	29.4228	91.7123	12.5	1.90	2.31	3.26	N29-21-51	W91-36-8	148
	Terrebonne, Timballer Bay	2	29.0397	90.5419	155	29.0000	90.5000	6.0	1.59	2.07	3.18	N29-2-23	W90-32-31	155
	Barataria Bay	3	29.2814	89.8808	521	29.2300	89.7500	13.9	1.61	2.10	3.24	N29-16-53	W89-52-51	158
	Lake Borgne	3	30.1161	89.4358	510	30.2287	89.2088	25.1	5.49	6.78	9.78	N30-6-58	W89-26-9	169
MISSISSIPPI														
	Pearl River	1	30.1719	89.5239	510	30.2287	89.2088	30.9	5.49	6.78	9.78	N30-10-19	W89-31-26	169
	Heron Bay	1	30.1736	89.4819	510	30.2287	89.2088	26.9	5.49	6.78	9.78	N30-10-25	W89-28-55	169
	St louis Bays	2	30.2933	89.3069	510	30 2287	89.2088	11.8	5.49	6.78	9.78	N30-17-36	W89-18-25	169
	Biloxi Bay	2	30.3461	88.7878	509	30.2799	88.8542	9.7	4.68	6.13	9.50	N30-20-46	W88-47-16	170
	Graveline Bay	2	30.3542	88.6619	508	30.1605	88.5204	25.4	2.53	3.29	5.05	N30-21-15	W88-39-43	171
	Pascagoula Bay	2	30.3439	88.6047	508	30.1605	88.5204	21.9	2.53	3.29	5.05	N30-20-38	W88-36-17	171
	Pascagoula River	2	30.3381	88.5669	508	30.1605	88.5204	20.2	2.53	3.29	5.05	N30-20-17	W88-34-1	171
	Bayou Casotte	2	30.3300	88.5169	508	30.1605	88.5204	18.8	2.53	3.29	5.05	N30-19-48	W88-31-1	171
	Point Aux Chenes Bay	2	30.3403	88.4286	508	30.1605	88.5204	21.8	2.53	3.29	5.05	N30-20-25	W88-25-43	171
FLORIDA														
	Pensacola Bay	1	30.3114	87.3072	502	30.3567	87.2582	6.9	1.79	2.13	2.92	N30-18-41	W87-18-26	177
(destin)	Choctawhatchee Bay	1	30.3819	86.5144	499	30.3567	86.5072	2.9	1.30	1.53	2.06	N30-22-55	W86-30-52	180
	West, N, E Bay	1	30.1172	85.7347	495	30.0495	85.6727	9.6	1.17	1.38	1.87	N30-7-2	W85-44-5	184
	(Panama city)	1	30.0656	85.6314	495	30.0495	85.6727	4.4	1.17	1.38	1.87	N30-3-56	W85-37-53	184
	St Joseph Bay	2	29.8808	85.3739	494	29.9216	85.5684	19.3	1.02	1.19	1.58	N29-52-51	W85-22-26	145
	Apalachicola Bay	2	29.6722	85.2281	491	29.6315	85.2763	6.5	1.54	1.89	2.70	N29-40-20	W85-13-41	188
		2	29.6197	85.1133	491	29.6315	85.2763	15.8	1.54	1.89	2.70	N29-37-11	W85-6-48	188
		2	29.7667	84.6767	488	29.6912	84.6504	8.8	2.03	2 56	3.79	N29-46-0	W84-40-36	190
	Ochlockonee Bay	3	29.9639	84.3319	486	29.9642	84.2540	7 5	2.98	3.71	5.41	N29-57-50	W84-19-55	193
	Dickerson Bay, Levy Bay	3	30.0133	84.3628	486	29.9642	84.2540	11.8	2.98	3.71	5.41	N30-0-48	W84-21-46	193
	Oyster Bay	3	30.0094	84.3592	486	29.9642	84.2540	11.3	2.98	3.71	5.41	N30-0-34	W84-21-33	193
		3	30.0394	84.3083	486	29.9642	84.2540	9.9	2.98	3.71	5.41	N30-2-22	W84-18-30	193
	Walker Creek	3	30.0539	84.2814	486	29.9642	84.2540	10.3	2.98	3.71	5.41	N30-3-14	W84-16-53	193
	Goose Creek Bay	3	30.0736	84.2494	486	29.9642	84.2540	12.2	2.98	3.71	5.41	N30-4-25	W84-14-58	193

State	Waterway Name	Map #	Lat.	Long.	Adcirc #	Adcir lat.	Adcirc long.	Difference (km)	ADCIRC results 50 year (m)	100 year (m)	500 year (m)	Lat.	Long.	WIS #
	St Marks River	3	30.0769	84.1992	486	29.9642	84.2540	13.6	2.98	3.71	5.41	N30-4-37	W84-11-57	193
	Aucilla River	3	30.0781	83.9947	485	29.9984	83.9724	9.1	3.50	4.21	5.86	N30-4-41	W83-59-41	194
	Henderson River		29.9714	83.7864	484	29.8362	83.6803	18.1	3.77	4.65	6.69	N29-58-17	W83-47-11	195
	Deadman Bay	4	29.6603	83.4242	483	29.6656	83.5238	9.6	3.80	5.01	7.82	N29-39-37	W83-25-27	197
	Suwannee River	4	29.2942	83.1753	480	29.2701	83.2025	3.8	3.45	4.60	7.27	N29-17-39	W83-10-31	199
	Waccasassa River	4	29.1414	82.8250	478	29.0227	82.8270	13.2	3.30	3.99	5.59	N29-8-29	W82-49-30	201
	Crystal Bay	4	28.8950	82.7128	477	28.7486	82.7436	16.5	2.58	3.06	4.17	N28-53-42	W82-42-46	202
	Homosassa Bay	4	28.7503	82.7000	477	28.7486	82.7436	4.2	2.58	3.06	4.17	N28-45-1	W82-42	202
	Chassahowitzka Bay	4	28.6956	82.6494	477	28.7486	82.7436	10.9	2.58	3.06	4.17	N28-41-44	W82-38-58	202
	Pithlachascotee River		28.2761	82.7494	475	28.2291	82.8583	11.9	2.28	2.71	3.71	N28-16-34	W82-44-58	204
	Anclote River	5	28.1781	82.8050	475	28.2291	82.8583	7.7	2.28	2.71	3.71	N28-10-41	W82-48-18	204
	Tampa Bay	5	27.5506	82.7639	208	27.5000	82.7500	5.8	2.78	3.54	5.30	N27-33-2-	W82-45-50	208
	Lemon Bay		26.8914	82.3478	467	26.8298	82.3576	6.9	3.09	4.00	6.11	N26-53-29	W82-20-52	211
	Charlotte Harbor		26.7092	82.2647	466	26.7104	82.2011	6.3	3.60	4.51	6.62	N26-42-33	W82-15-53	212
			26.6094	82.2289	466	26.7104	82.2011	11.5	3.66	4.51	6.48	N26-36-34	W82-13-44	212
			26.4469	81.9878	464	26.4288	82.0134	3.2	3.83	4.80	7.05	N26-26-49	W81-59-16	214
Sarasota Bay	Longboat Pass	5b	27.4428	82.6972	471	27.4954	82.6914	5.9	2.92	3.83	5.94	N27-26-34	W82-41-50	208
	New Pass	5b	27.3269	82.5942	470	27.2820	82.6080	5.2	3.05	4.00	6.21	N27-19-37	W82-35-39	209
	Big Sarasota Bay	5b	27.2906	82.5750	470	27.2820	82.6080	3.4	3.05	4.00	6.21	N27-17-26	W82-34-30	209
	Venice Inlet	5b	27.1119	82.4750	469	27.1455	82.5662	9.8	2.93	3.83	5.92	N27-6-43	W82-28-30	210
	Estero Bay		26.4706	81.9731	464	26.4288	82.0134	6.1	3.83	4.80	7.05	N26-28-14	W81-58-23	214
			26.3961	81.8942	463	26.2581	81.8882	15.3	3.67	4.60	6.76	N26-23-46	W81-53-39	216
	Gordon Pass	6	26.0931	81.8086	462	26.0448	81.8361	6.0	3.43	4.32	6.39	N26-5-35	W81-48-31	217
	Big Marco Pass	6	25.9700	81.7556	461	25.8998	81.8256	10.5	3.37	4.18	6.06	N25-58-12	W81-45-20	218
	Caxambas Bay	6	25.9000	81.7286	461	25.8998	81.8256	9.7	3.37	4.18	6.06	N25-54	W81-43-43	223
	First Bay	7	25.5411	81.2247	457	25.4390	81.2102	11.4	3.27	3.92	5.43	N25-32-28	W81-13-29	240
	Whitewater Bay	7	25.3564	81.1544	457	25.4390	81.2102	10.7	3.27	3.92	5.43	N25-21-23	W81-9-16	240
Water way	Biscayne Bay	7	25.6567	80.2161	443	25.7547	80.1566	12.4	1.00	1.21	1.70	N25-39-24	W80-12-58	
	Miami	7	25.7514	80.1311	443	25.7547	80.1566	2.6	1.00	1.21	1.70	N25-45-5	W80-7-52	
	Bakers Haulover Inlet	8	25.9000	80.1172	442	25.9936	80.0836	10.9	0.82	0.99	1.38	N25-54	W80-7-2	
	Turning Basin	8	26.0922	80.1028	442	25.9936	80.0836	11.1	0.82	0.99	1.38	N26-5-32	W80-6-10	
	Hillsboro Bay	8	26.2547	80.0806	441	26.2441	80.0648	2.0	0.77	0.91	1.24	N26-15-17	W80-4-50	
	Boca Raton Inlet	8	26.3364	80.0650	441	26.2441	80.0648	10.2	0.77	0.91	1.24	N26-20-11	W80-3-54	
	South Lake worth Inlet	9	26.5456	80.0361	440	26.4830	80.0231	7.1	0.77	0.90	1.20	N26-32-44	W80-2-10	
	Lake Worth Inlet	9	26.7728	80.0264	439	26.7560	80.0231	1.9	0.79	0.94	1.29	N26-46-22	W80-1-35	
	Loxahatchee River	9	26.9442	80.0653	438	27.0035	80.0544	6.7	0.76	0.94	1.36	N26-56-39	W80-3-55	
	St Lucie River	9	27.1644	80.1472	437	27.2338	80.1483	7.7	0.91	1.13	1.64	N27-9-52	W80-8-50	
	Fort Pierce Inlet	9	27.4731	80.2833	436	27.4813	80.2422	4.2	1.17	1.45	2.10	N27-28-23	W80-17	
	Sebastian Inlet	10	27.8608	80.4417	435	27.7202	80.3256	19.3	1.41	1.75	2.54	N27-51-39	W80-26-30	

State	Waterway Name	Map #	Lat.	Long.	Adcirc #	Adcir lat.	Adcirc long.	Difference (km)	ADCIRC results 50 year (m)	100 year (m)	500 year (m)	Lat.	Long.	WIS #
	Cape Canaveral	10	28.4092	80.5797	432	28.4710	80.4821	11.7	0.84	0.97	1.27	N28-24-33	W80-34-47	
	Ponce De Leon Inlet	11	29.0769	80.9111	430	28.9745	80.7846	16.7	0.95	1.10	1.45	N29-4-37	W80-54-40	
	Matanzas Inlet	11	29.7072	81.2208	427	29.7424	81.1914	4.8	2.12	2.46	3.25	N29-42-26	W81-13-15	
	St Augustine Inlet	11	29.9136	81.2797	426	29.9984	81.2749	9.4	2.17	2.51	3.30	N29-54-49	W81-16-47	
	St Johns River	12	30.4114	81.3944	424	30.5018	81.4105	10.2	2.58	3.02	4.04	N30-24-41	W81-23-40	
	Nassau Sound	12	30.5611	81.4147	424	29.9984	81.2749	63.9	2.17	2.51	3.30	N30-3-22	W81-24-53	
GEORGIA														
	St Marys River		30.7133	81.4375	423	30.7321	81.4418	2.1	3.06	3.60	4.85	N30-42-48	W81-26-15	
	St Andrew Sound	1	31.0003	81.4064	422	31.0052	81.4105	0.7	3.53	4.32	6.15	N31-0-1	W81-24-23	
	St Simons Sound	1	31.1197	81.3928	422	31.0052	81.4105	12.8	3.53	4.32	6.15	N31-7-11	W81-23-34	
	Hampton River	1	31.2181	81.2739	421	31.2612	81.2436	5.6	3.31	3.96	5.47	N31-13-5	W81-16-26	
	Altamaha River	1	31.3050	81.2489	421	31.2612	81.2436	4.9	3.31	3.96	5.47	N31-18-18	W81-14-56	
	Sapelo	1	31.3700	81.2664	421	31.2612	81.2436	12.3	3.31	3.96	5.47	N31-22-12	W81-15-59	
	Sapelo Sound	1	31.5358	81.1694	420	31.5171	81.1497	2.8	3.86	4.71	6.68	N31-32-9	W81-10-10	
	St catherines Sound	1	31.7111	81.1278	420	31.5171	81.1497	21.6	3.86	4.71	6.68	N31-42-40	W81-7-40	
	Ossabaw Sound	1	31.8328	81.0089	419	31.8840	80.8993	11.8	3.42	4.30	6.34	N31-49-58	W81-0-32	
	Wassaw Sound	1	31.9250	80.9150	419	31.8840	80.8993	4.8	3.42	4.30	6.34	N31-55-30	W80-54-54	
	Savannah River	1	32.0681	80.8208	419	31.8840	80.8993	21.7	3.42	4.30	6.34	N32-4-5	W80-49-15	
SOUTH CAROLINA														
	Calibogue Sound	1	32.0994	80.8339	419	31.8840	80.8993	24.7	3.42	4.30	6 34	N32-5-58	W80-50-2	
	Port Royal Sound	1	32.2350	80.6444	418	32.1763	80.6573	6.6	3.34	4.05	5 70	N32-14-6	W80-38-40	
	St Helena Sound	1	32.4347	80.3786	417	32.3213	80.4070	12 9	3.02	3.52	4.68	N32-26-5	W80-22-43	
	North Edisto River	1	32.5433	80.1892	416	32.5602	80.0836	10.1	3.06	3.64	4.99	N32-32-36	W80-11-21	
	Stono Inlet	1	32.6253	79.9778	416	32.5602	80.0836	12.3	3.06	3.64	4 99	N32-37-31	W79-58-40	
	Lighthouse Inlet	1	32.6919	79.8825	416	32.5602	80.0836	23.8	3.06	3.64	4.99	N32-41-31	W79-52-57	
	Charleston Harbor	1	32.7417	79.8514	415	32.8333	79.6351	22.6	2 92	3.59	5.15	N32-44-30	W79-51-5	
	Breach Inlet	1	32.7700	79.8089	415	32.8333	79.6351	17.7	2 92	3.59	5.15	N32-46-12	W79-48-32	
	Bulls Bay	1	32.9539	79.5136	415	32.8333	79.6351	17.5	2.92	3.59	5.15	N32- 57-14	W79-30-49	
	North Santee Bay	1	33.1272	79 2372	414	33.1063	79.2282	2.5	3.06	3.94	5.98	N33-7-38	W79-14-14	
	Winyah Bay	1	33.1972	79.1725	413	33.2599	79.1448	7.4	3.42	4.39	6.64	N33-11-50	W79-10-21	
	North Inlet	2	33.3256	79.1564	413	33.2599	79.1448	7 4	3.42	4.39	6.64	N33-19-32	W79-9-23	
	Pawleys Inlet	2	33.3975	79.1347	413	33.2599	79 1448	15.3	3.42	4.39	6.64	N33-23-51	W79-8-5	
	Midway Inlet	2	33 4486	79.1028	413	33.2599	79.1448	21.3	3.42	4.39	6.64	N33-26-55	W79-6-10	
	Murrells Inlet	3	33.5258	79.0311	412	33.6097	78.9153	14.2	3 24	4.16	6.30	N33-31-33	W79-1-52	
	Hog Inlet	4	33.8342	78.6003	411	33.8316	78.5398	5.6	3.24	4.02	5.83	N33-50-3	W78-36-1	
	Little River Inlet	4	33.8428	78.5469	411	33.8316	78.5398	1.4	3.24	4.02	5.83	N33-50-34	W78-32-49	

State	Waterway Name	Map #	Lat.	Long.	Adcirc #	Adcir lat.	Adcirc long.	Difference (km)	ADCIRC results 50 year (m)	100 year (m)	500 year (m)	Lat.	Long.	WIS #
NORTH CAROLINA														
	Tubbs Inlet	1	33.8678	78.4775	411	33.8316	78.5398	7.0	3.24	4.02	5.83	N33-52-4	W78-28-39	
	Shallotte Inlet	1	33.8947	78.3800	411	33.8316	78.5398	16.3	3.24	4.02	5.83	N33-53-41	W78-22-48	
	Lockwoods Folly Inlet	2	33.9075	78.2339	410	33.8486	78.0182	20.9	2.07	2.53	3.60	N33-54-27	W78-14-2	
	Cape Fear River	3	33.8722	78.0261	410	33.8486	78.0182	2.7	2.07	2.53	3.60	N33-52-20	W78-1-34	
	Carolina Beach Inlet	3	34.0778	77.8644	409	34.0534	77.8618	2.7	2.59	3.18	4.55	N34-4-40	W77-51-52	
	Masonboro Inlet	4	34.1814	77.8089	409	34.0534	77.8618	15.0	2.59	3.18	4.55	N34-10-53	W77-48-32	
	Mason Inlet	4	34.2442	77.7586	409	34.0534	77.8618	23.2	2.59	3.18	4.55	N34-14-39	W77-45-31	
	Rich Inlet	5	34.2950	77.7056	408	34.3776	77.5280	18.7	2.54	3.21	4.77	N34-17-42	W77-42-20	
	New Topsail Inlet	5	34.3397	77.6481	408	34.3776	77.5280	11.8	2.54	3.21	4.77	N34-20-23	W77-38-53	
	New River Inlet	6	34.5247	77.3347	407	34.5142	77.2880	4.4	2.67	3.39	5.06	N34-31-29	W77-20-5	
	White Oak River	6	34.6333	77.1081	406	34.6165	77.0586	4.9	2.75	3.48	5.18	N34-38-00	W77-6-29	
	Beaufort Inlet	7	34.6853	76.6731	404	34.6848	76.5683	9.6	2.42	3.11	4.71	N34-41-7	W76-40-23	
	Nelson Bay	7	34.8444	76.3950	403	34.8111	76.3200	7.8	1.98	2.45	3.54	N34-50-40	W76-23-42	
	Thorofare Bay		34.9114	76.2992	403	34.8111	76.3200	11.3	1.98	2.45	3.54	N34-54-41	W76-17-57	
	Cedar Bay	8	34.9653	76.2625	402	34.9305	76.1218	13.4	1.76	2.14	3.02	N34-57-55	W76-15-45	
	Stumpy Point Bay		35.6631	75.7286	397	35.7753	75.5064	23.6	1.80	2.37	3.69	N35-39-47	W75-43-43	
VIRGINIA														
	Chesapeake Bay	1	37.0056	75.9664	392	37.0978	75.9132	11.3	2.86	3.55	5.15	N37-0-20	W75-57-59	
	Metonplain Bay	1	37.6822	75.5831	389	37.7718	75.4542	15.1	2.24	2.73	3.87	N37-40-56	W75-34-59	
		1	37.6986	75.5647	389	37.7718	75.4542	12.7	2.24	2.73	3.87	N37-41-55	W75-33-53	
	Kegotank Bay	1	37.7919	75.5150	389	37.7718	75.4542	5.8	2.24	2.73	3.87	N37-47-31	W75-30-54	
	Chincoteague Bay	1	37.8689	75.4156	389	37.7718	75.4542	11.3	2.24	2.73	3.87	N37-52-8	W75-24-56	
MARYLAND														
	Chincoteague Bay	1	37.8689	75.4156	389	37.7718	75.4542	11.3	2.24	2.73	3.87	N37-52-8	W75-24-56	
	Ocean City Inlet (Assowoman Inlet)	2	38.3231	75.0794	386	38.2411	75.0787	9.1	1.57	2.05	3.16	N38-19-23	W75-4-46	
NEW JERSEY														
	Delaware Bay	1	38.8083	74.9917	298	38 7500	75.0000	6.5	1.68	2.21	3.44	N38-48-30	W74-59-30	
	Cape May Inlet	1	38.9353	74.8686	384	39.0091	74.7240	14.9	1.59	2.14	3.42	N38-56-7	W74-52-7	
	Hereford Inlet	1	39.0111	74.7775	384	39.0091	74.7240	4.6	1.59	2.14	3.42	N39-0-40	W74-46-39	
	Townsend Inlet	1	39.1189	74.7094	384	39.0091	74.7240	12.3	1.59	2.14	3.42	N39-7-8	W74-42-34	
	Corson Inlet	1	39.2106	74.6419	383	39.2906	74.4633	17.7	1.66	2.30	3.79	N39-12-38	W74-38-31	
	Great Egg Harbor Inlet	1	39.2950	74 5403	383	39.2906	74.4633	6.6	1.66	2.30	3.79	N39-17-42	W74-32-25	
	Absecon Inlet	1	39.3694	74.4014	383	39.2906	74.4633	10.2	1.66	2.30	3.79	N39-22-10	W74-24-5	
	Brigantine Inlet	1	39.4419	74.3192	382	39.4869	74.3277	5 0	1.81	2.48	4.04	N39-26-31	W74-19-9	

State	Waterway Name	Map #	Lat.	Long.	Adcirc #	Adcir lat.	Adcirc long.	Difference (km)	ADCIRC results 50 year (m)	100 year (m)	500 year (m)	Lat.	Long.	WIS #
	Little Egg Inlet	1	39.4939	74.2897	382	39.4869	74.3277	3.3	1.81	2.48	4 04	N39-29-38	W74-17-23	
	Barnegat Inlet	1	39.7614	74.0936	379	39.7497	74.0544	3.6	2 04	2.89	4.86	N39-45-41	W74-5-37	
	Manasquan Inlet	1	40.1008	74.0256	378	40.0056	74.0231	10.6	1.84	2.56	4.23	N40-6-3	W74-1-32	
	Shark River	1	40.1878	74.0033	377	40.2360	73.9396	7.6	1.86	2.60	4.32	N40-11-16	W74-0-12	
	Raritan Bay	2	40.4906	74.2606	305	40.5000	73.7500	43.1	1.95	2.74	4.57	N40-29-26	W74-15-38	
NEW YORK														
	Lower Bay	1	40.5092	73.9944	305	40.5000	73.7500	20.7	1.95	2.74	4.57	N40-30-33	W73-59-40	
	Upper NY Bay	1	40.5511	74.0442	305	40.5000	73.7500	25.5	1.95	2.74	4.57	N40-33-4	W74-2-39	
	Raritan Bay	1	40.4906	74.2606	305	40.5000	73.7500	43.1	1.95	2.74	4.57	N40-29-26	W74-15-38	
	Rockaway Inlet	1	40.5611	73.9639	376	40.5517	73.7519	17.9	2.11	2.90	4.73	N40-33-40	W73-57-50	
	East Rockaway Inlet	1	40.5844	73.7608	376	40.5517	73.7519	3.7	2.11	2.90	4.73	N40-35-4	W73-45-39	
	Jones Inlet	2	40 5792	73.5747	376	40.5517	73.7519	15.3	2.11	2 90	4.73	N40-34-45	W73-34-29	
	Great South Bay	2	40.6239	73.3225	374	40.6115	73.2616	5.3	2.48	3.69	6.50	N40-37-26	W73-19-21	
	Moriches Bay	2	40.7583	72.7542	372	40.7394	72.7400	2.4	2.05	2.90	4.87	N40-45-30	W72-45-15	
	Shinnecock Bay	2	40.8333	72.4758	371	40.8077	72.5001	3.5	2.02	2.74	4.41	N40-50-0	W72-28-33	
	Mecox Bay	2	40.8342	72.3256	370	40.8760	72 2706	6.5	1.85	2.45	3.84	N40-50-3	W72-19-32	
	Gardiners Bay	2	41.1717	72.1292	368	41 2761	71.7574	33.1	2.07	2.78	4.43	N41-10-18	W72-7-45	
	Smithtown Bay	1	40.9672	73.2717	368	41.2761	71.7574	131.2	2.07	2.78	4.43	N40-58-2	W73-16-18	
	Huntigton Bay	1	40 9606	73.4269	368	41.2761	71.7574	144.0	2.07	2.78	4 43	N40-57-38	W73-25-37	
	Oyster Bay	1	40.9297	73.5156	368	41.2761	71.7574	152.0	2.07	2.78	4 43	N40-55-47	W73-30-56	
	Sea Cliff	1	40.8781	73.6728	368	41.2761	71.7574	166.3	2.07	2.78	4.43	N40-52-41	W73-40-22	
	Manhasset Bay	1	40.8503	73.7494	368	41.2761	71.7574	173.3	2.07	2.78	4.43	N40-51-1	W73-44-58	
	Little Neck Bay	1	40.8086	73.7742	368	41.2761	71.7574	176.7	2.07	2.78	4.43	N40-48-31	W73-46-27	
	Little Bay	1	40.8039	73.7814	368	41.2761	71.7574	177.4	2.07	2.78	4.43	N40-48-14	W73-46-53	
	Eastchester Bay	1	40.8233	73.7906	368	41 2761	71.7574	177.5	2.07	2.78	4.43	N40-49-24	W73-47-26	
	Echo Bay	1	40.9028	73.7583	368	41.2761	71.7574	172.5	2.07	2.78	4.43	N40-54-10	W73-45-30	
	Larchmont Harbor	1	40.9144	73.7361	368	41.2761	71.7574	170.4	2.07	2.78	4.43	N40-54-52	W73-44-10	
	Mamaroneck Harbor	1	40.9300	73.7108	368	41.2761	71.7574	167.9	2.07	2.78	4.43	N40-55-48	W73-42-39	
CONNECTICUT						Connecticut values were obtained from FEMA reports for 100 and 500 year events.								
	Greenwich Harbor	1	41.0011	73.6164	368	41.2761	71.7574	158.4	3.47	3.66	4.21	N41-0-4	W73-36-59	
	Cos Cob Harbor	1	40.9944	73.6189	368	41.2761	71.7574	158.8	3.41	3.60	4.08	N40-59-40	W73-37-8	
	Stamford Harbor	1	41.0111	73.5428	368	41.2761	71.7574	152.2	3.35	3.51	3.90	N41-0-40	W73-32-34	
	Cove Harbor, Goodwives River	2	41.0300	73.4889	368	41.2761	71.7574	147.3	3.32	3.47	3.84	N41-1-48	W73-29-20	
	Scott Cove	2	41.0469	73.4603	368	41.2761	71.7574	144.6	3.32	3 47	3.84	N41-2-49	W73-27-37	
	Fivemile River	2	41.0503	73.4458	368	41.2761	71.7574	143.3	3.32	3.47	3.84	N41-3-1	W73-26-45	
	Norwalk Harbor	2	41.0739	73.3942	368	41.2761	71.7574	138.6	3.26	3.41	3.78	N41-4-26	W73-23-39	
	Saugatuck River	3	41.0939	73.3567	368	41.2761	71.7574	135.2	3.20	3.35	3.75	N41-5-38	W73-21-24	

State	Waterway Name	Map #	Lat.	Long.	Adcirc #	Adcir lat.	Adcirc long.	Difference (km)	ADCIRC results 50 year (m)	100 year (m)	500 year (m)	Lat.	Long.	WIS #
	Mill River	3	41.1194	73.2875	368	41.2761	71.7574	129.0	3.17	3.35	3.72	N41-7-10	W73-17-15	
	Black Rock Harbor	4	41.1347	73.2211	368	41.2761	71.7574	123.3	3.11	3.32	3.69	N41-8-5	W73-13-16	
	Pequonnock River	4	41.1536	73.1781	368	41.2761	71.7574	119.4	2.96	3.17	3.47	N41-9-13	W73-10-41	
	Housatonic River	4	41.1664	73.0986	368	41.2761	71.7574	112.7	2.93	3.11	3.47	N41-9-59	W73-5-55	
	The Gulf		41.1942	73.0497	368	41.2761	71.7574	108.3	2.99	3.17	3.66	N41-11-39	W73-2-59	
	New Haven Harbor	5	41.2439	72.9258	368	41.2761	71.7574	97.6	3.05	3.23	3.75	N41-14-38	W72-55-33	
	Branford Harbor	5	41.2431	72.8269	368	41.2761	71.7574	89.3	3.05	3.23	3.78	N41-14-35	W72-49-37	
	Clinton Harbor	6	41.2475	72.5231	368	41.2761	71.7574	64.0	2.90	3.17	3.78	N41-14-51	W72-31-23	
	Patchoguee River	6	41.2636	72.4725	368	41.2761	71.7574	59.7	2.90	3.17	3.78	N41-15-49	W72-28-21	
	Oyster River	6	41.2722	72.4031	368	41.2761	71.7574	53.9	2.87	3.17	3.78	N41-16-20	W72-24-11	
	Connecticut River	7	41.2678	72.3281	368	41.2761	71.7574	47.6	2.83	3.14	3.78	N41-16-4	W72-19-41	
	Niantic Bay	7	41.2850	72.1758	368	41.2761	71.7574	34.9	2.77	3.08	3.78	N41-17-6	W72-10-33	
	New London Harbor	7	41.3031	72.0797	368	41.2761	71.7574	27.1	2.74	3.05	3.78	N41-18-11	W72-4-47	
	Poquonock River	7	41.3100	72.0578	368	41.2761	71.7574	25.3	2.87	3.17	3.78	N41-18-36	W72-3-28	
	Mystic River	7	41.3144	71.9639	368	41.2761	71.7574	17.7	2.90	3.23	3.81	N41-18-52	W71-57-50	
	Stonington Harbor	7	41.3222	71.9131	368	41.2761	71.7574	14.0	2.93	3.29	3.84	N41-19-20	W71-54-47	
	Little Narragansett Bay	7	41.3153	71.9028	368	41.2761	71.7574	12.9	2.93	3.29	3.84	N41-18-55	W71-54-10	
MAINE														
	Portsmouth River	1	43.0497	70.6939	352	43.0082	70.6830	4.7	0.77	0.97	1.43	N43-2-59	W70-41-38	
	Brave Boat Harbor	1	43.0994	70.6483	352	43.0082	70.6830	10.5	0.77	0.97	1.43	N43-5-58	W70-38-54	
	York River	1	43.1267	70.6217	352	43.0082	70.6830	14.1	0.77	0.97	1.43	N43-7-36	W70-37-18	
	Cape Neddick Harbor	1	43.1822	70.5939	330	43.2500	70.5000	10.7	0.99	0.78	0.29	N43-10-56	W70-35-38	
	Webhannet River		43.3189	70.5506	330	43.2500	70.5000	8.7	0.99	0.78	0.29	N43-19-8	W70-33-2	
	Mousam River		43.3383	70.5158	351	43.3154	70.4639	4.9	0.82	1.03	1.52	N43-20-18	W70-30-57	
	Kennebunk River		43.3378	70.4786	351	43.3154	70.4639	2.8	0.82	1.03	1.52	N43-20-16	W70-28-43	
	Saco River		43.4619	70.3675	350	43.5116	70.2866	8.5	0.88	1.09	1.58	N43-27-43	W70-22-3	
	Scarborough River		43.5247	70.3333	350	43.5116	70.2866	4.0	0.88	1.09	1.58	N43-31-29	W70-20	
	Spurwink River		43.5475	70.2753	350	43.5116	70.2866	4.1	0.88	1.09	1.58	N43-32-51	W70-16-31	
	Casco Bay	2	43.6203	69.9958	349	43.6823	69.8631	12.7	0.71	0.86	1.21	N43-37-13	W69-59-45	
	Sheepscott Bay	2	43.7739	69.6903	348	43.8273	69.5606	12.0	0.69	0.87	1.29	N43-46-26	W69-41-25	
	Linekin Bay	2	43.7964	69.6194	348	43.8273	69.5606	5.8	0.69	0.87	1.29	N43-47-47	W69-37-10	
	Johns Bay	2	43.8281	69.5328	348	43.8273	69.5606	2.2	0.69	0.87	1.29	N43-49-41	W69-31-58	
	Muscongus Bay	2	43.8719	69.3581	348	43.8273	69.5606	17.0	0.69	0.87	1.29	N43-52-19	W69-21-29	
	Penobscot Bay	3	43.9928	68.8633	335	44.0000	68.5000	29.0	0.52	0.65	0.95	N43-59-34	W68-51-48	
	Blue hill Bay	3	44.0375	68.4231	335	44.0000	68.5000	7.4	0.52	0.65	0.95	N44-2-15	W68-25-23	
	Frenchman Bay	3	44.2917	68.1208	345	44.3393	68.0794	6.2	0.74	1.00	1.60	N44-17-30	W68-7-15	
	Gouldsboro, Dyer Bay	3	44.3917	67.9325	345	44.3393	68.0794	13.0	0.74	1.00	1.60	N44-23-30	W67-55-57	

State	Waterway Name	Map #	Lat.	Long.	Adcirc #	Adcir lat.	Adcirc long.	Difference (km)	ADCIRC results 50 year (m)	100 year (m)	500 year (m)	Lat.	Long.	WIS #
	Narraguagus, Pleasant	3	44.4756	67.7789	344	44.4673	67.6517	10.1	0.60	0.79	1.23	N44-28-32	W67-46-44	
	Western Bay	3	44.4908	67.6531	344	44.4673	67.6517	2.6	0.60	0.79	1.23	N44-29-27	W67-39-11	
	Chandler, Englishman Bay	3	44.5314	67.5244	344	44.4673	67.6517	12.3	0.60	0.79	1.23	N44-31-53	W67-31-28	
		3	44.5658	67.4358	344	44.4673	67.6517	20.3	0.60	0.79	1.23	N44-33-57	W67-26-9	
	Machias Bay	3	44.5903	67.3522	343	44.6209	67.1197	18.7	0.66	0.85	1.29	N44-35-25	W67-21-8	
Cheasapeake Bay														
	Entrance to Bay	1	37.0978	75.9132	1	37.0978	75.9132		2.17	2.68	3.86			
	Entrance to Bay	1	36.7394	75.8923	2	36.7394	75.8923		1.92	2.38	3.45			
	Ocean City	7	38.3267	75.0833	3	38.3267	75 0833		1.52	1.98	3.05			
	Near Wachapreague	7	37.6067	75.6867	4	37.6067	75.6867		1.96	2.44	3.55			
	Bay Tunnel	1	36.9667	76.1133	5	36.9667	76.1133		1.97	2.46	3.60			
	Mouth of James River	1	36.9467	76.3300	6	36.9467	76.3300		2.46	3.08	4.52			
	York River	1	37.2467	76.5000	7	37 2467	76.5000		1.31	1.61	2 31			
	Potomac River	2	37.9967	76.4633	8	37 9967	76.4633		1.36	1.68	2 42			
	Coles Point, Potomac	3	38.1333	76.5333	9	38.1333	76.5333		1.1	1.36	1.96			
	Lexington Park	3	38.3167	76.4533	10	38.3167	76.4533		1.12	1.46	2 25			
	Severn River	5	38.9833	76.4800	11	38.9833	76.4800		1.39	1.90	3.08			
	Dundalk	5	39.2667	76.5783	12	39.2667	76.5783		3.45	4.58	7.20			
	NA	6	39.5367	76.0900	13	39.5367	76.0900		NA	NA	NA			
	NA	6	39.5267	75.8100	14	39.5267	75.8100		NA	NA	NA			
	Cambridge, MD	4	38.5750	76.0717	15	38.5750	76.0717		1 42	1.73	2.45			
	Cape Charles	1	37.1667	75.9883	16	37.1667	75.9883		1.64	2.08	3.10			
	Near Chincoteague	7	38.0333	75.3667	17	38 0333	75.3667		0.96	1.19	1.72			
	NA	2	37.9833	75.8667	18	37.9833	75.8667		NA	NA	NA			
	Chesapeake Bay	3	38.2500	76.2500	19	38.2500	76.2500		1.27	1.58	2.30			
	James River	1	36.9332	76.4423	20	36.9332	76.4423		0.98	1 20	1.71			
	Mouth of Rappahanoc	2	37.5871	76.2869	21	37.5871	76.2869		1.63	2.00	2.86			
	Mouth of Potomac	2	37.9923	76.2995	22	37.9923	76.2995		1.05	1.31	1.91			
	Potomac River	NA	38.3659	77.2629	23	38.3659	77.2629		1.07	1.33	1.93			
	Mouth of Severn	5	38.9587	76.4512	24	38.9587	76.4512		1.07	1.43	2 27			
	Chesapeake Bay	5	39.1447	76.4124	25	39.1447	76.4124		1.28	1.68	2.61			
	Chesapeake Bay	6	39.3237	76.2207	26	39.3237	76.2207		1.40	1.76	2 60			
	Entrance to C&D Canal	6	39.4858	75.9397	27	39.4858	75.9397		1.07	1.37	2 07			
	Susquehanna	6	39.5344	76.0734	28	39.5344	76.0734		1.01	1.26	1.84			
	Chesapeake Bay	5	39.0916	76.2925	29	39.0916	76.2925		0.93	1.19	1.79			
	Eastern Bay	5	38.8040	76.3542	30	38.8040	76.3542		0.71	0.86	1.21			
	Tred Avon River	4	38.6365	76.3289	31	38.6365	76.3289		0.64	0.79	1.14			
	Holland Straits	3	38.2057	75.9883	32	38.2057	75.9883		1.00	1.21	1.70			

State	Waterway Name	Map #	Lat.	Long.	Adcirc #	Adcir lat.	Adcirc long.	Difference (km)	ADCIRC results			Lat.	Long.	WIS #
									50 year (m)	100 year (m)	500 year (m)			
	Tangier Sound	3	38.0820	75.9429	33	38.0820	75.9429		0 92	1.11	1.55			
	Pocomoke Sound	2	37.8615	75.8351	34	37.8615	75.8351		1.79	2.25	3.32			
	Chesapeake Bay	2	37.7071	76.0831	35	37.7071	76.0831		1.73	2.08	2.89			
	Mouth of Bay	1	37.0908	76.1344	36	37.0908	76.1344		0 99	1.16	1.55			
	Paramore Island	7	37.5526	75.5469	37	37.5526	75.5469		1.46	1.90	2.92			
	Chincoteague	7	38.0287	75.3160	38	38 0287	75.3160		NA	NA	NA			
	Ocean City	7	38.3243	75.0072	39	38.3243	75.0072		NA	NA	NA			

APPENDIX B
Tidal Waterway Maps

LOUISIANA - 1

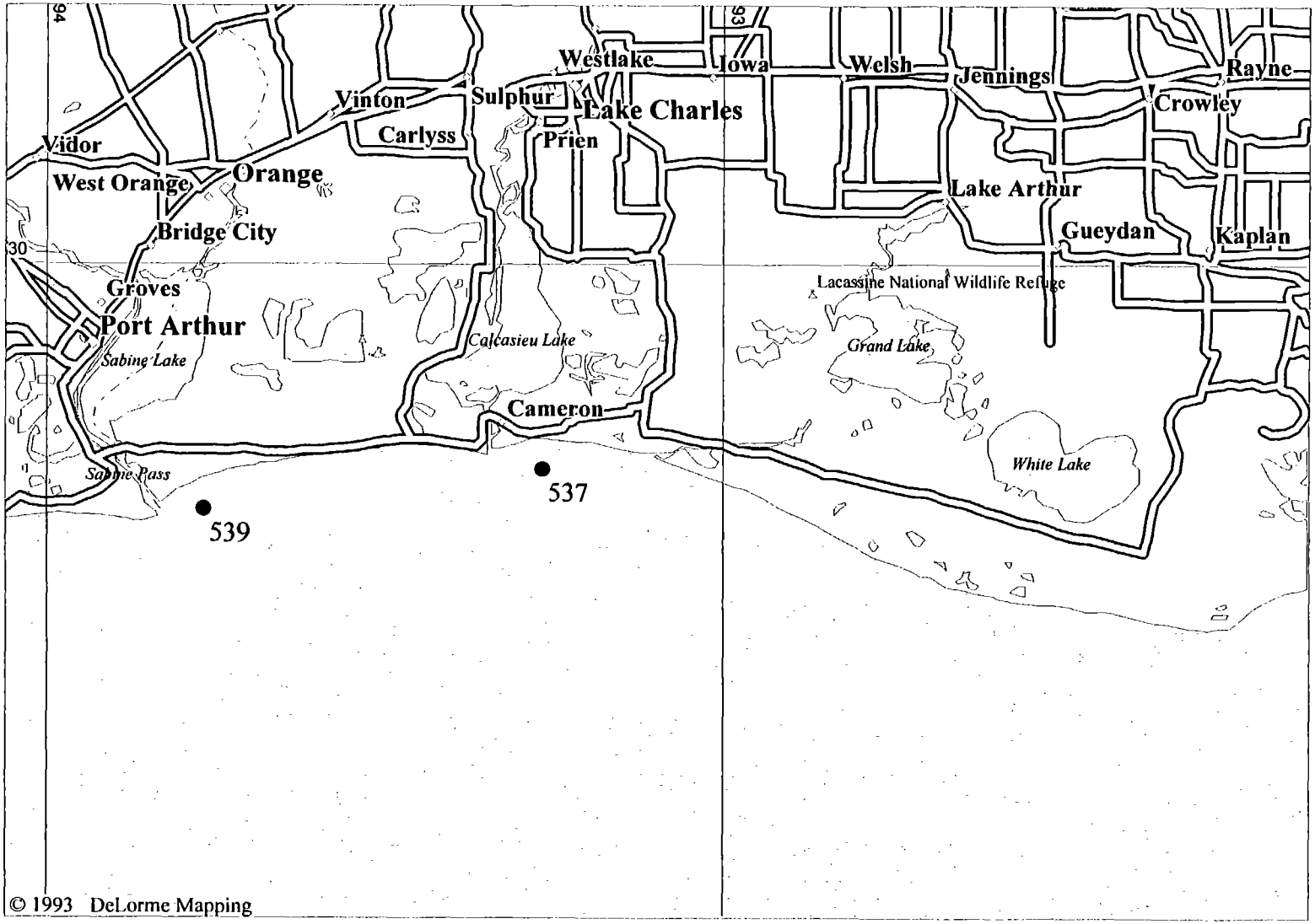
94
93
30
Westlake
Iowa
Welsh
Jennings
Rayne
Crowley
Vinton
Sulphur
Lake Charles
Carlyss
Prien
Vidor
West Orange
Orange
Bridge City
Lake Arthur
Gueydan
Kaplan
Groves
Port Arthur
Sabine Lake
Lacassine National Wildlife Refuge
Calcasieu Lake
Grand Lake
Cameron
Sabine Pass
White Lake
537
539
© 1993 DeLorme Mapping

LOUISIANA - 2

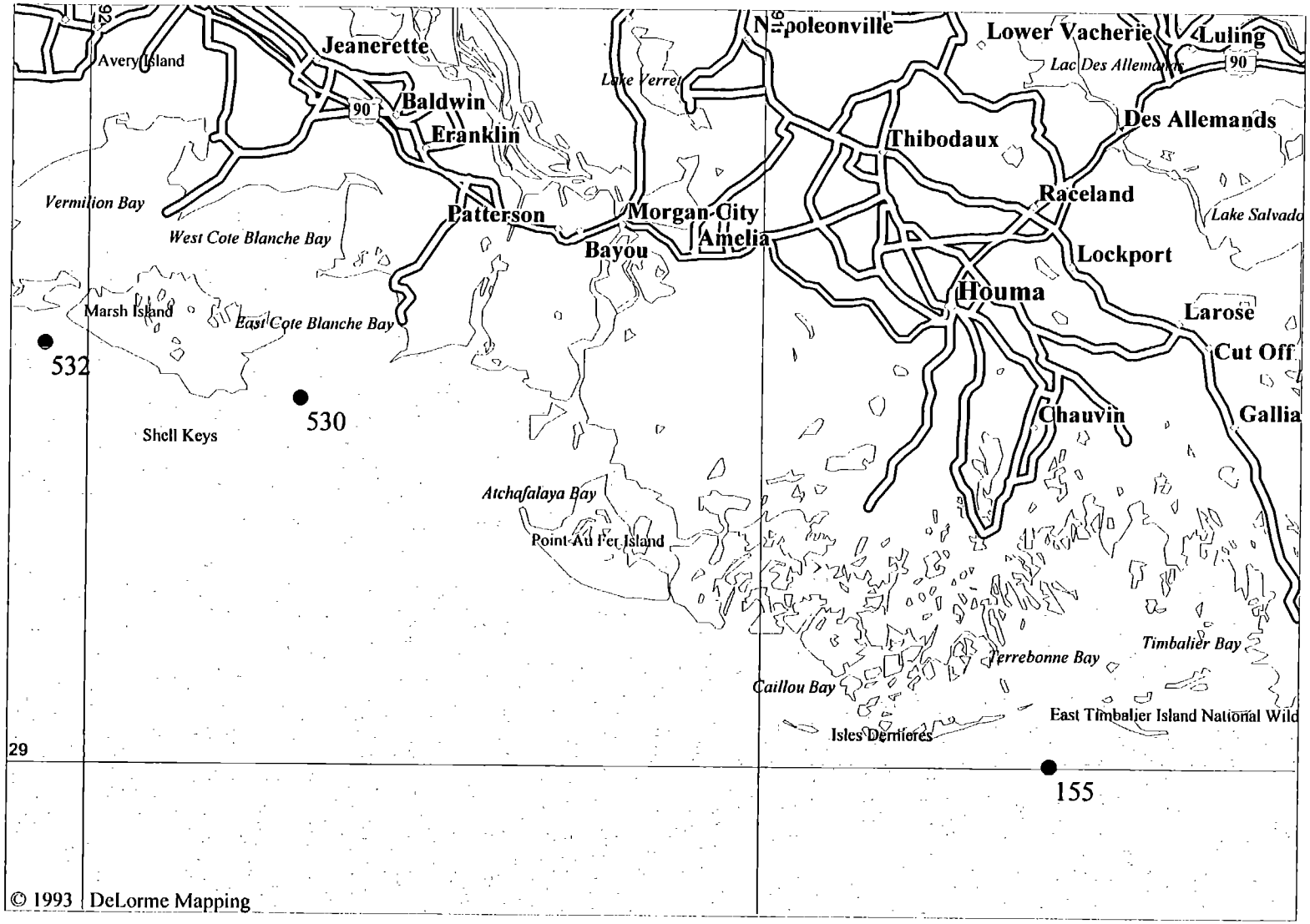
Jeanerette
Avery Island
Baldwin
Franklin
Lake Verret
Napoleonville
Lower Vacherie
Luling
Lac Des Allemands
Des Allemands
Thibodaux
Raceland
Lake Salvado
Vermilion Bay
West Cote Blanche Bay
Patterson
Morgan City
Amelia
Bayou
Lockport
Houma
Larose
Cut Off
Marsh Island
East Cote Blanche Bay
532
530
Shell Keys
Chauvin
Gallia
Atchafalaya Bay
Point Au Fer Island
Timbalier Bay
Terrebonne Bay
Caillou Bay
East Timbalier Island National Wild
Isles Dernieres
29
155
© 1993 DeLorme Mapping

LOUISIANA - 3

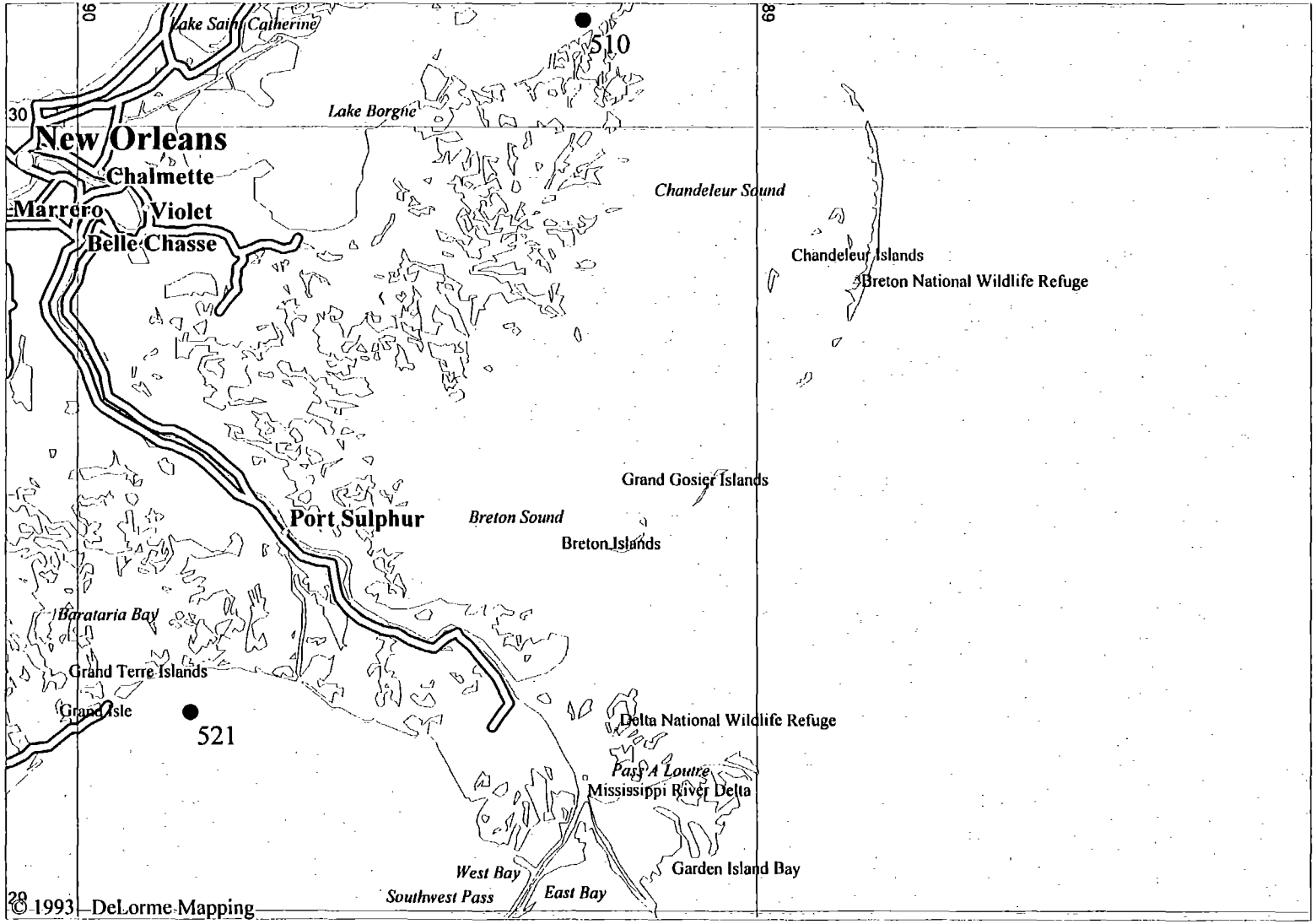
90
89
30
28
Lake Saint Catherine
510
Lake Borgne
New Orleans
Chalmette
Marrero
Violet
Belle Chasse
Chandeleur Sound
Chandeleur Islands
Breton National Wildlife Refuge
Grand Gosier Islands
Port Sulphur
Breton Sound
Breton Islands
Barataria Bay
Grand Terre Islands
Grand Isle
521
Delta National Wildlife Refuge
Pass A Loutre
Mississippi River Delta
Garden Island Bay
West Bay
Southwest Pass
East Bay
© 1993 DeLorme Mapping

MISSISSIPPI - 1

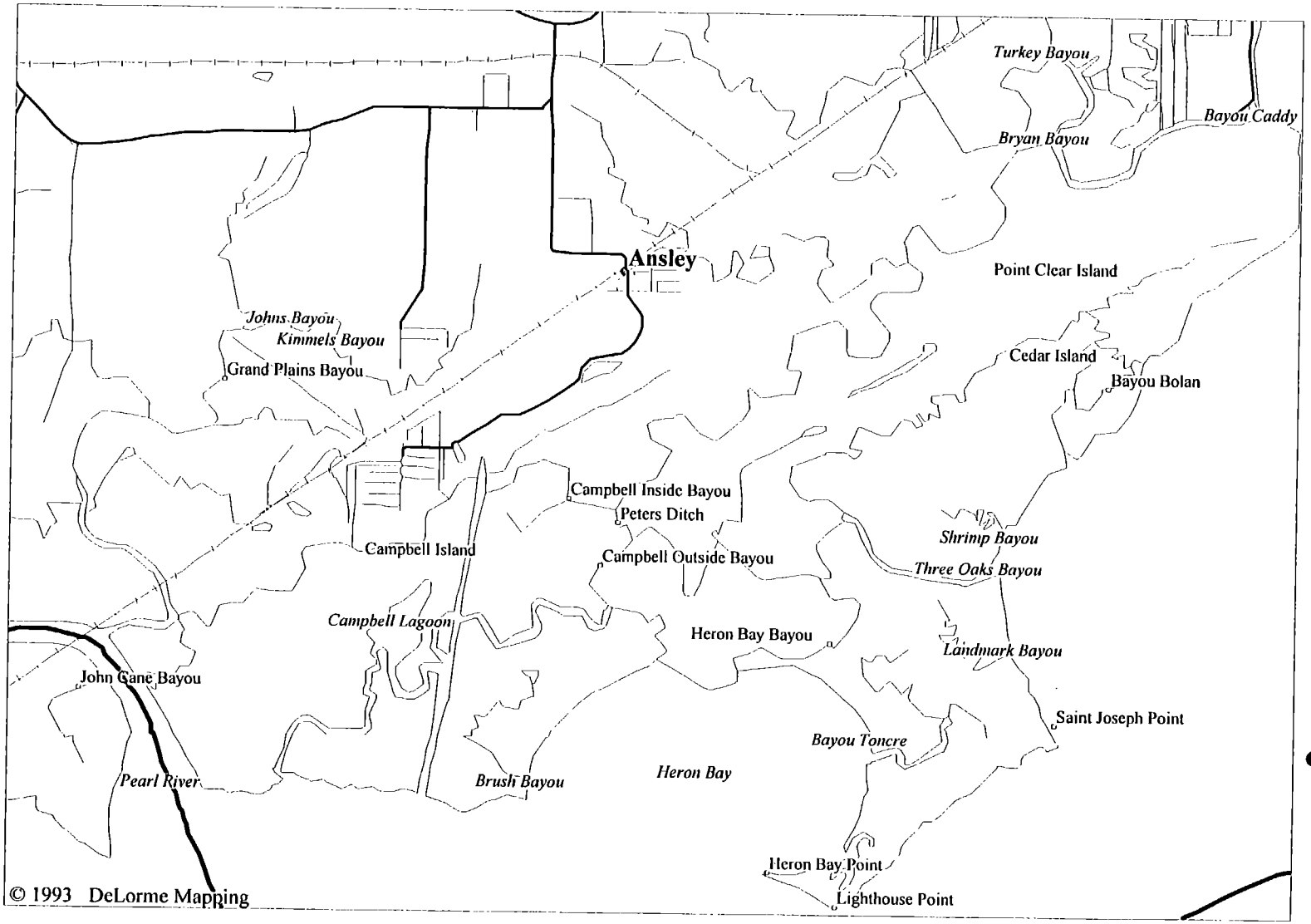

MISSISSIPPI- 2

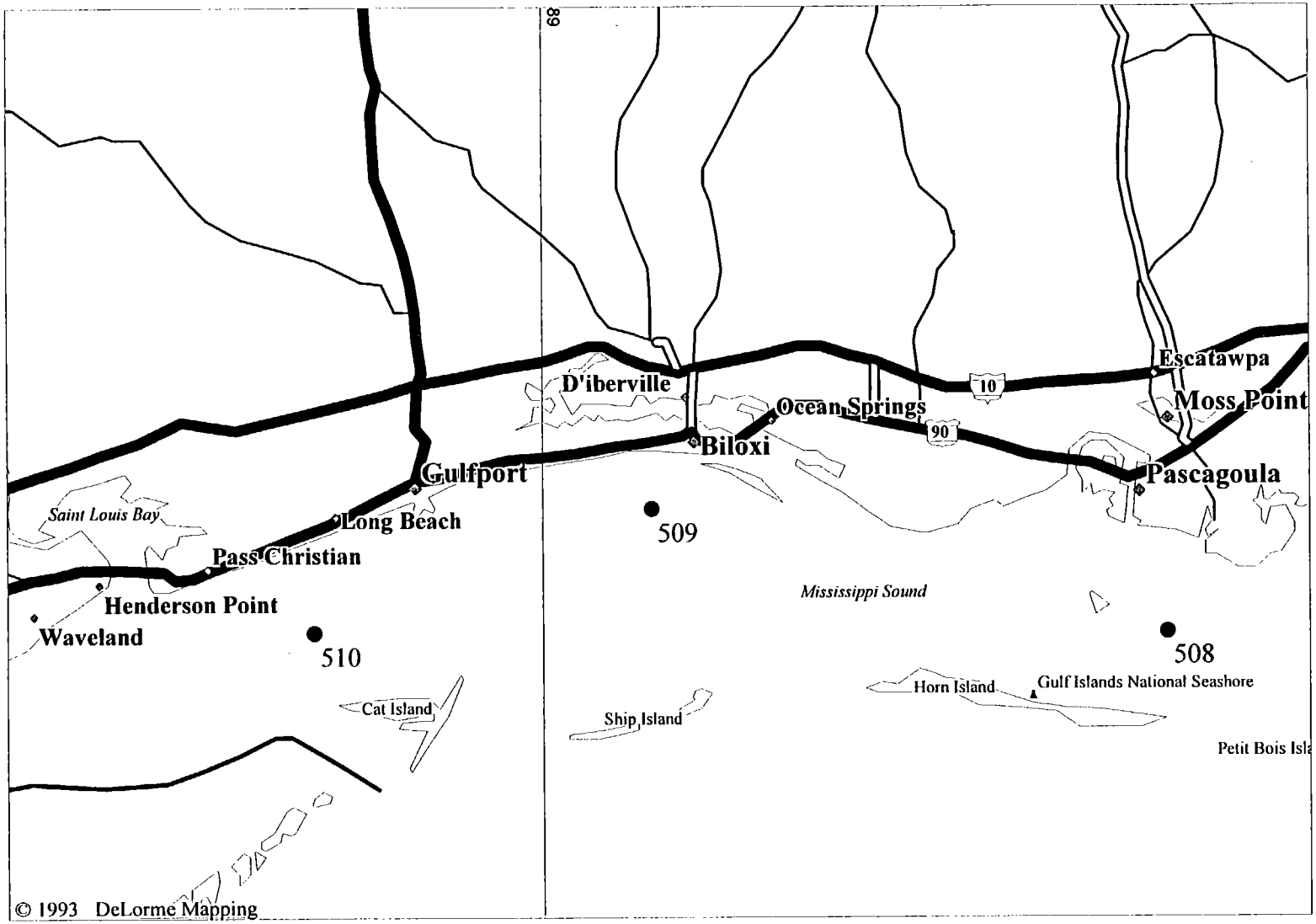

ALABAMA- 1

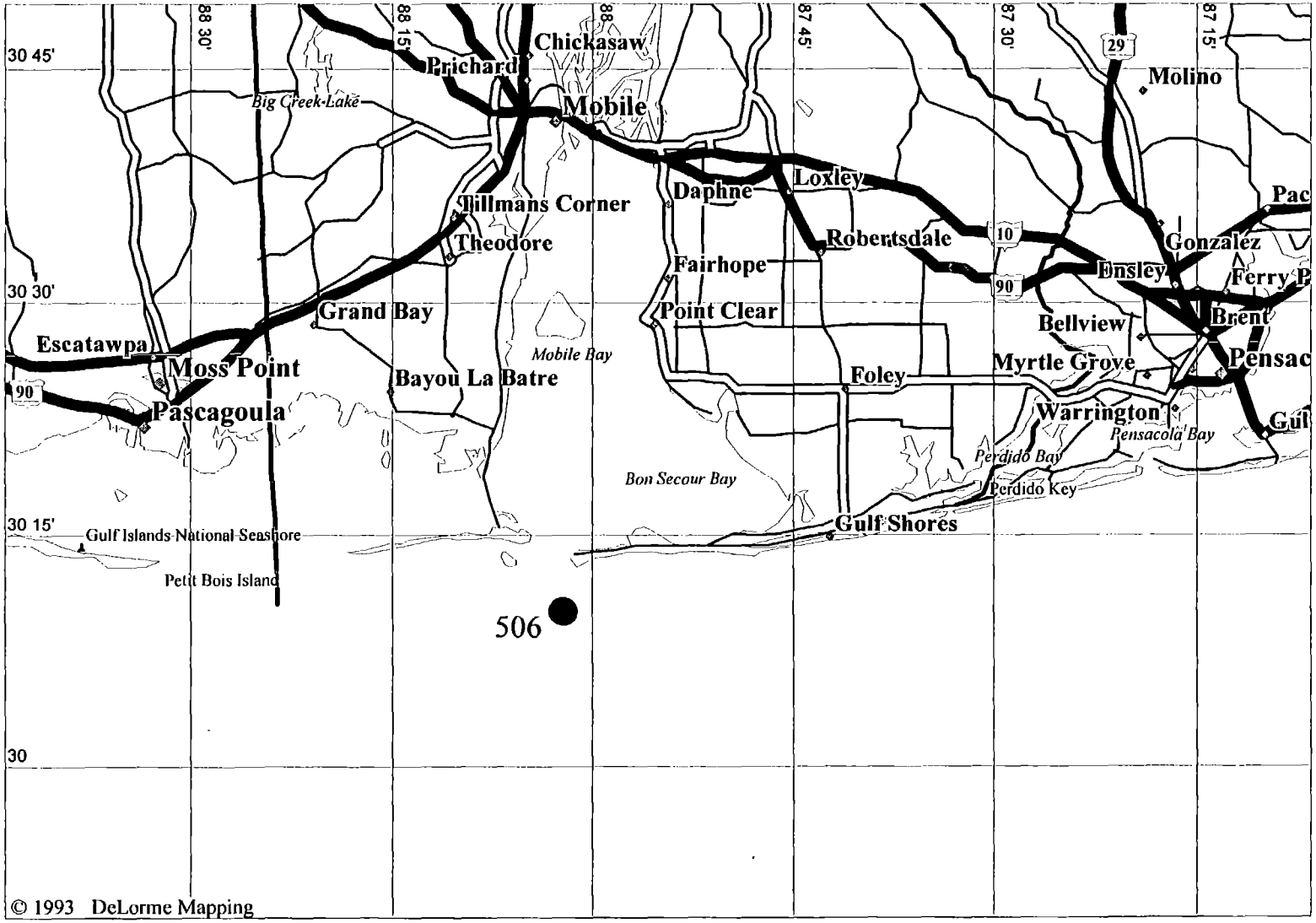
30 45'
30 30'
30 15'
30
88 30'
88 15'
88
87 45'
87 30'
87 15'
29
10
90
90
Chickasaw
Prichard
Mobile
Big Creek-Lake
Molino
Daphne
Loxley
Tillmans Corner
Theodore
Robertsdale
Fairhope
Point Clear
Grand Bay
Escatawpa
Moss Point
Pascagoula
Bayou La Batre
Mobile Bay
Foley
Bellview
Myrtle Grove
Gonzalez
Ensley
Ferry P
Brent
Pensac
Warrington
Pensacola Bay
Perdido Bay
Perdido Key
Bon Secour Bay
Gulf Shores
Gulf Islands National Seashore
Petit Bois Island
506
© 1993 DeLorme Mapping

FLORIDA - 1

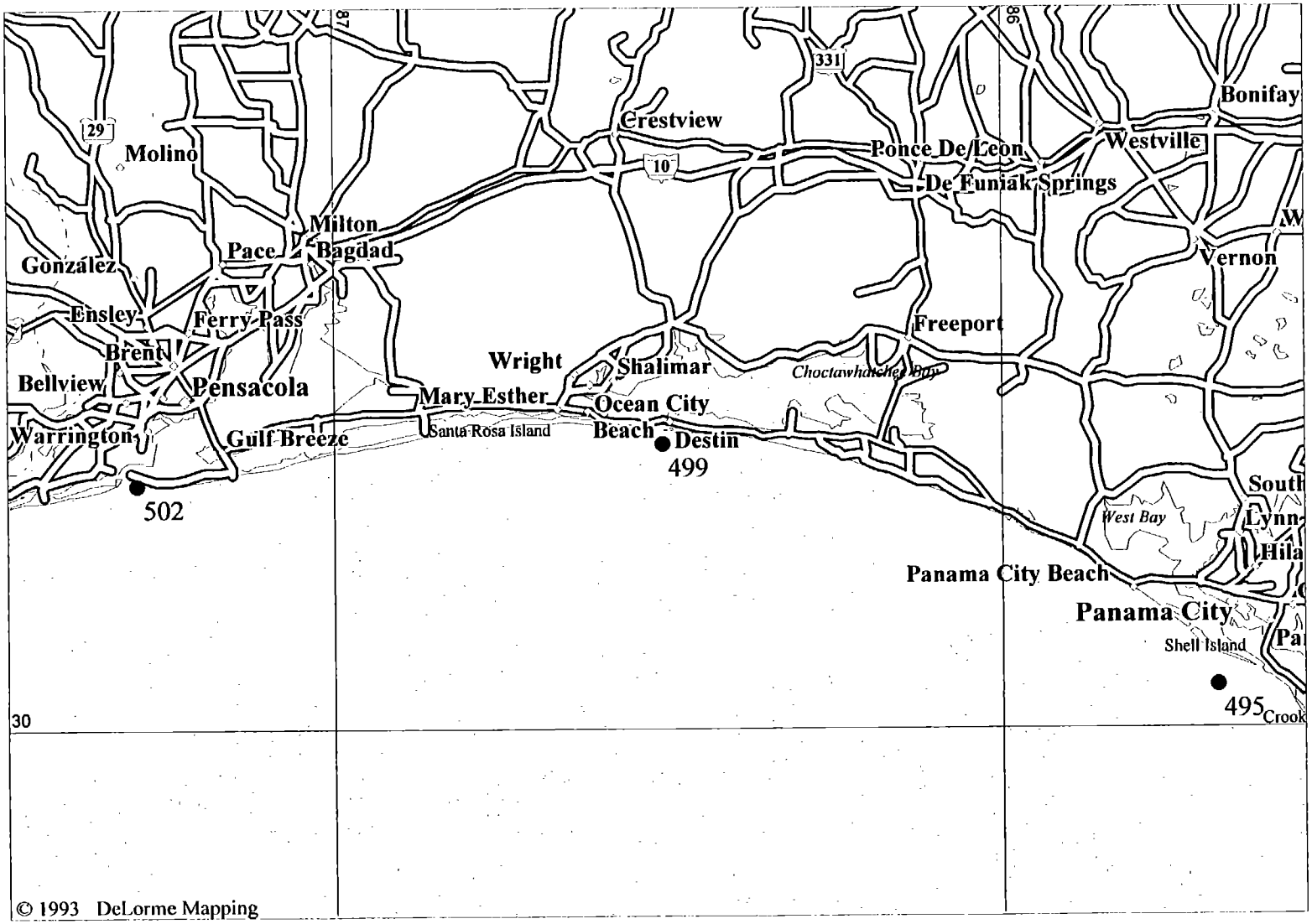
87
331
98
29
10
Molino
Crestview
Ponce De Leon
Westville
Bonifay
De Funiak Springs
Milton
Pace
Bagdad
Gonzalez
Vernon
Ensley
Ferry Pass
Freeport
Brent
Wright
Shalimar
Choctawhatchee Bay
Bellview
Pensacola
Mary Esther
Ocean City
Beach
Destin
499
Santa Rosa Island
Warrington
Gulf Breeze
502
West Bay
Panama City Beach
Panama City
Shell Island
495
30
© 1993 DeLorme Mapping

FLORIDA - 2

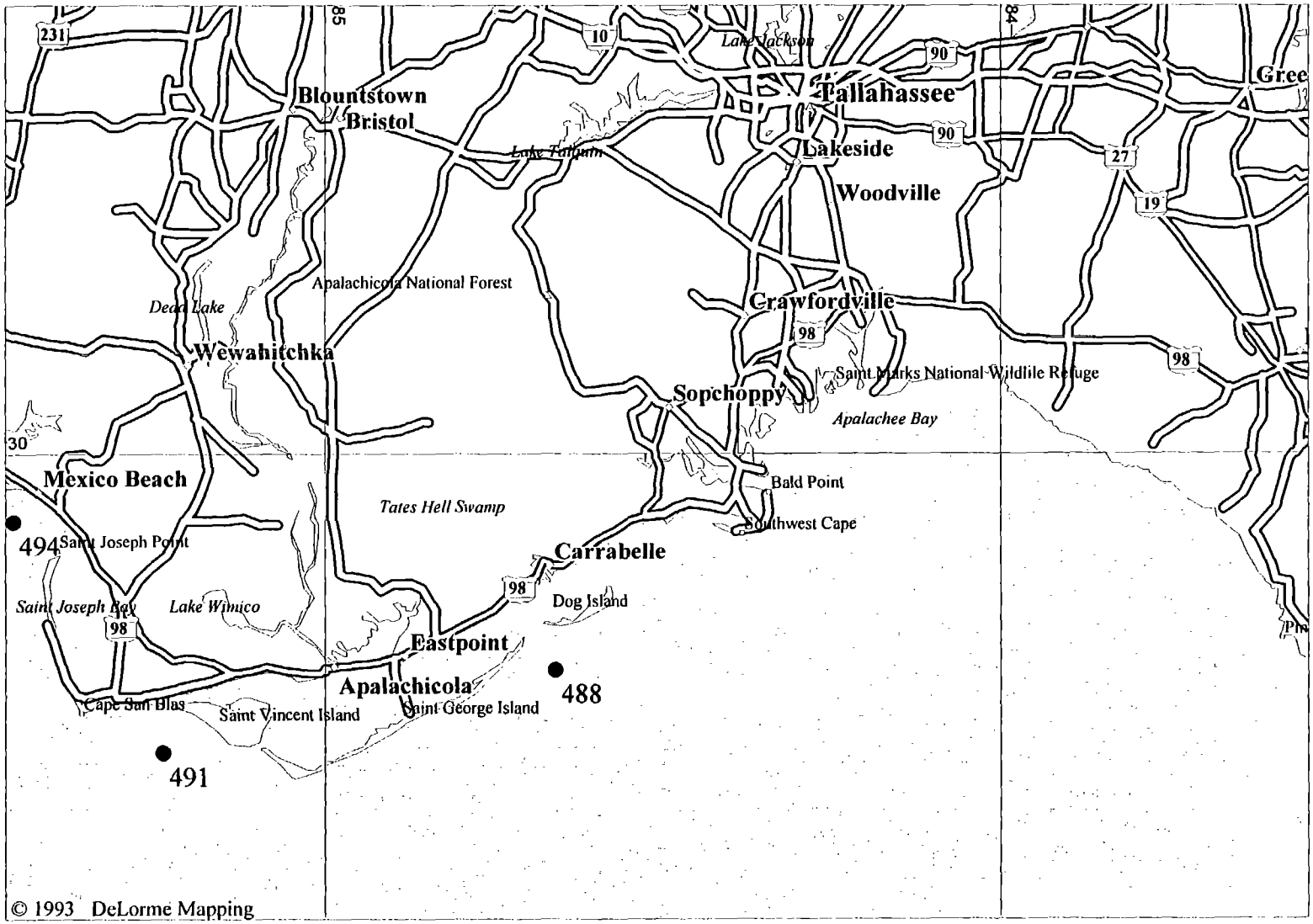
231
85
10
Lake Jackson
90
Tallahassee
Gree
Blountstown
Bristol
Lake Talquin
Lakeside
90
27
Woodville
19
Apalachicola National Forest
Dead Lake
Crawfordville
98
Wewahitchka
98
Saint Marks National Wildlife Refuge
Sopchoppy
Apalachee Bay
30
Mexico Beach
Bald Point
Tates Hell Swamp
Southwest Cape
494
Saint Joseph Point
Carrabelle
98
Dog Island
Saint Joseph Bay
Lake Wimico
98
Eastpoint
Apalachicola
488
Cape San Blas
Saint Vincent Island
Saint George Island
491
© 1993 DeLorme Mapping

FLORIDA - 3

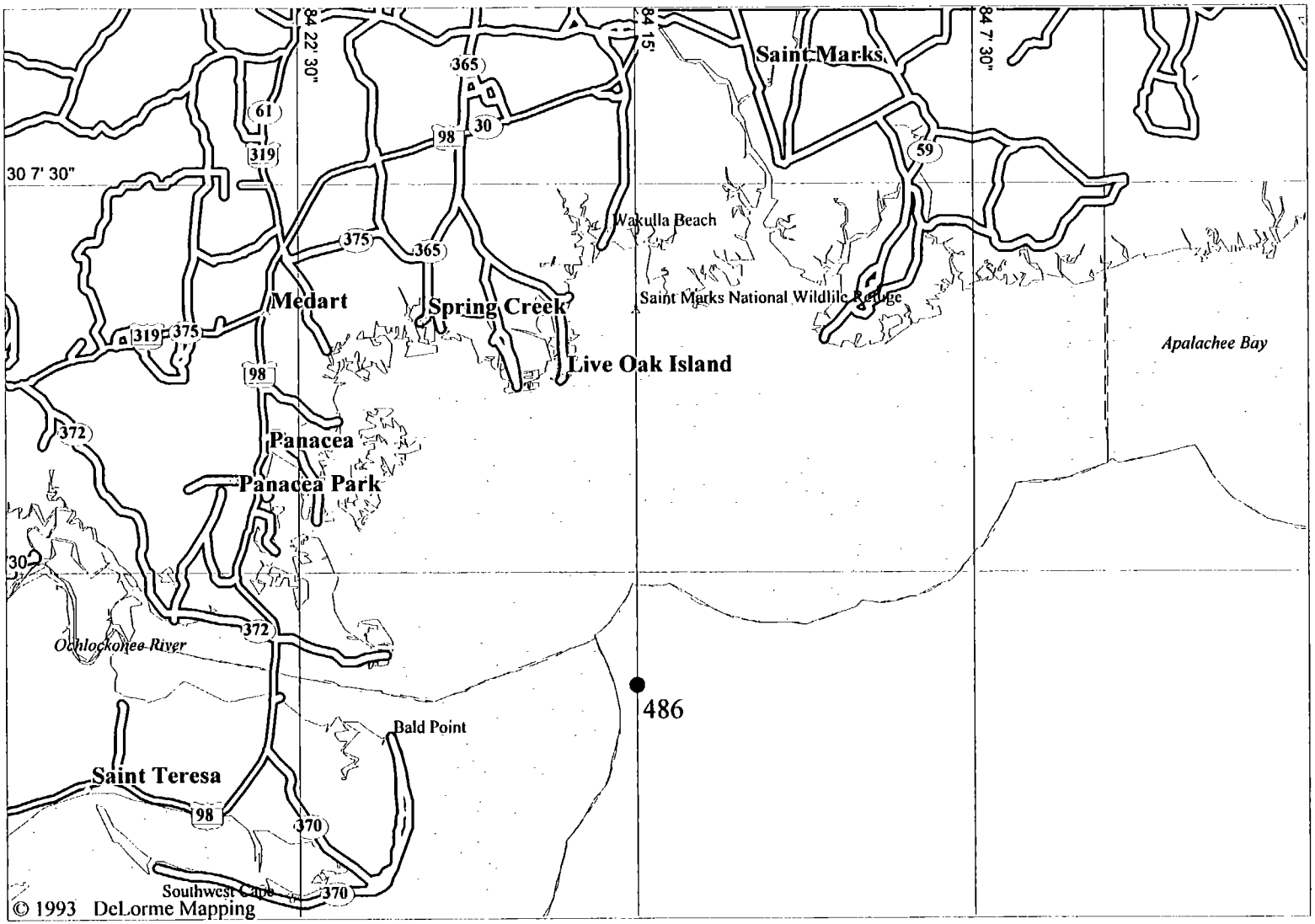
84 22' 30"
84 15'
84 7' 30"
30 7' 30"
Saint Marks
Wakulla Beach
Saint Marks National Wildlife Refuge
Apalachee Bay
Medart
Spring Creek
Live Oak Island
Panacea
Panacea Park
Ochlockonee River
Bald Point
Saint Teresa
Southwest Cape
© 1993 DeLorme Mapping
61
319
365
98
30
59
375
372
370
485
486

FLORIDA - 4

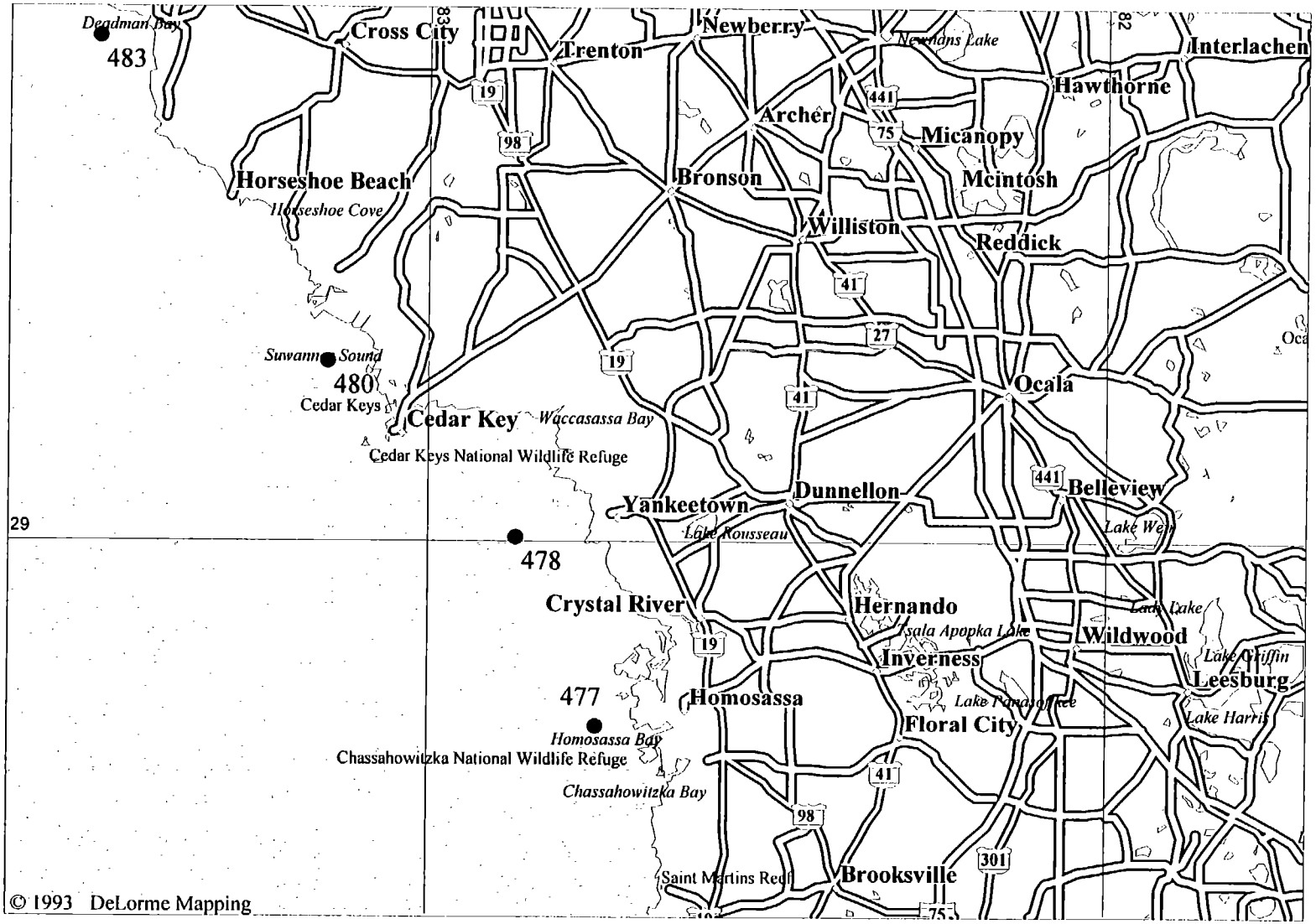
Deadman Bay
483
Cross City
Trenton
Newberry
Newnans Lake
Interlachen
Hawthorne
Archer
Micanopy
Mcintosh
Horseshoe Beach
Horseshoe Cove
Bronson
Williston
Reddick
Suwannee Sound
480
Cedar Keys
Cedar Key
Waccasassa Bay
Cedar Keys National Wildlife Refuge
Ocala
Yankeetown
Dunnellon
Belleview
Lake Rousseau
Lake Weir
29
478
Crystal River
Hernando
Lake Apopka
Wildwood
Lady Lake
Inverness
Lake Griffin
Leesburg
477
Homosassa
Lake Panasoffkee
Floral City
Lake Harris
Homosassa Bay
Chassahowitzka National Wildlife Refuge
Chassahowitzka Bay
Saint Martins Reef
Brooksville
© 1993 DeLorme Mapping

FLORIDA - 5

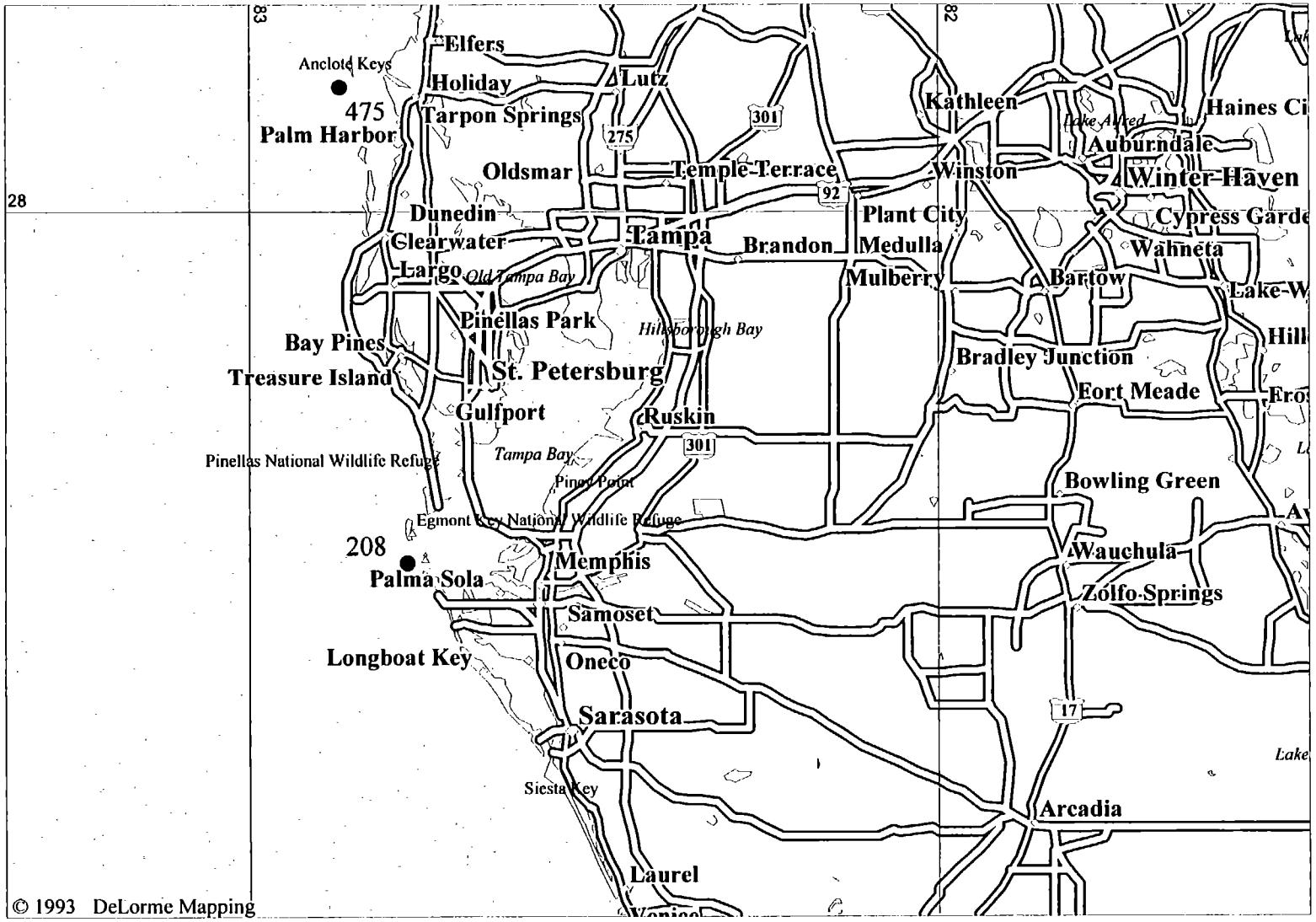
83
82
28
Elfers
Anclote Keys
Holiday
Lutz
475
Tarpon Springs
Palm Harbor
275
301
Kathleen
Lake Alfred
Haines Ci
Auburndale
Winter Haven
Oldsmar
Temple Terrace
Winston
92
Dunedin
Plant City
Cypress Garde
Clearwater
Tampa
Brandon
Medulla
Wahneta
Largo
Old Tampa Bay
Mulberry
Bartow
Lake W
Pinellas Park
Hillsborough Bay
Bay Pines
Hill
Bradley Junction
Treasure Island
St. Petersburg
Fort Meade
Gulfport
Ruskin
Fros
Pinellas National Wildlife Refuge
Tampa Bay
301
Piney Point
Bowling Green
Egmont Key National Wildlife Refuge
208
Memphis
Wauchula
Palma Sola
Zolfo Springs
Samoset
Longboat Key
Oneco
17
Sarasota
Lake
Siesta Key
Arcadia
Laurel
Venice
© 1993 DeLorme Mapping

FLORIDA - 5b

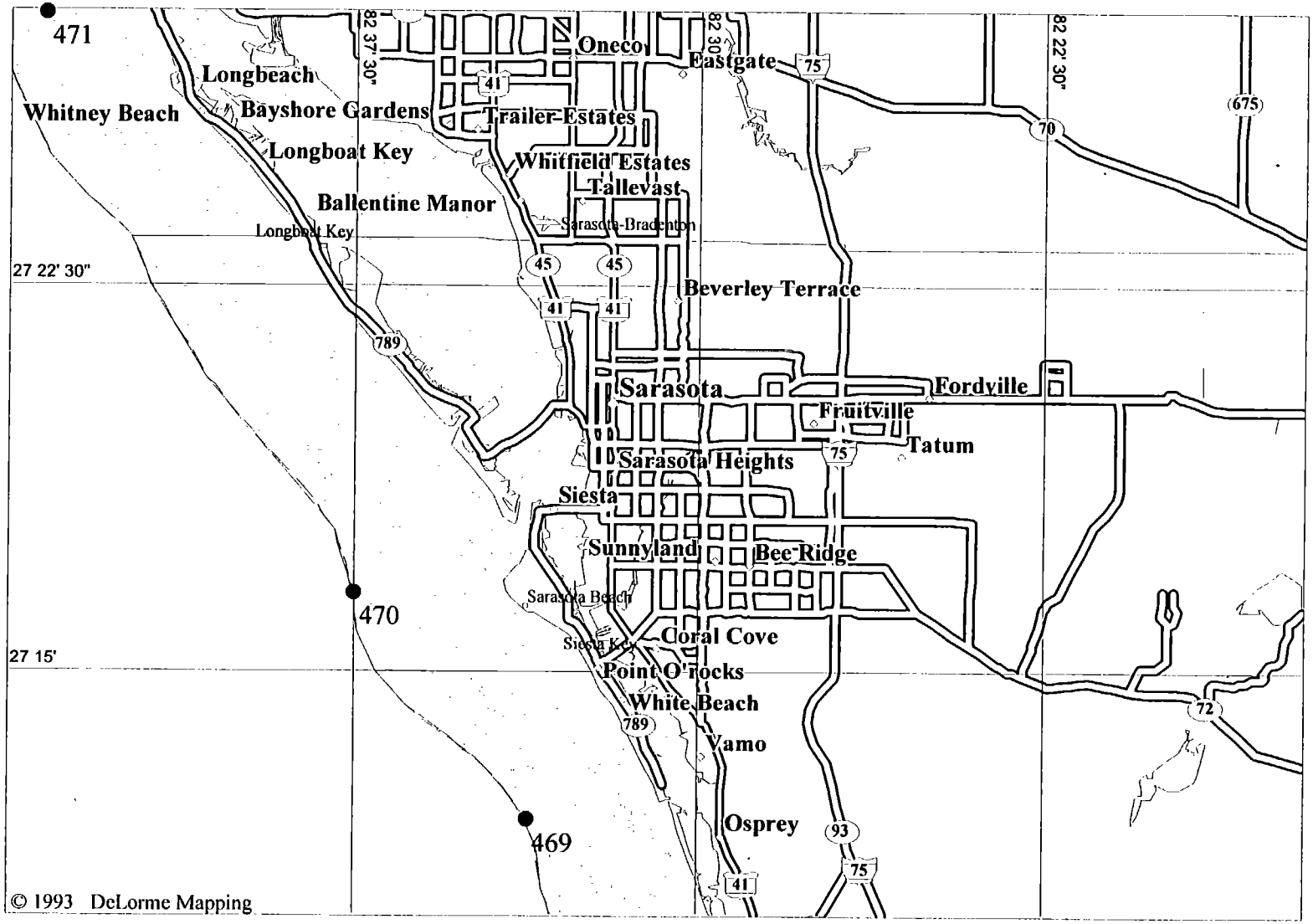
471
82 37' 30"
82 30'
82 22' 30"
Oneco
Eastgate
Longbeach
Whitney Beach
Bayshore Gardens
Trailer Estates
Longboat Key
Whitfield Estates
Tallevast
Ballentine Manor
Longboat Key
Sarasota-Bradenton
27 22' 30"
Beverley Terrace
Sarasota
Fordville
Fruitville
Tatum
Sarasota Heights
Siesta
Sunnyland
Bee Ridge
470
Sarasota Beach
Siesta Key
Coral Cove
27 15'
Point O'rocks
White Beach
Vamo
Osprey
469
41
75
70
675
45
789
72
93
© 1993 DeLorme Mapping

FLORIDA - 6

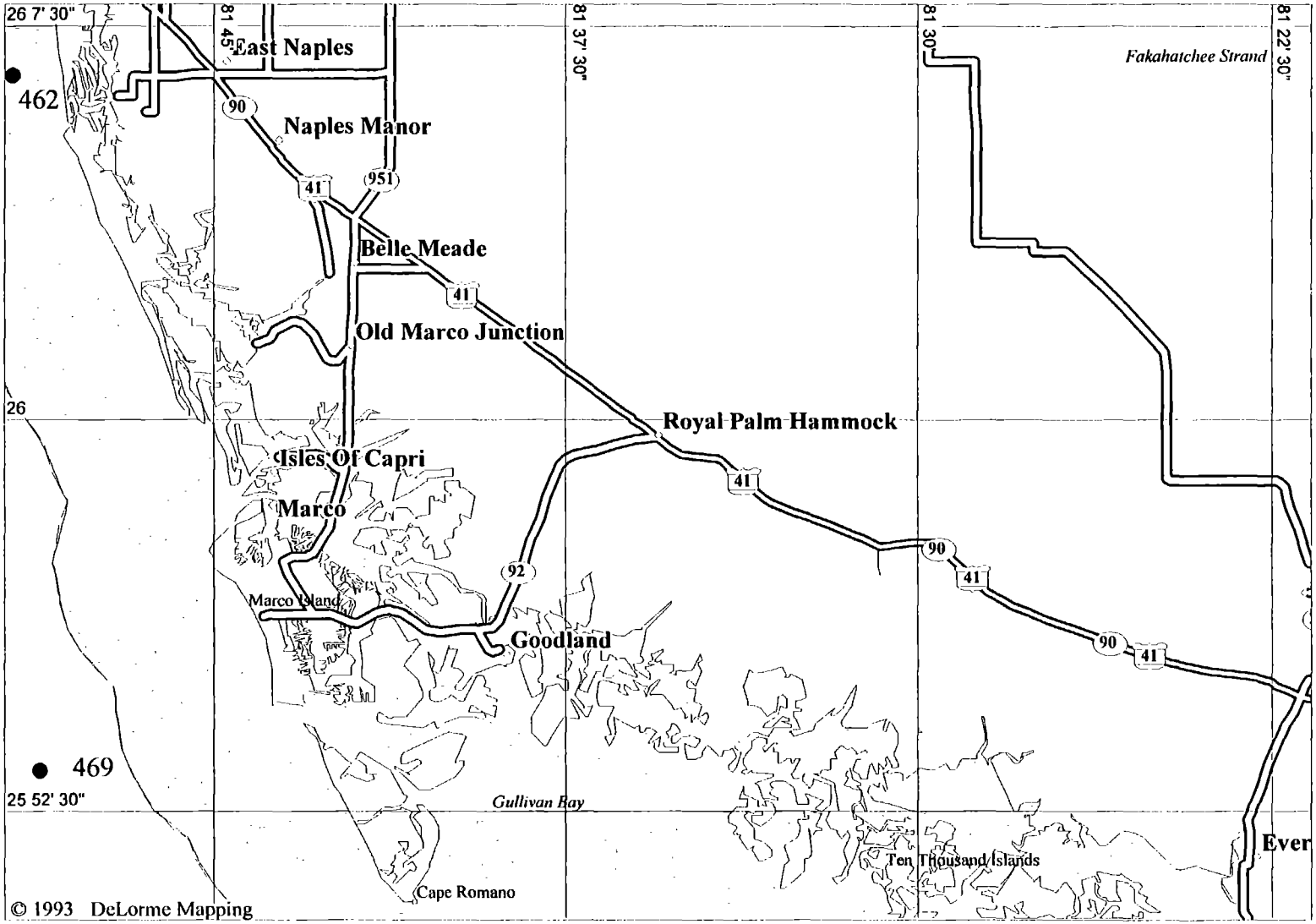
26 7' 30"
81 45'
81 37' 30"
81 30'
81 22' 30"
East Naples
462
90
Naples Manor
41
951
Belle Meade
41
Old Marco Junction
26
Royal Palm Hammock
Isles Of Capri
41
Marco
92
90
41
Marco Island
Goodland
90
41
469
25 52' 30"
Gullivan Bay
Fakahatchee Strand
Ten Thousand Islands
Ever
Cape Romano
© 1993 DeLorme Mapping

FLORIDA - 7

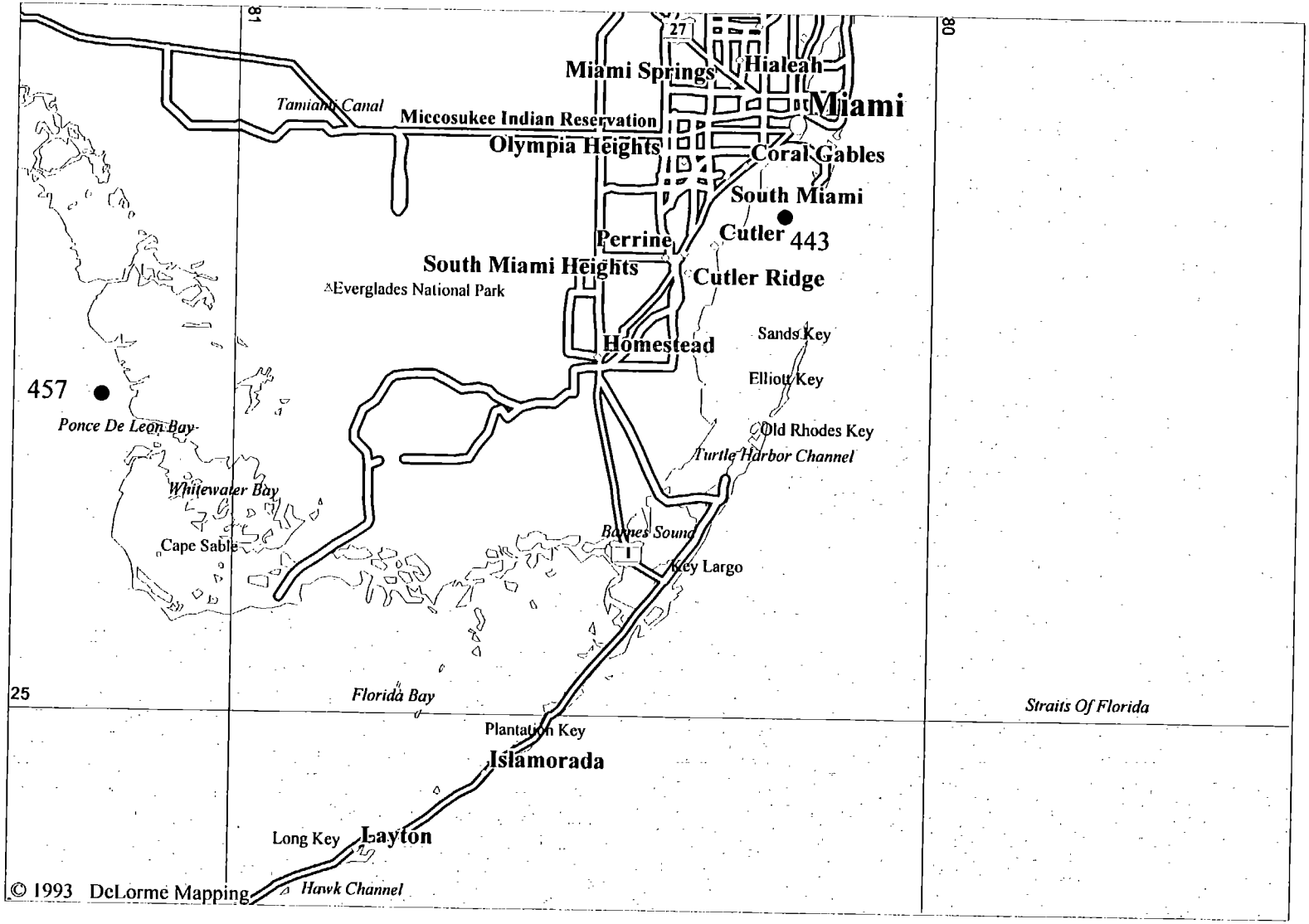
81
27
80
Miami Springs
Hialeah
Miami
Tamiami Canal
Miccosukee Indian Reservation
Olympia Heights
Coral Gables
South Miami
Perrine
Cutler
443
South Miami Heights
Cutler Ridge
Everglades National Park
Homestead
Sands Key
Elliott Key
457
Ponce De Leon Bay
Old Rhodes Key
Turtle Harbor Channel
Whitewater Bay
Barnes Sound
Cape Sable
Key Largo
25
Florida Bay
Straits Of Florida
Plantation Key
Islamorada
Long Key
Layton
Hawk Channel
© 1993 DeLorme Mapping

FLORIDA - 8

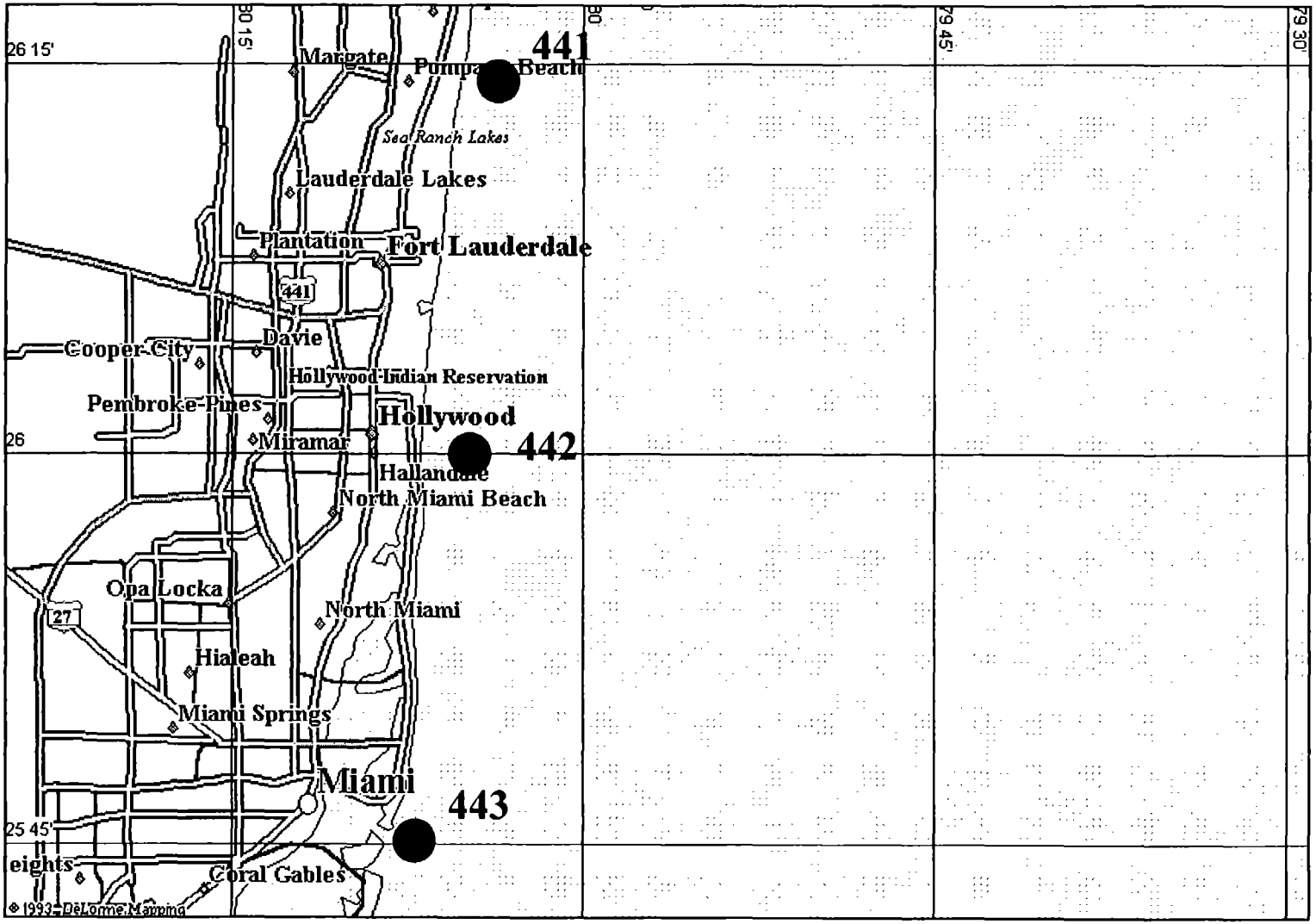
26 15'
80 15'
80
79 45'
79 30'
441
Margate
Pompano Beach
Sea Ranch Lakes
Lauderdale Lakes
Plantation
Fort Lauderdale
441
Davie
Cooper City
Hollywood Indian Reservation
Pembroke Pines
Hollywood
26
Miramar
442
Hallandale
North Miami Beach
Opa Locka
27
North Miami
Hialeah
Miami Springs
Miami
443
25 45'
eights
Coral Gables
© 1993 DeLorme Mapping

FLORIDA - 9

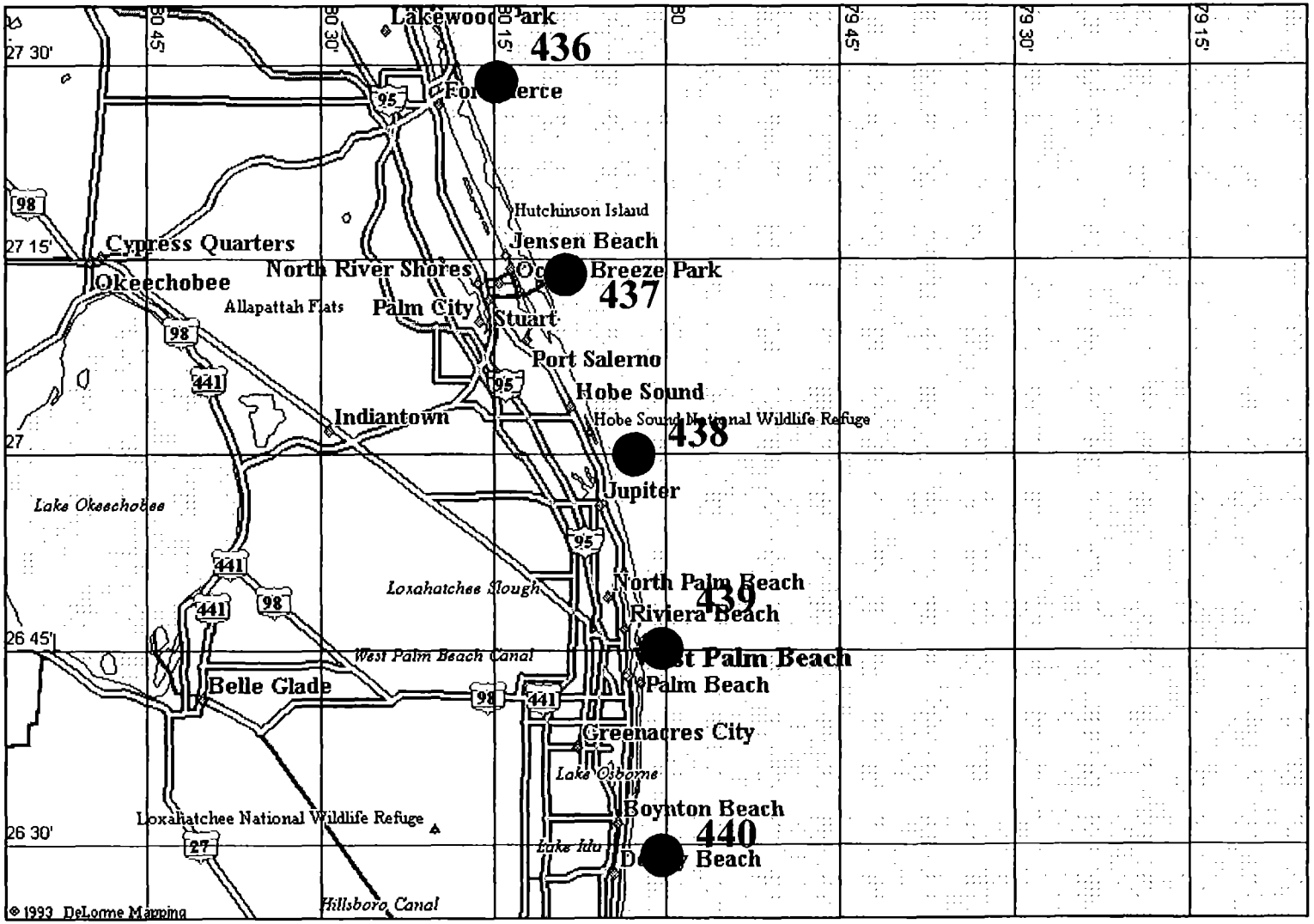
Lakewood Park
436
Fort Pierce
Hutchinson Island
Jensen Beach
Breeze Park
437
Cypress Quarters
North River Shores
Okeechobee
Allapattah Flats
Palm City
Stuart
Port Salerno
Hobe Sound
Hobe Sound National Wildlife Refuge
438
Indiantown
Jupiter
Lake Okeechobee
Loxahatchee Slough
North Palm Beach
439
Riviera Beach
West Palm Beach Canal
West Palm Beach
Palm Beach
Belle Glade
Greenacres City
Lake Osborne
Boynton Beach
440
Loxahatchee National Wildlife Refuge
Hillsboro Canal
© 1993 DeLorme Mapping
27 30'
27 15'
27
26 45'
26 30'
80 45'
80 30'
80 15'
80
79 45'
79 30'
79 15'
95
98
441
27

FLORIDA - 10

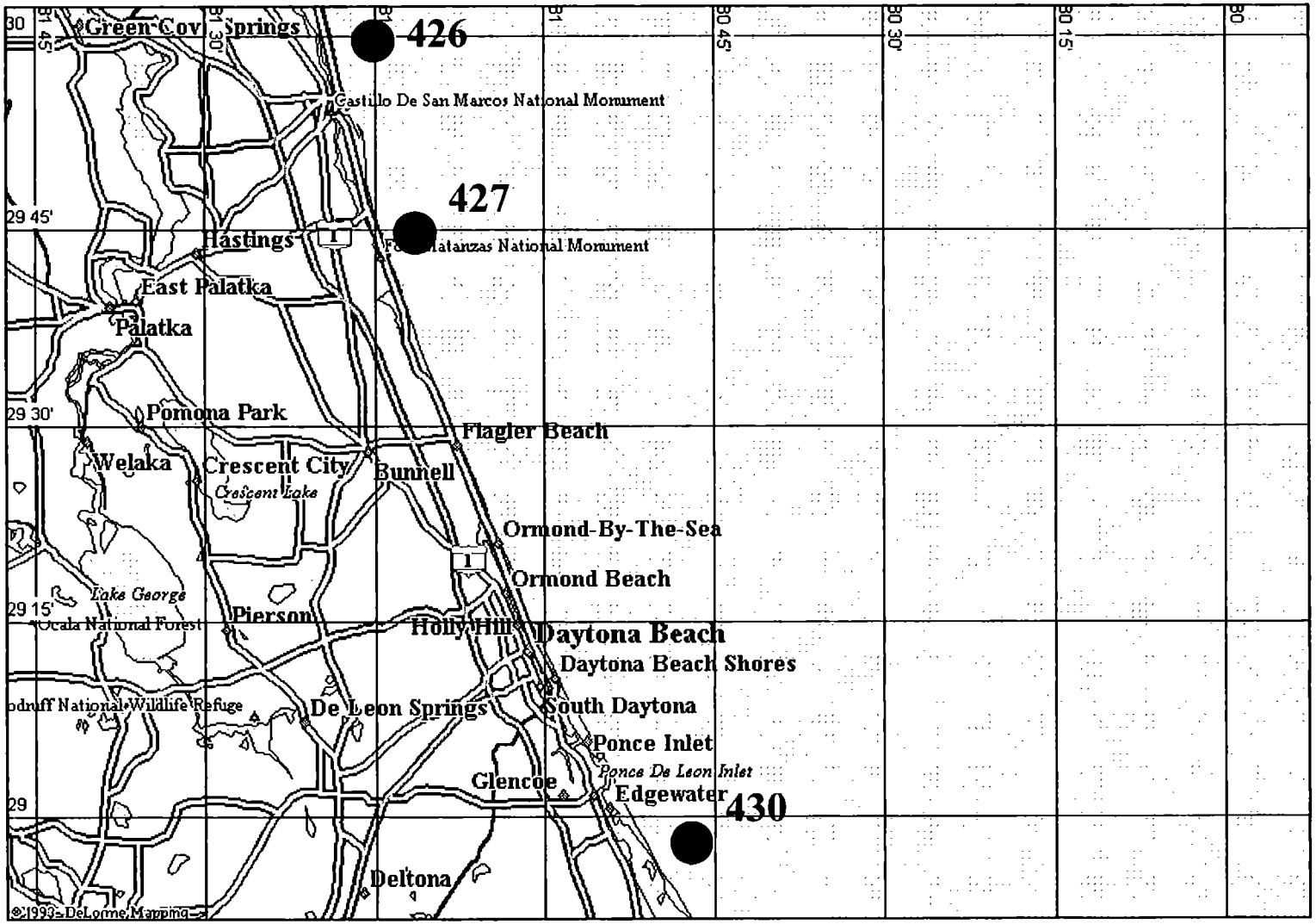
426
Castillo De San Marcos National Monument
427
Hastings
East Palatka
Palatka
Pomona Park
Flagler Beach
Welaka
Crescent City
Crescent Lake
Bunnell
Ormond-By-The-Sea
Ormond Beach
Lake George
Ocala National Forest
Pierson
Holly Hill
Daytona Beach
Daytona Beach Shores
De Leon Springs
South Daytona
Ponce Inlet
Ponce De Leon Inlet
Glencoe
Edgewater
430
Deltona
©1999 DeLorme Mapping

FLORIDA - 11

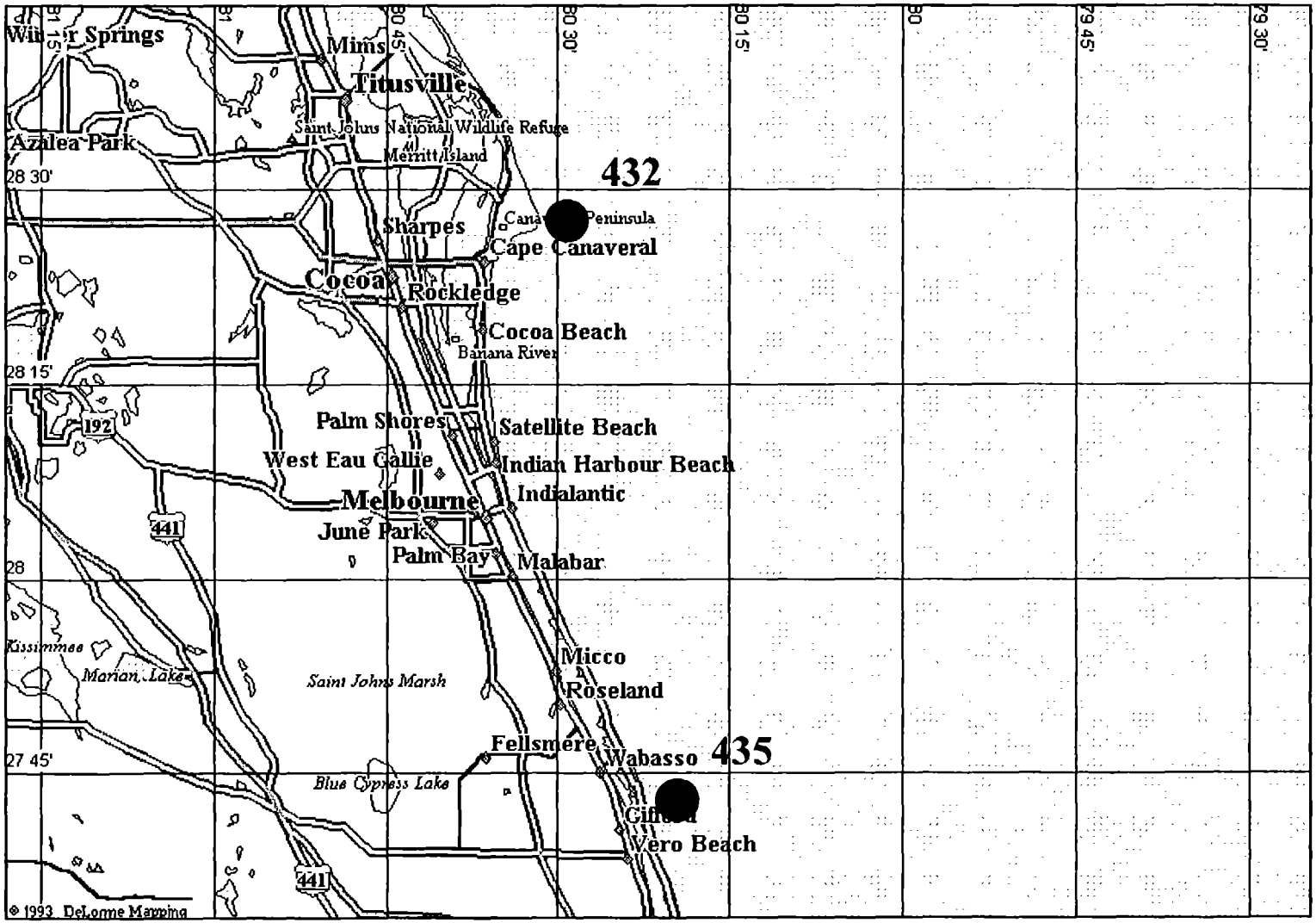
Mims
Titusville
Saint Johns National Wildlife Refuge
Merritt Island
Azalea Park
28 30'
432
Sharpes
Cape Canaveral
Cocoa
Rockledge
Cocoa Beach
Banana River
28 15'
192
Palm Shores
Satellite Beach
West Eau Gallie
Indian Harbour Beach
Melbourne
Indialantic
441
June Park
Palm Bay
Malabar
28
Micco
Roseland
Saint Johns Marsh
Fellsmere
Wabasso
435
27 45'
Blue Cypress Lake
Vero Beach
441
© 1993 DeLorme Mapping
80 45'
80 30'
80 15'
80
79 45'
79 30'

FLORIDA - 12

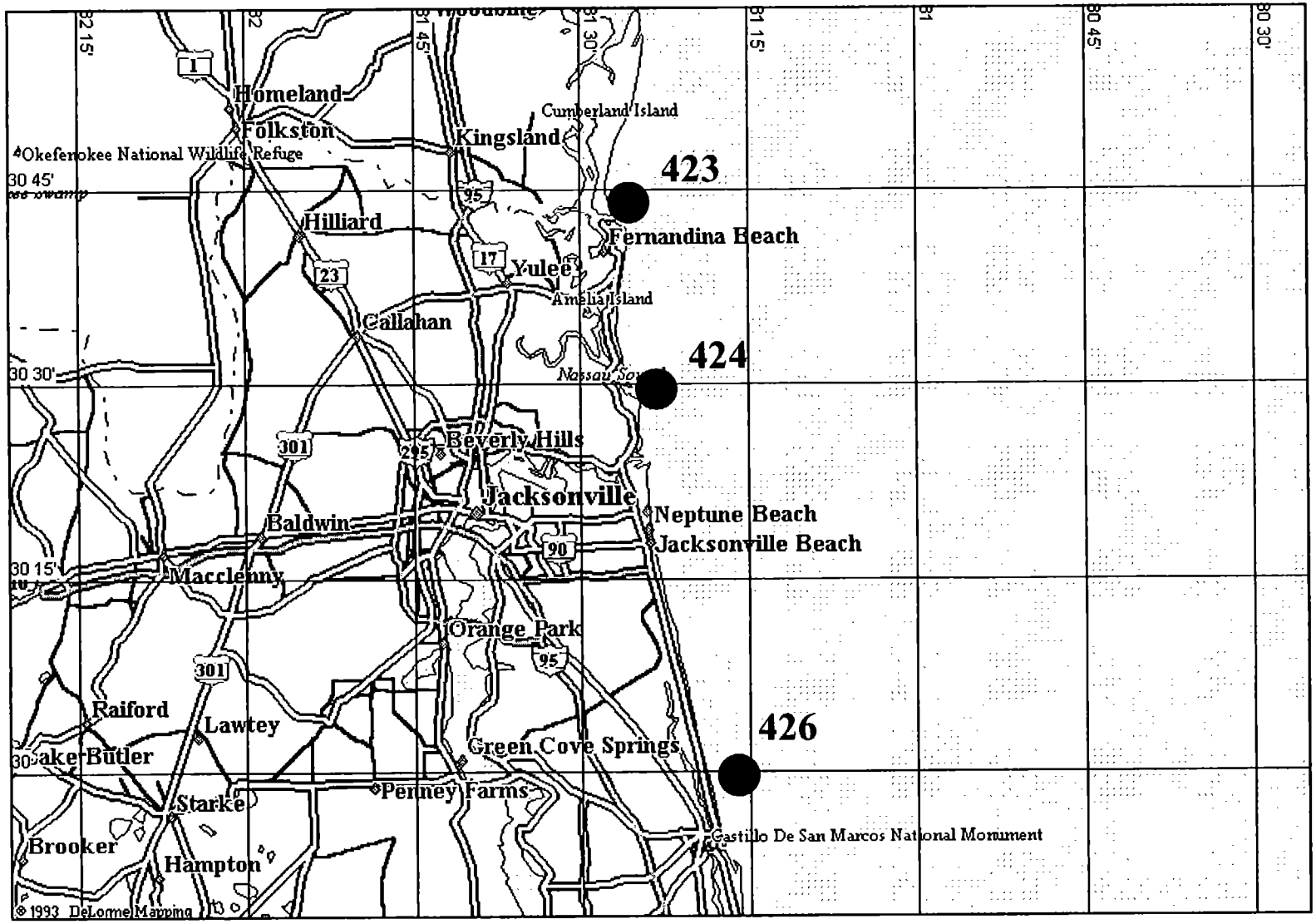
82 15'
82
81 45'
81 30'
81 15'
81
80 45'
80 30'
1
Homeland
Folkston
Okefenokee National Wildlife Refuge
30 45'
Hilliard
23
Callahan
30 30'
301
Baldwin
30 15'
Macclenny
301
Raiford
Lawtey
Lake Butler
Starke
Brooker
Hampton
95
Kingsland
Cumberland Island
17
Yulee
Amelia Island
Nassau Sound
Beverly Hills
295
Jacksonville
90
Orange Park
95
Green Cove Springs
Penney Farms
Fernandina Beach
Neptune Beach
Jacksonville Beach
Castillo De San Marcos National Monument
423
424
426
© 1993 DeLorme Mapping

GEORGIA - 1

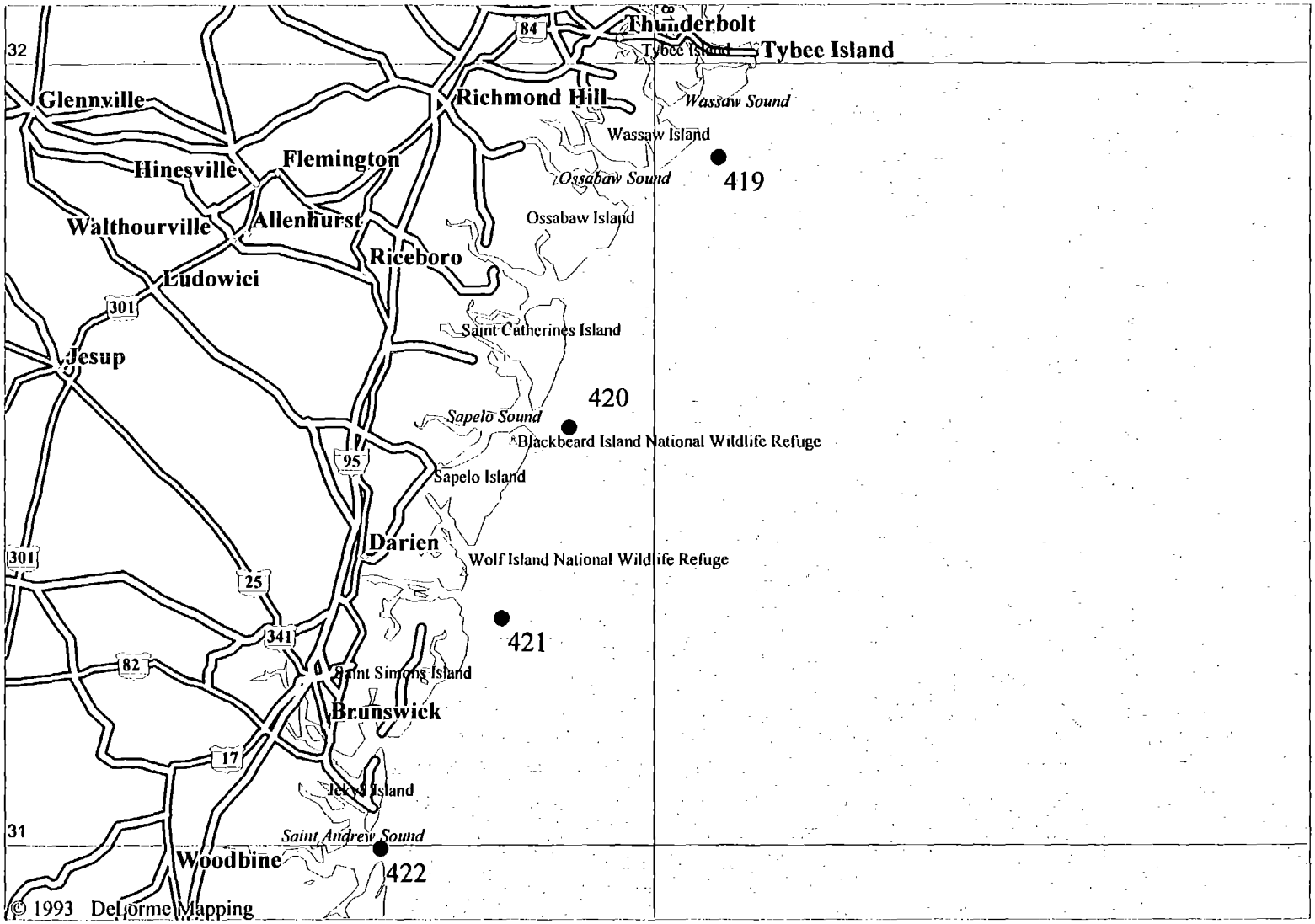
Thunderbolt
Tybee Island
Tybee Island
Wassaw Sound
Wassaw Island
Richmond Hill
Glennville
Hinesville
Flemington
Ossabaw Sound
419
Ossabaw Island
Walthourville
Allenhurst
Riceboro
Ludowici
Saint Catherines Island
Jesup
420
Sapelo Sound
Blackbeard Island National Wildlife Refuge
Sapelo Island
Darien
Wolf Island National Wildlife Refuge
421
Saint Simons Island
Brunswick
Jekyll Island
Saint Andrew Sound
Woodbine
422
32
31
84
95
301
25
341
82
17
© 1993 DeLorme Mapping

SOUTH CAROLINA - 1

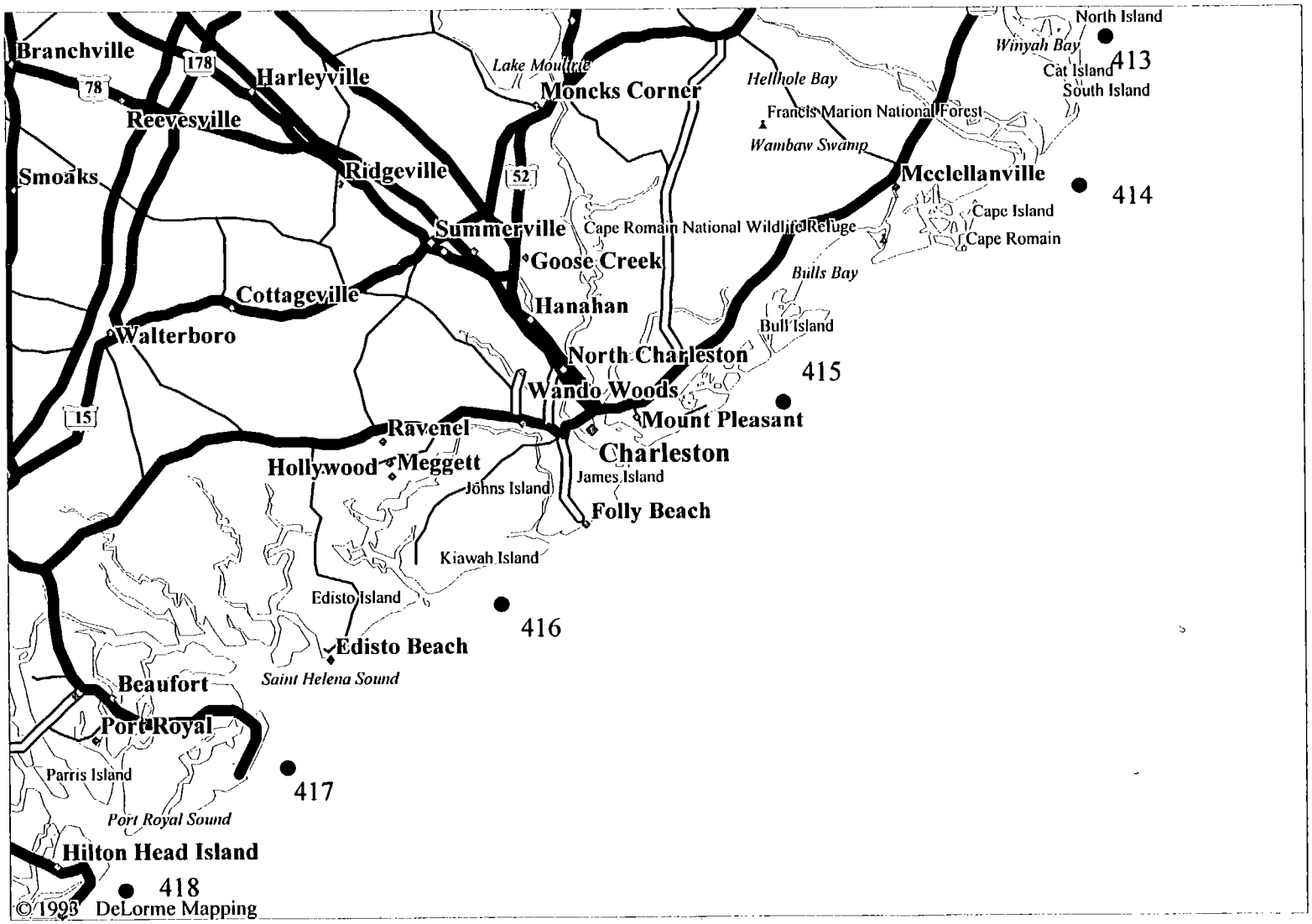

419

SOUTH CAROLINA - 2

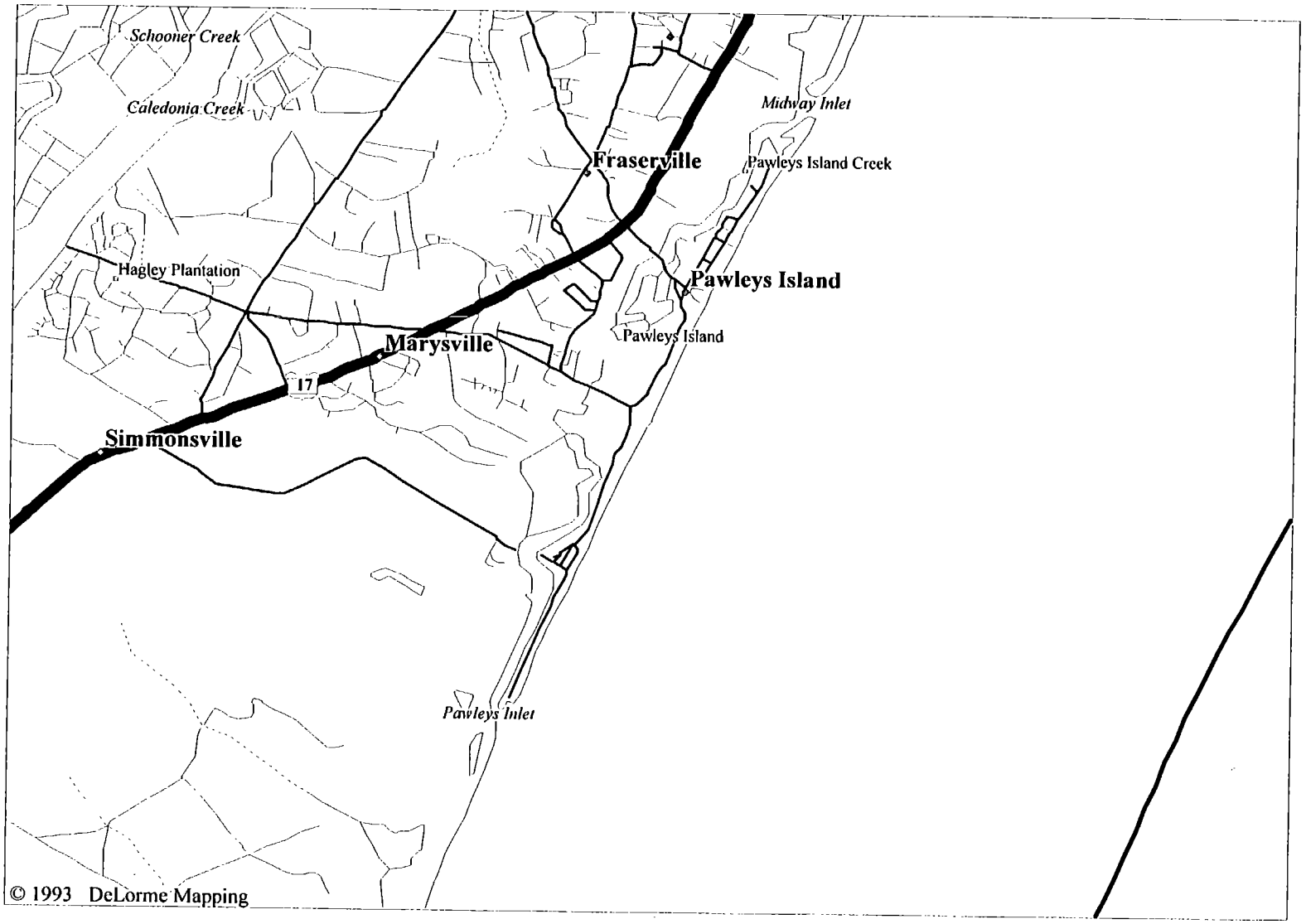

SOUTH CAROLINA - 3

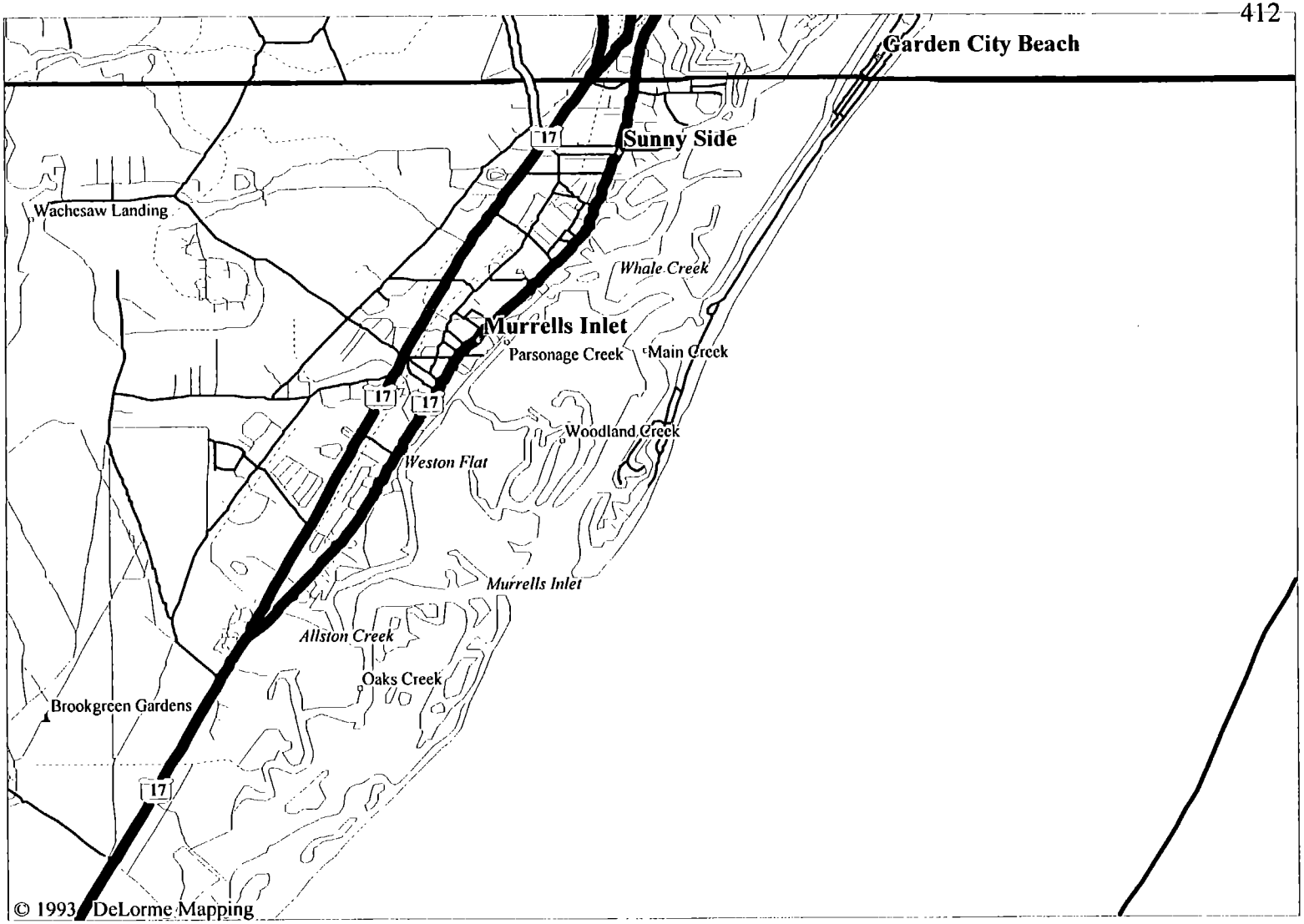

SOUTH CAROLINA - 4

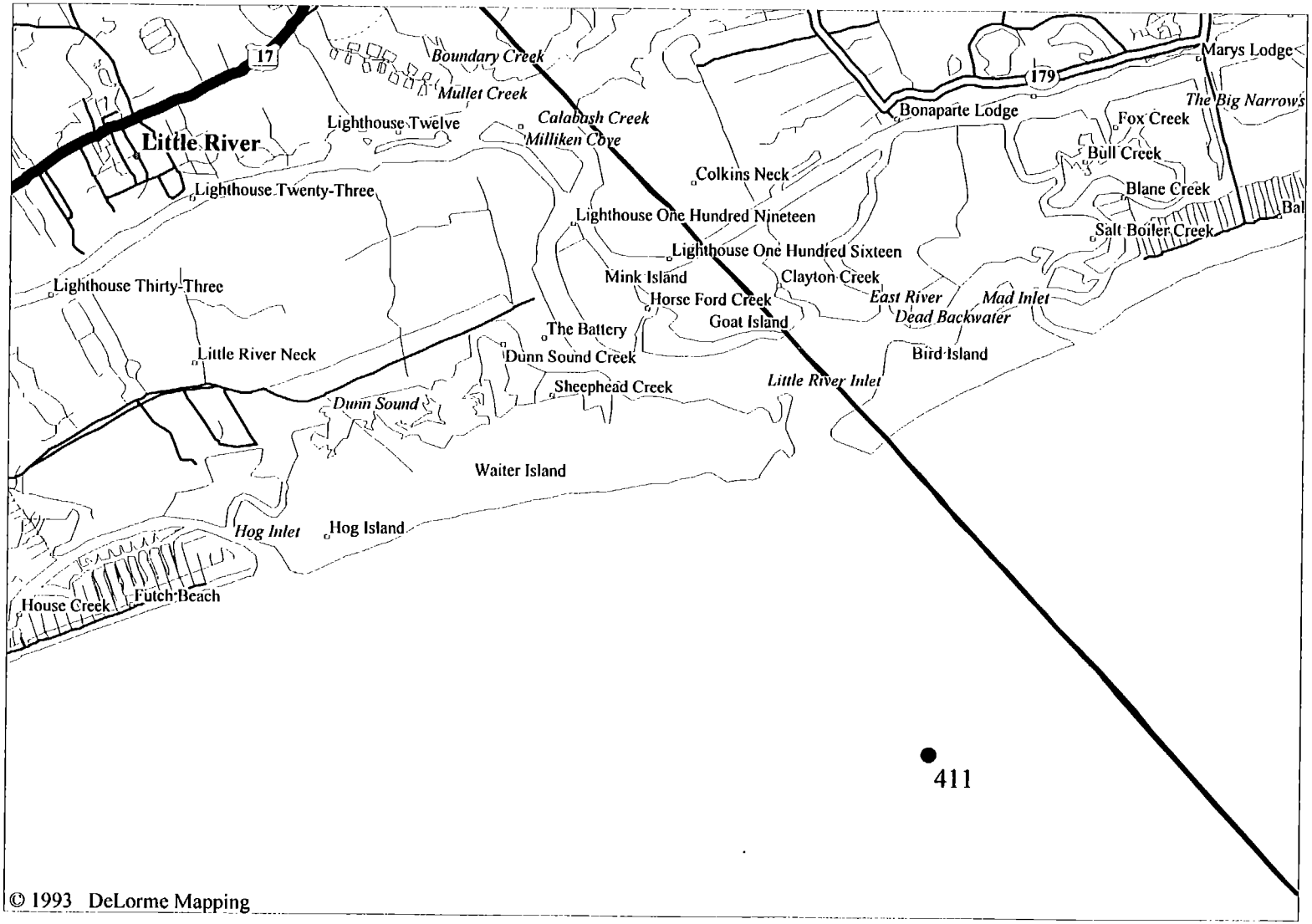

NORTH CAROLINA- 1

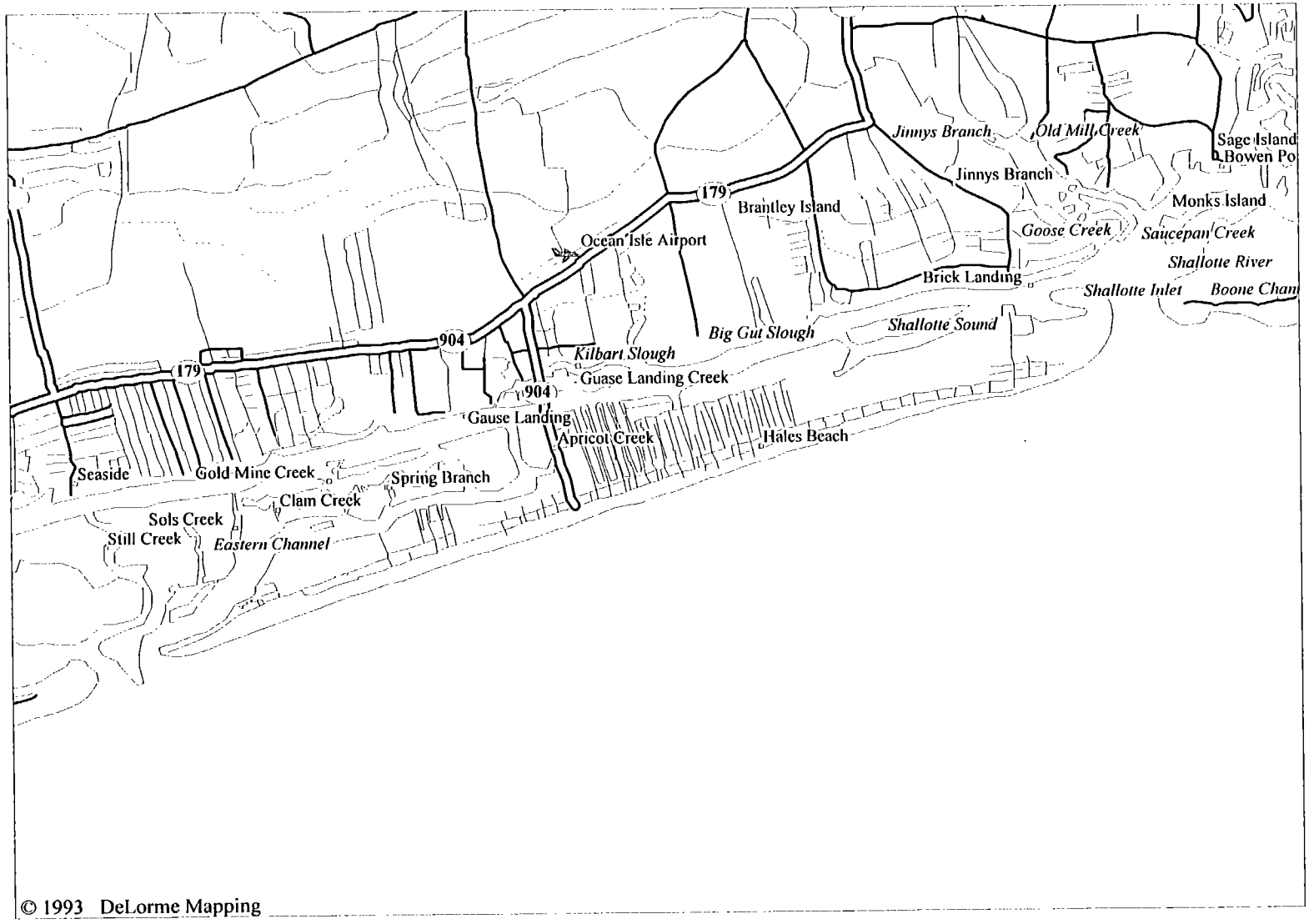

NORTH CAROLINA- 2

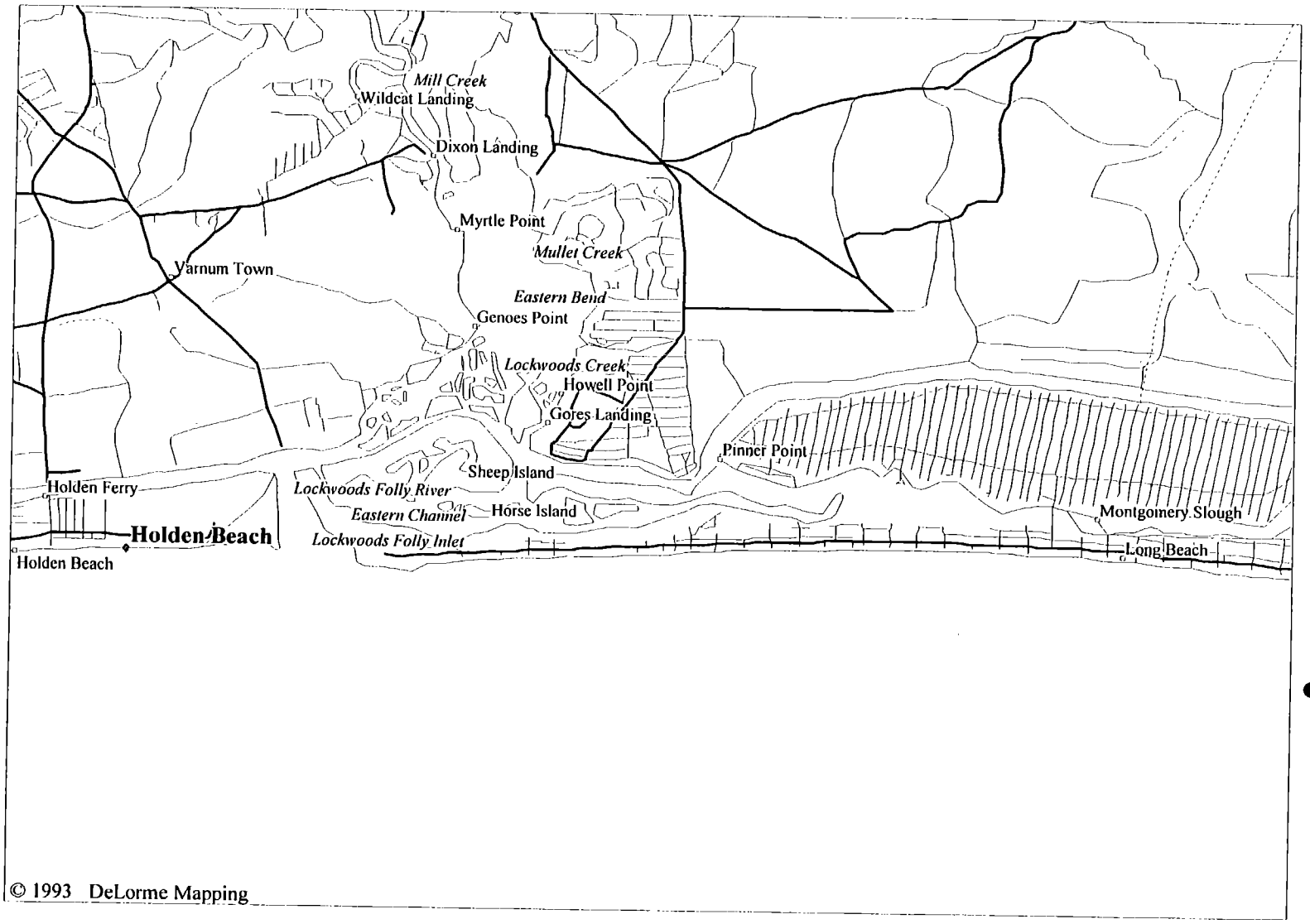

410

NORTH CAROLINA- 3

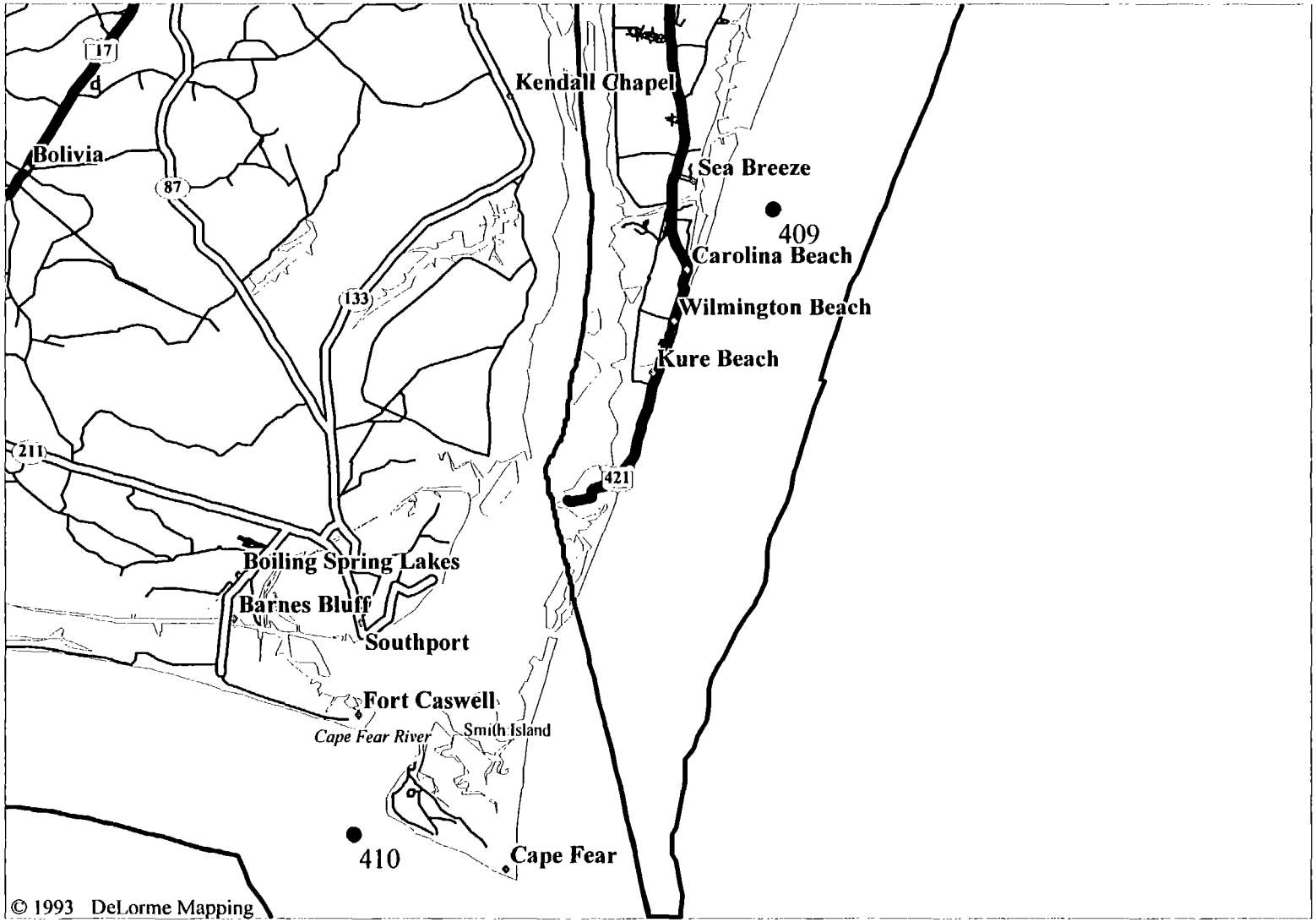

NORTH CAROLINA- 4

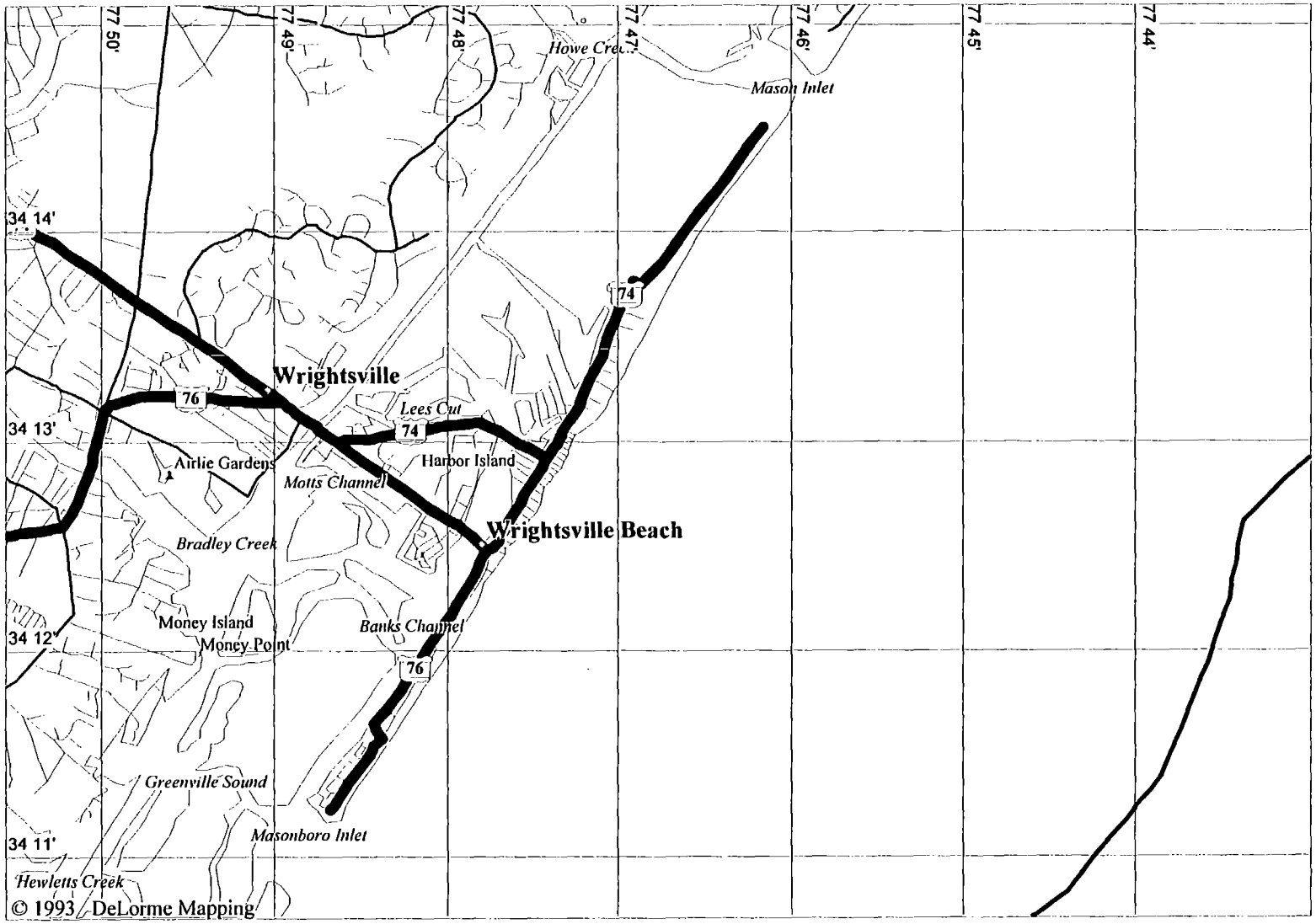

NORTH CAROLINA- 5

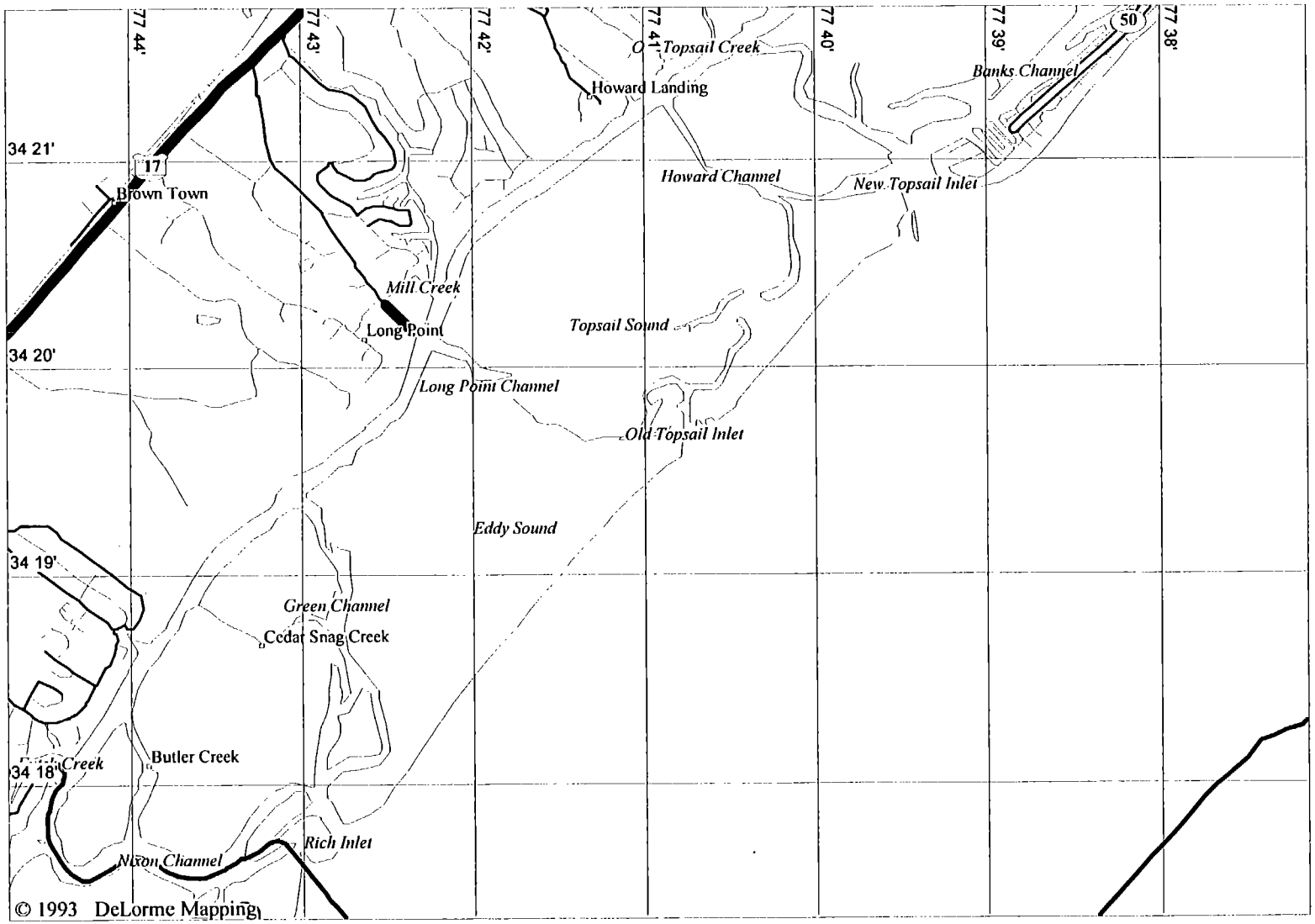

B-40

NORTH CAROLINA- 6

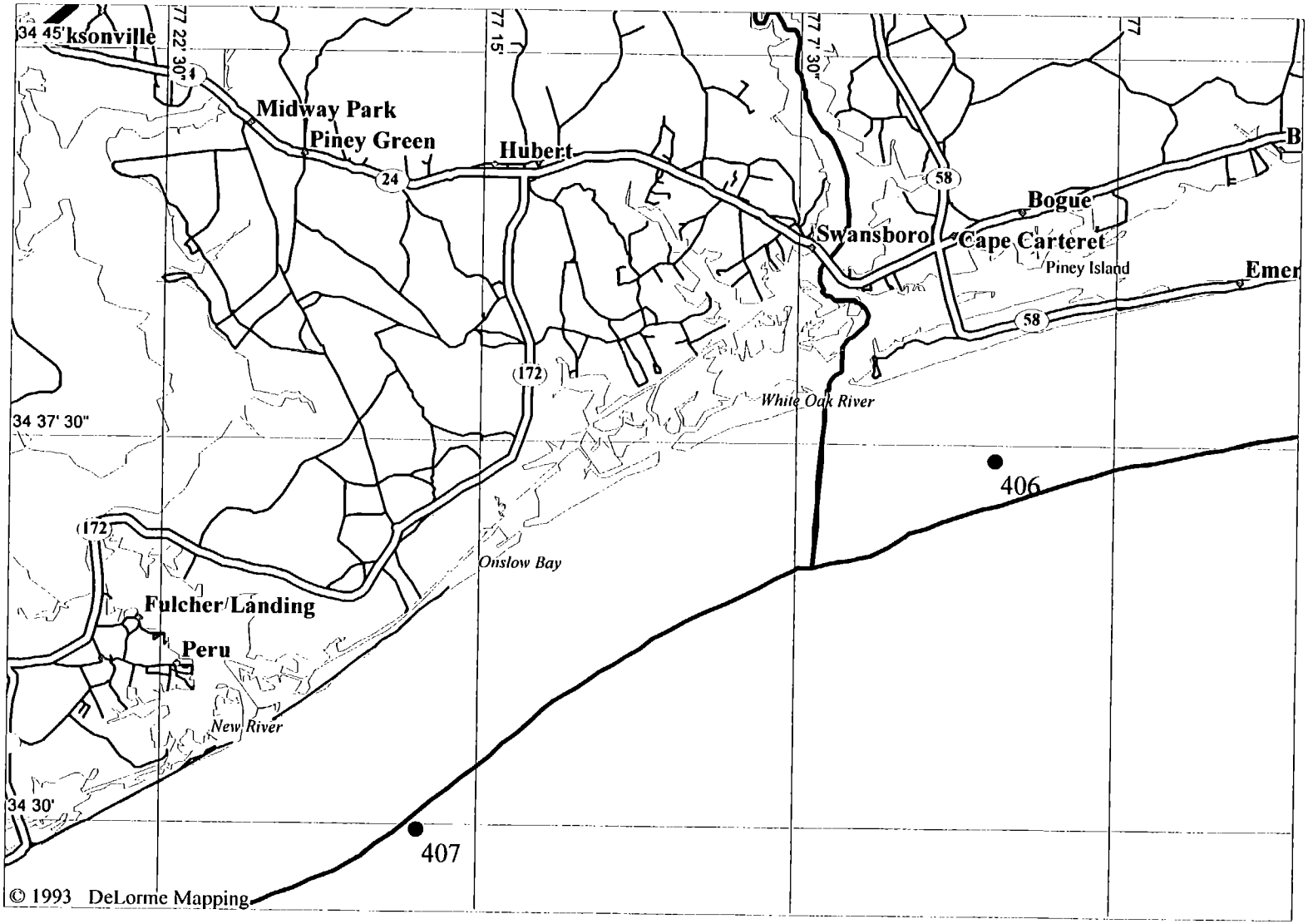

NORTH CAROLINA- 7

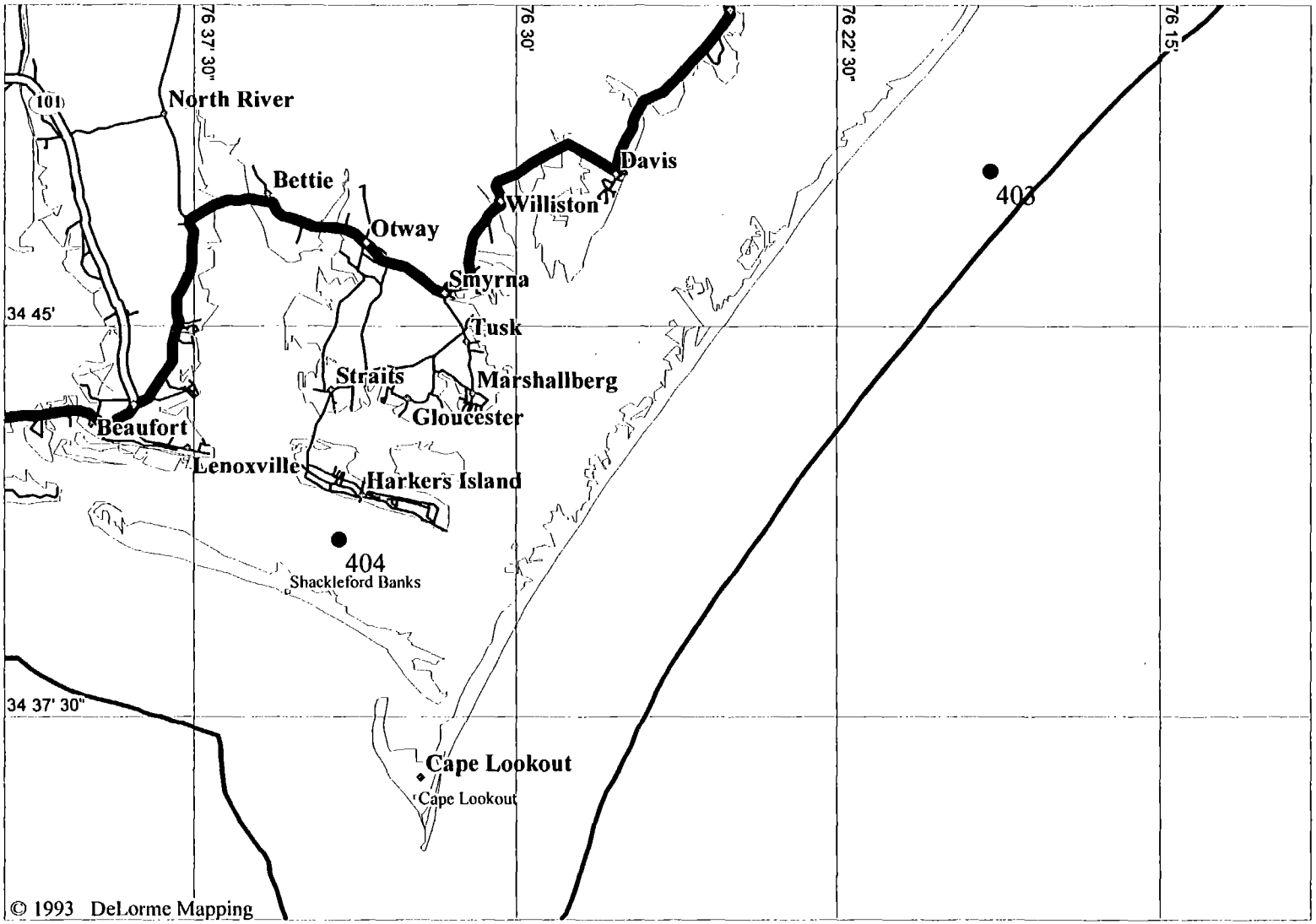

NORTH CAROLINA- 8

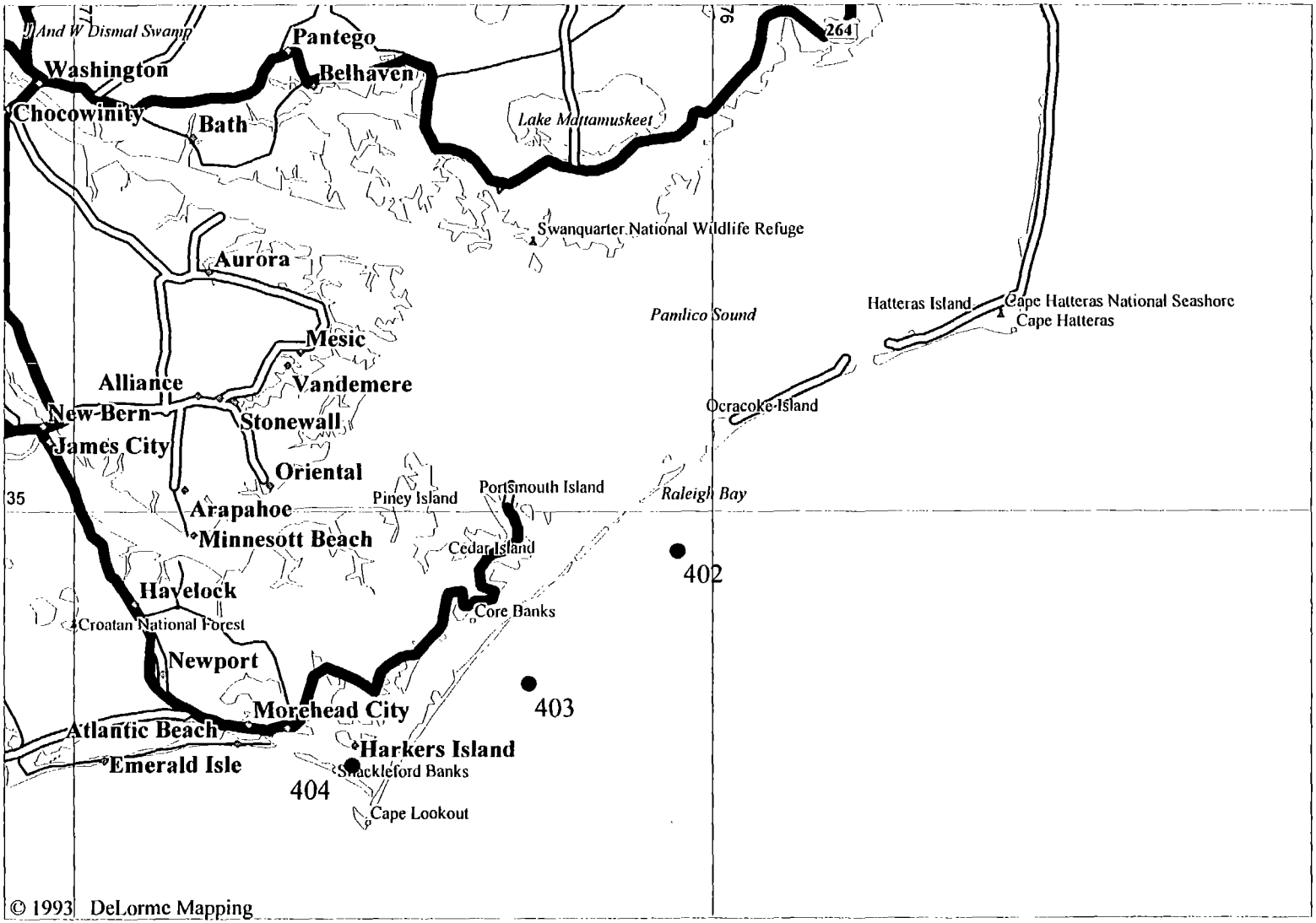

VIRGINIA- 1

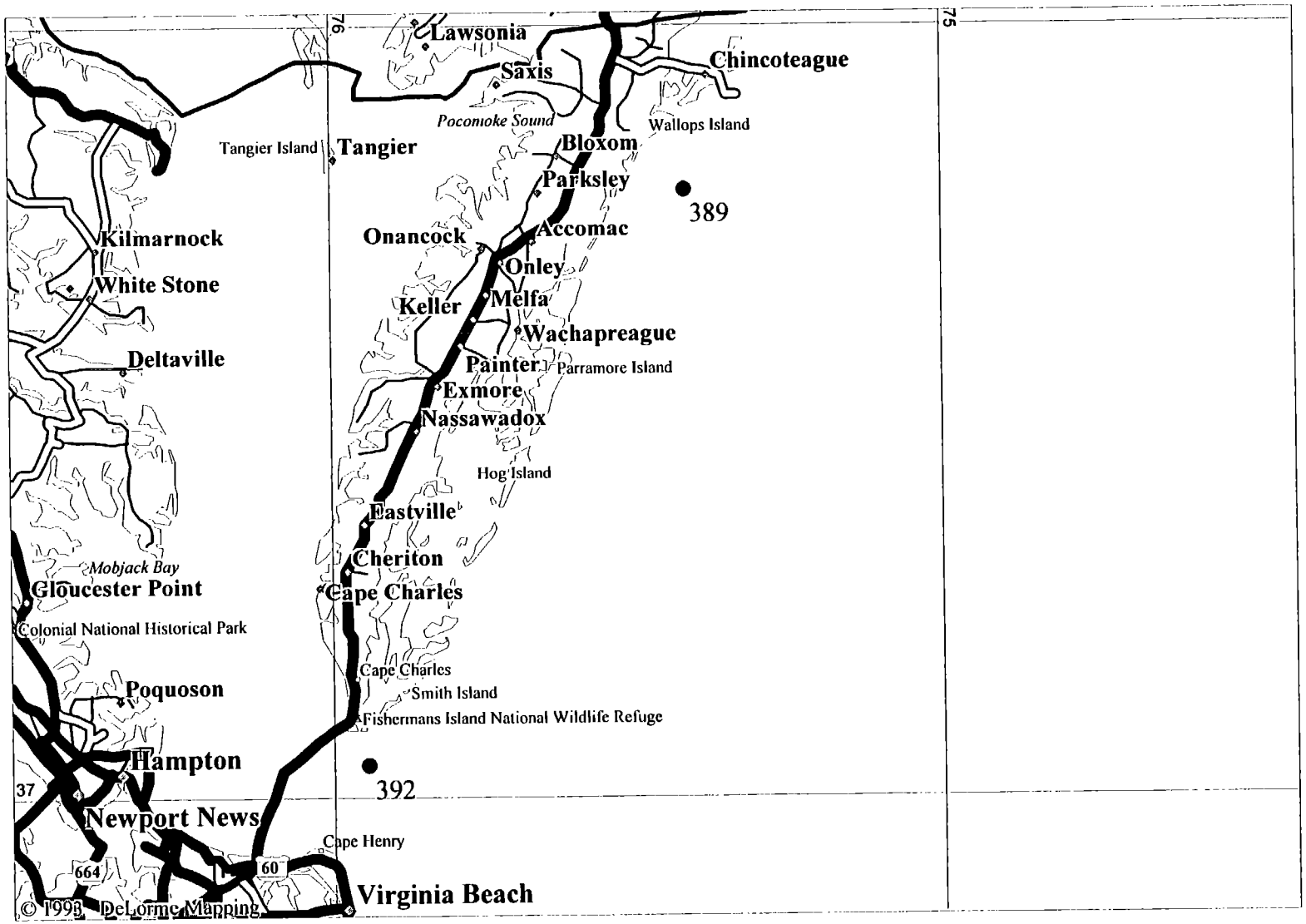
Lawsonia
Saxis
Chincoteague
Pocomoke Sound
Wallops Island
Tangier Island
Tangier
Bloxom
Parksley
389
Kilmarnock
Onancock
Accomac
Onley
White Stone
Keller
Melfa
Wachapreague
Deltaville
Painter
Parramore Island
Exmore
Nassawadox
Hog Island
Eastville
Cheriton
Mobjack Bay
Gloucester Point
Cape Charles
Colonial National Historical Park
Cape Charles
Poquoson
Smith Island
Fishermans Island National Wildlife Refuge
Hampton
392
37
Newport News
Cape Henry
664
60
Virginia Beach
© 1993 DeLorme Mapping
76
75

Chesapeake Bay - 1

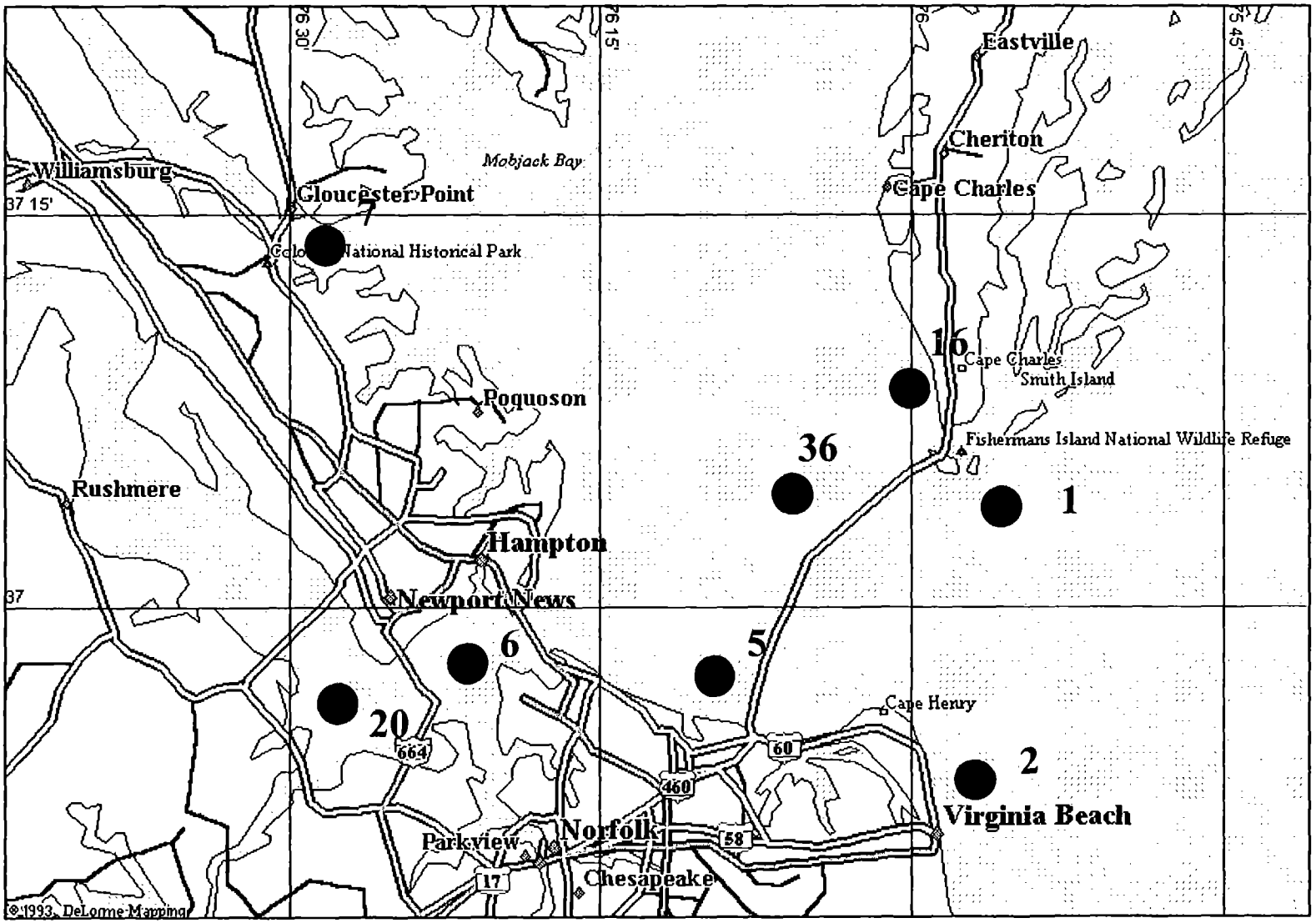

Chesapeake Bay - 2

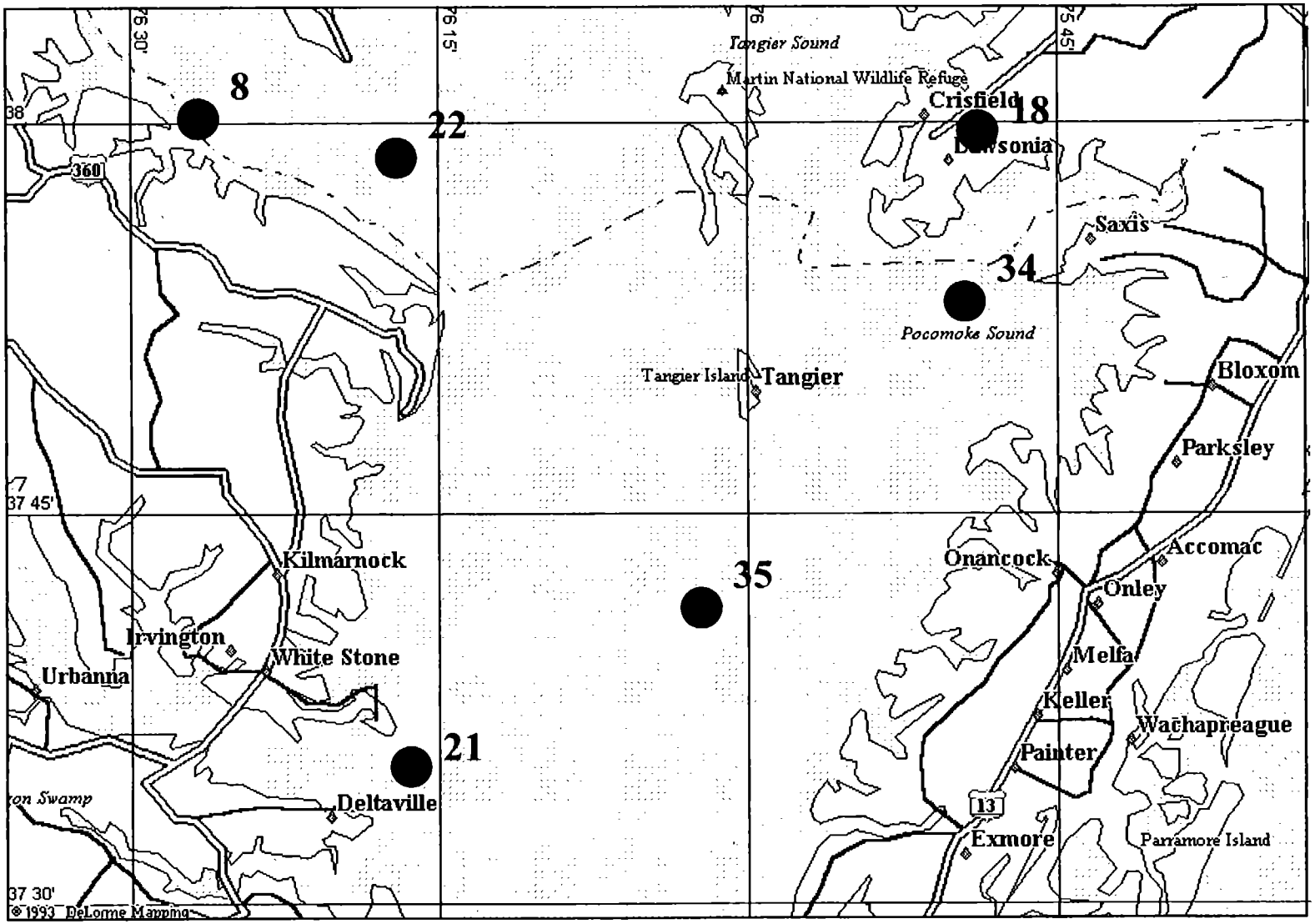

Chesapeake Bay - 3

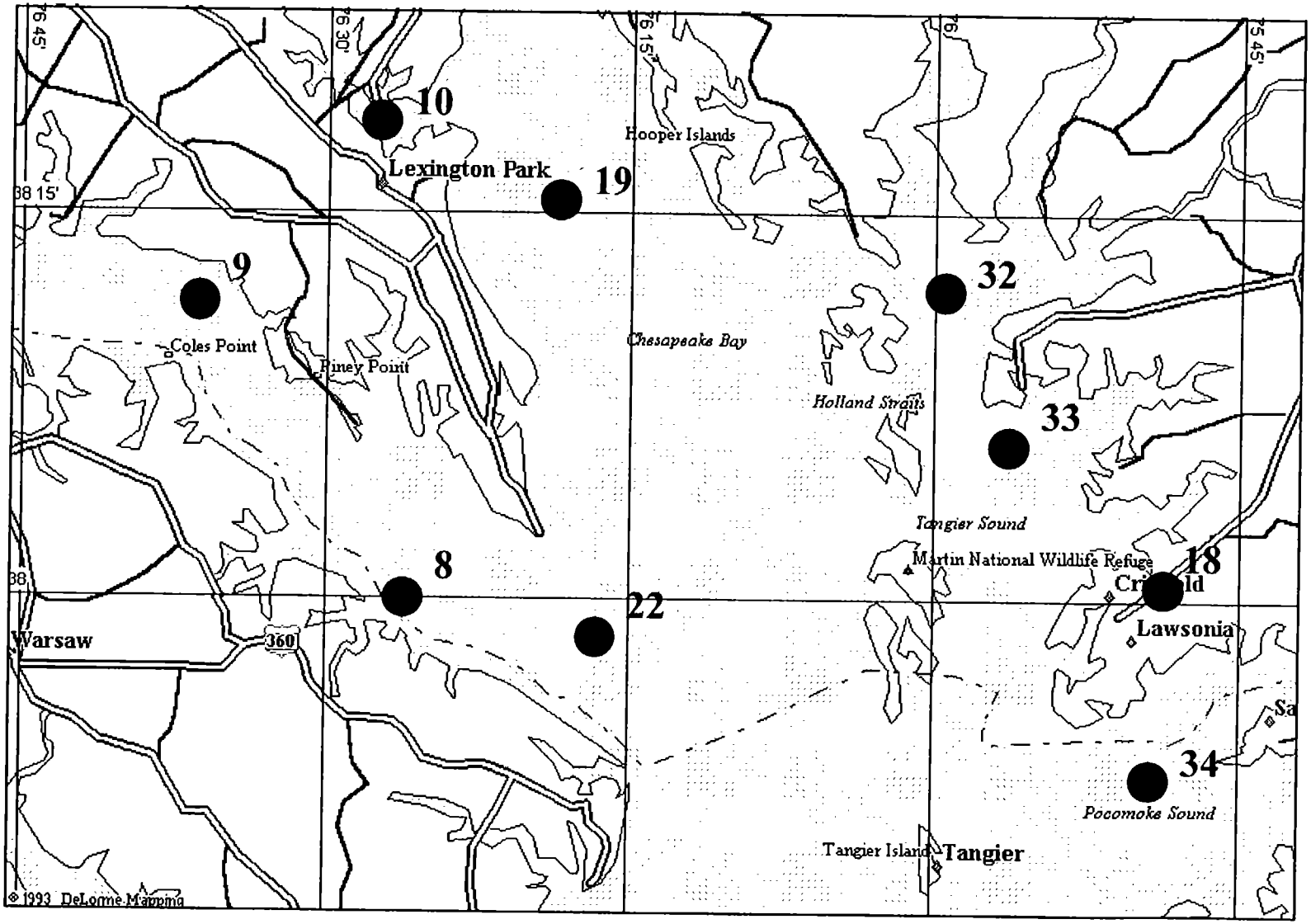

Chesapeake Bay - 4

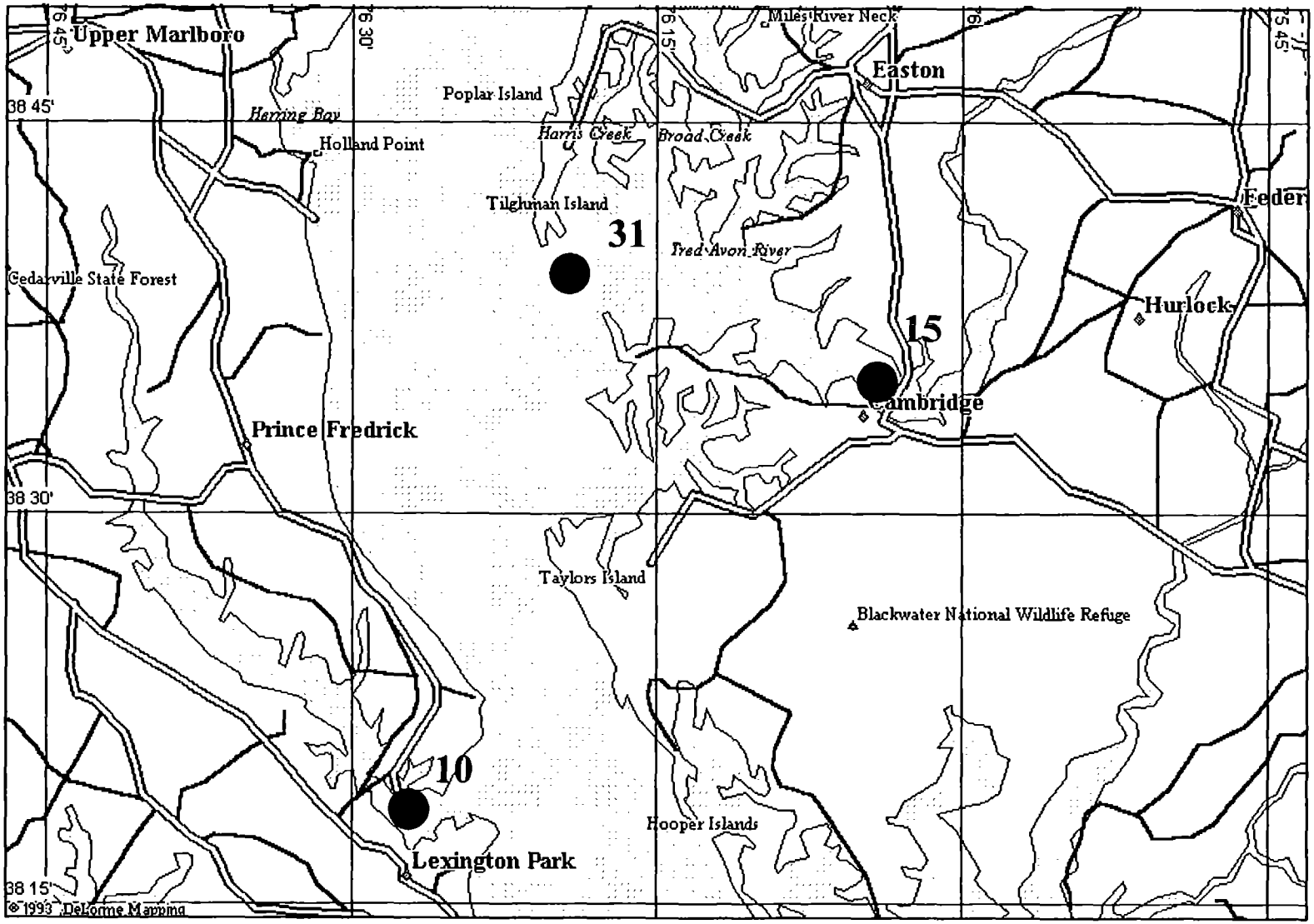

Chesapeake Bay - 5

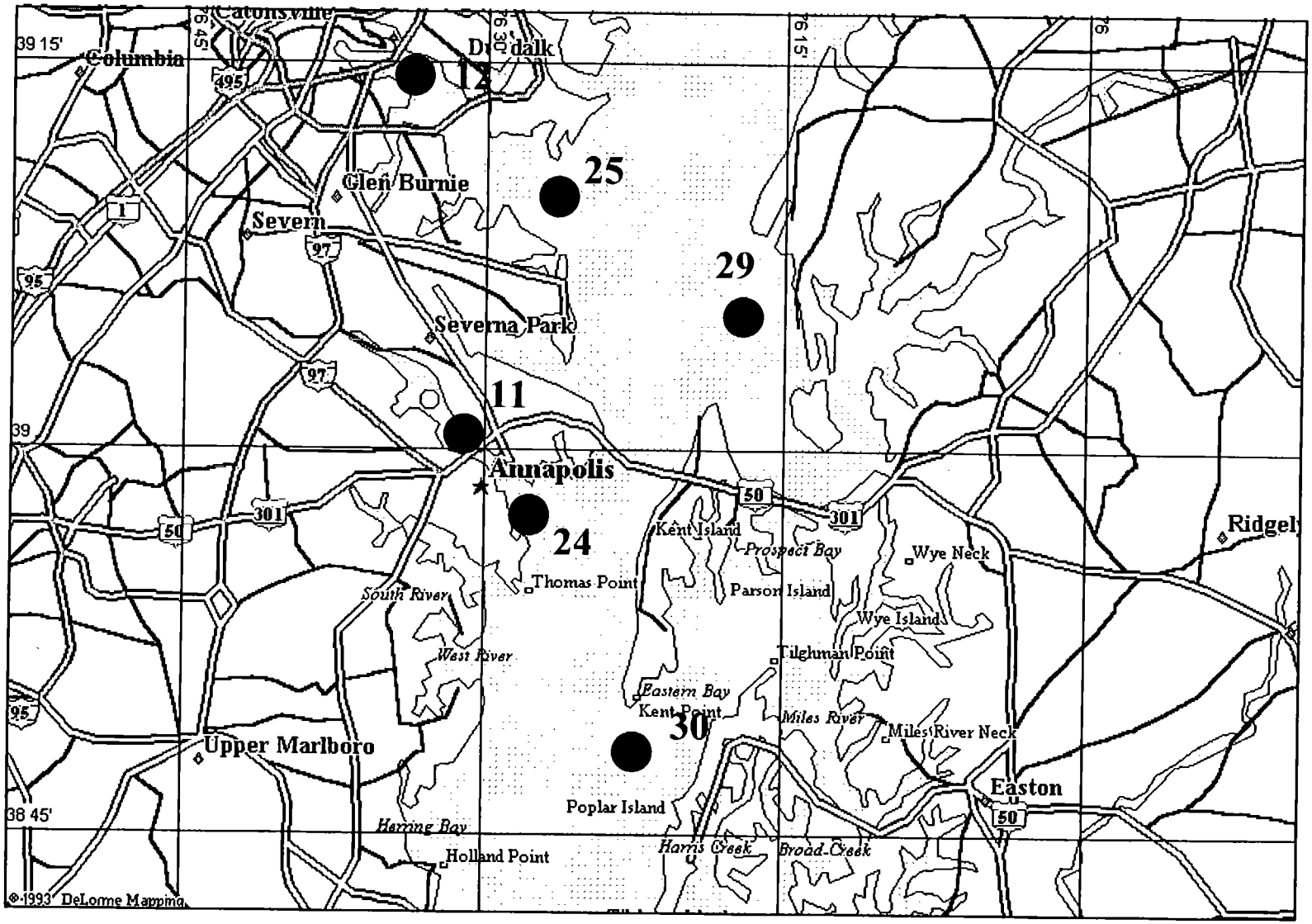

Chesapeake Bay - 6

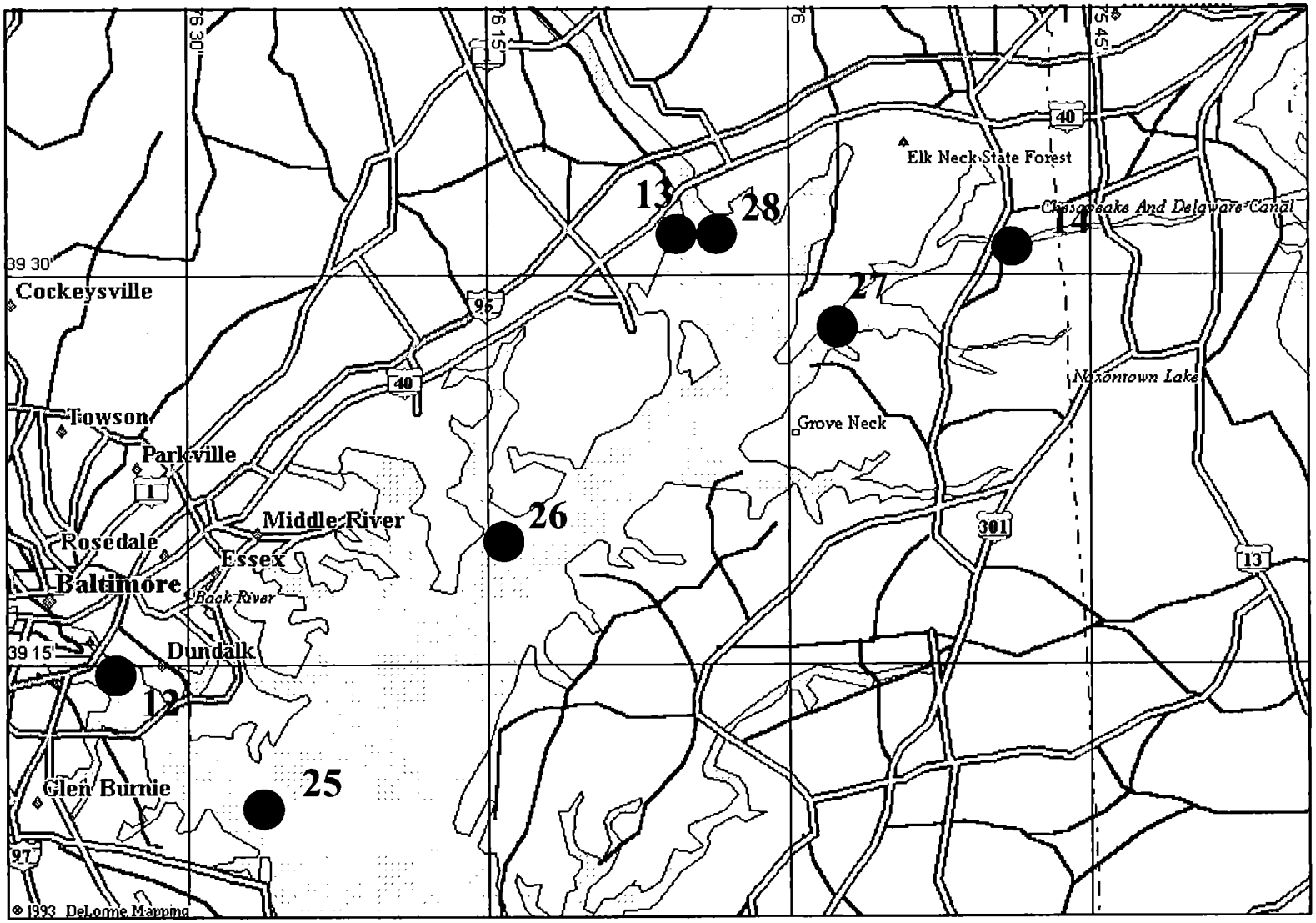

Chesapeake Bay - 7

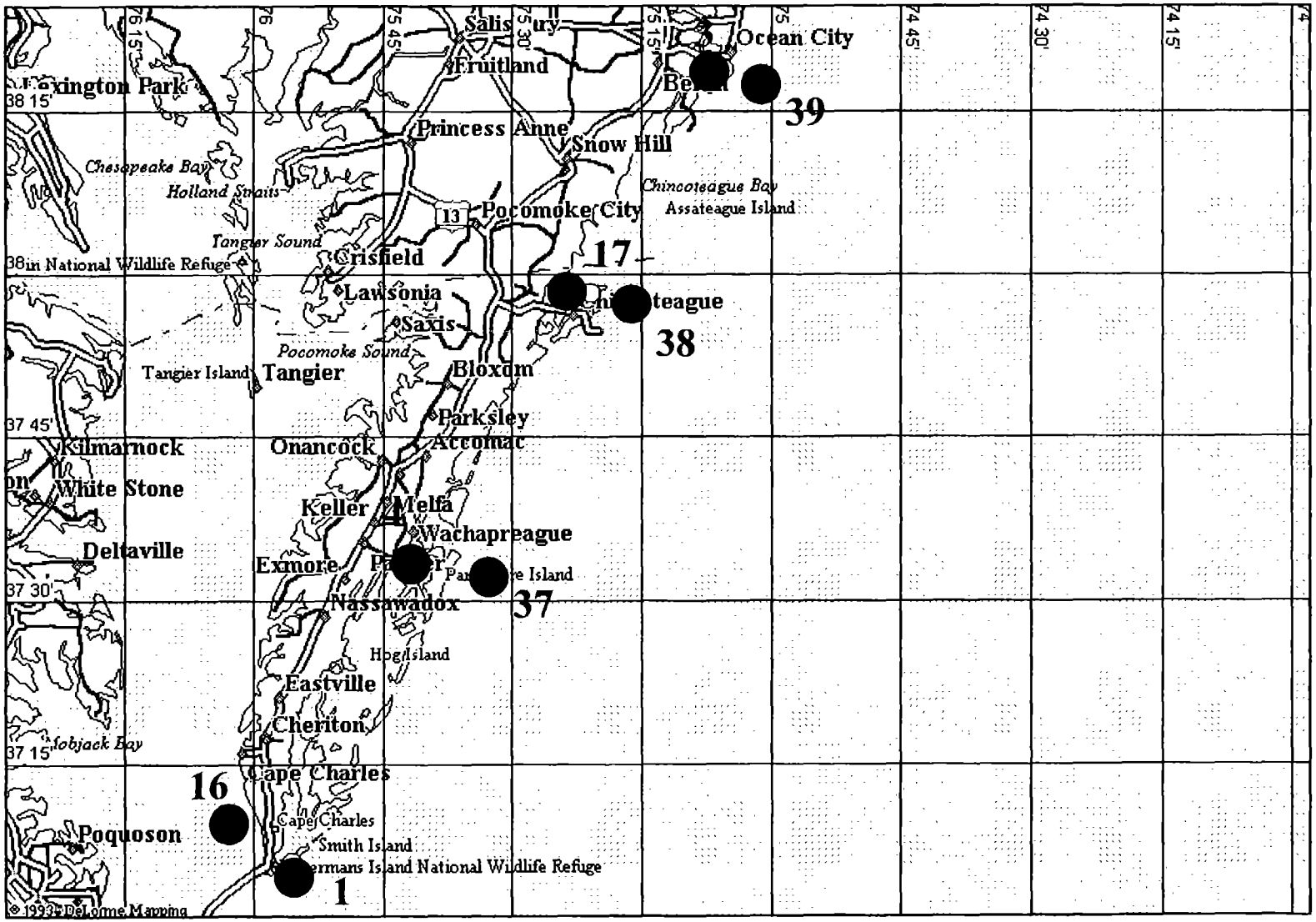

MARYLAND- 1

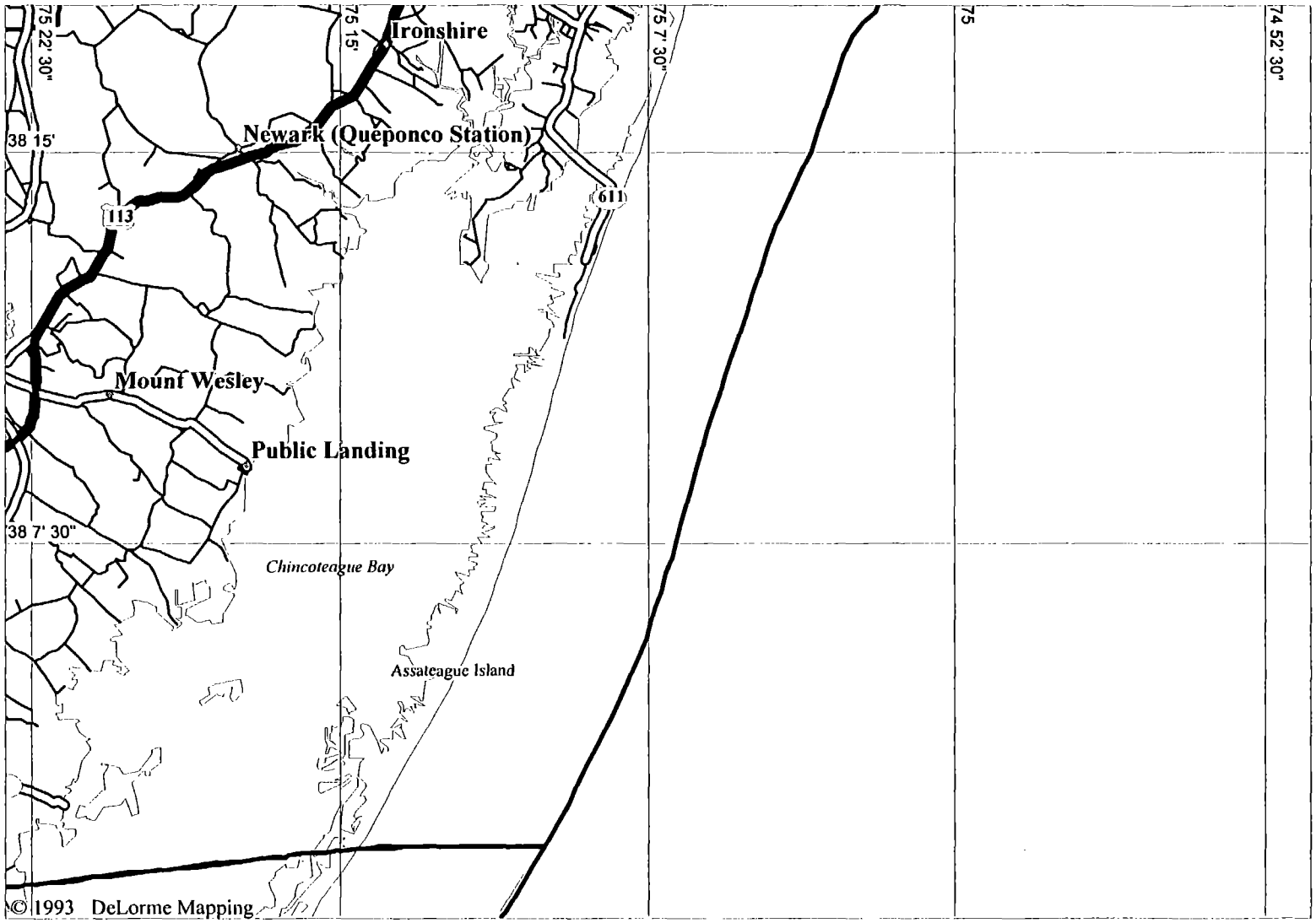
75 22' 30"
75 15'
75 7' 30"
75
74 52' 30"
38 15'
38 7' 30"
Ironshire
Newark (Queponco Station)
113
611
Mount Wesley
Public Landing
Chincoteague Bay
Assateague Island
© 1993 DeLorme Mapping

MARYLAND- 2

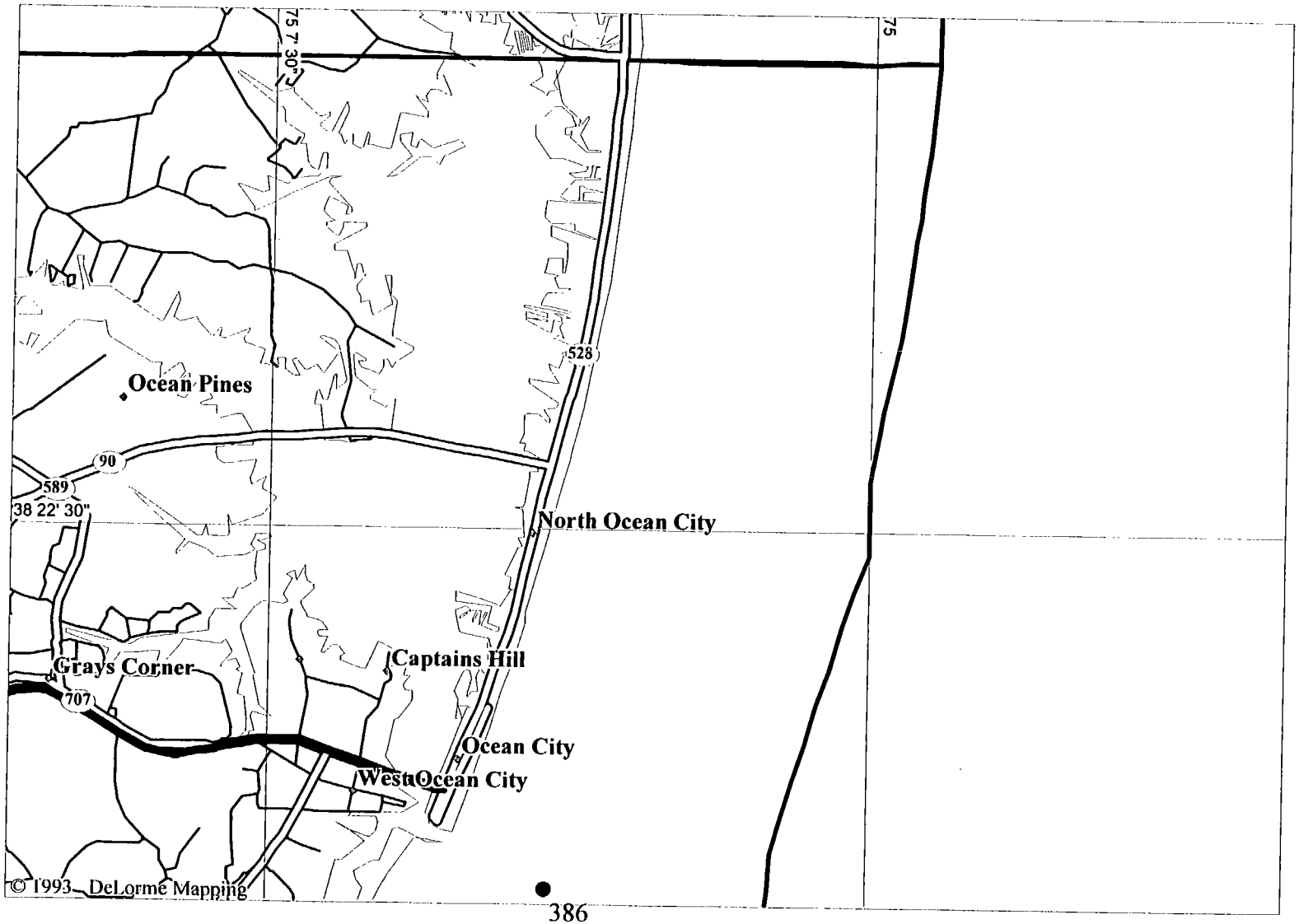
75 7' 30"
75
528
Ocean Pines
90
589
38 22' 30"
North Ocean City
Captains Hill
Grays Corner
707
Ocean City
West Ocean City
© 1993 DeLorme Mapping

NEW JERSEY- 1

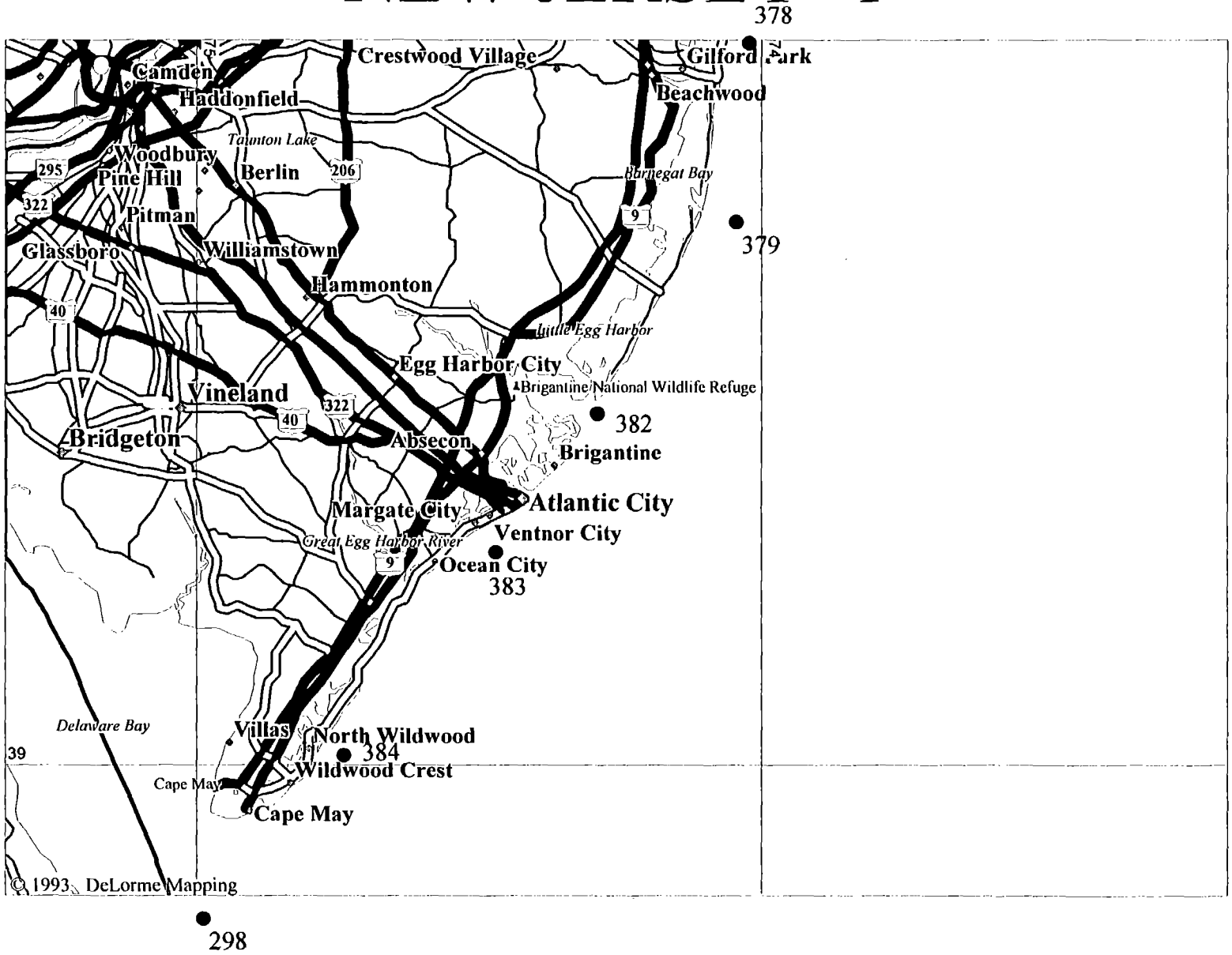
378
Crestwood Village
Gilford Park
Camden
Haddonfield
Beachwood
Taunton Lake
Woodbury
Pine Hill
Berlin
206
295
Barnegat Bay
322
9
Pitman
379
Glassboro
Williamstown
Hammonton
40
Little Egg Harbor
Egg Harbor City
Brigantine National Wildlife Refuge
Vineland
322
382
40
Bridgeton
Absecon
Brigantine
Atlantic City
Margate City
Ventnor City
Great Egg Harbor River
9
Ocean City
383
Delaware Bay
Villas
North Wildwood
39
384
Wildwood Crest
Cape May
Cape May
© 1993 DeLorme Mapping
298

NEW JERSEY- 2

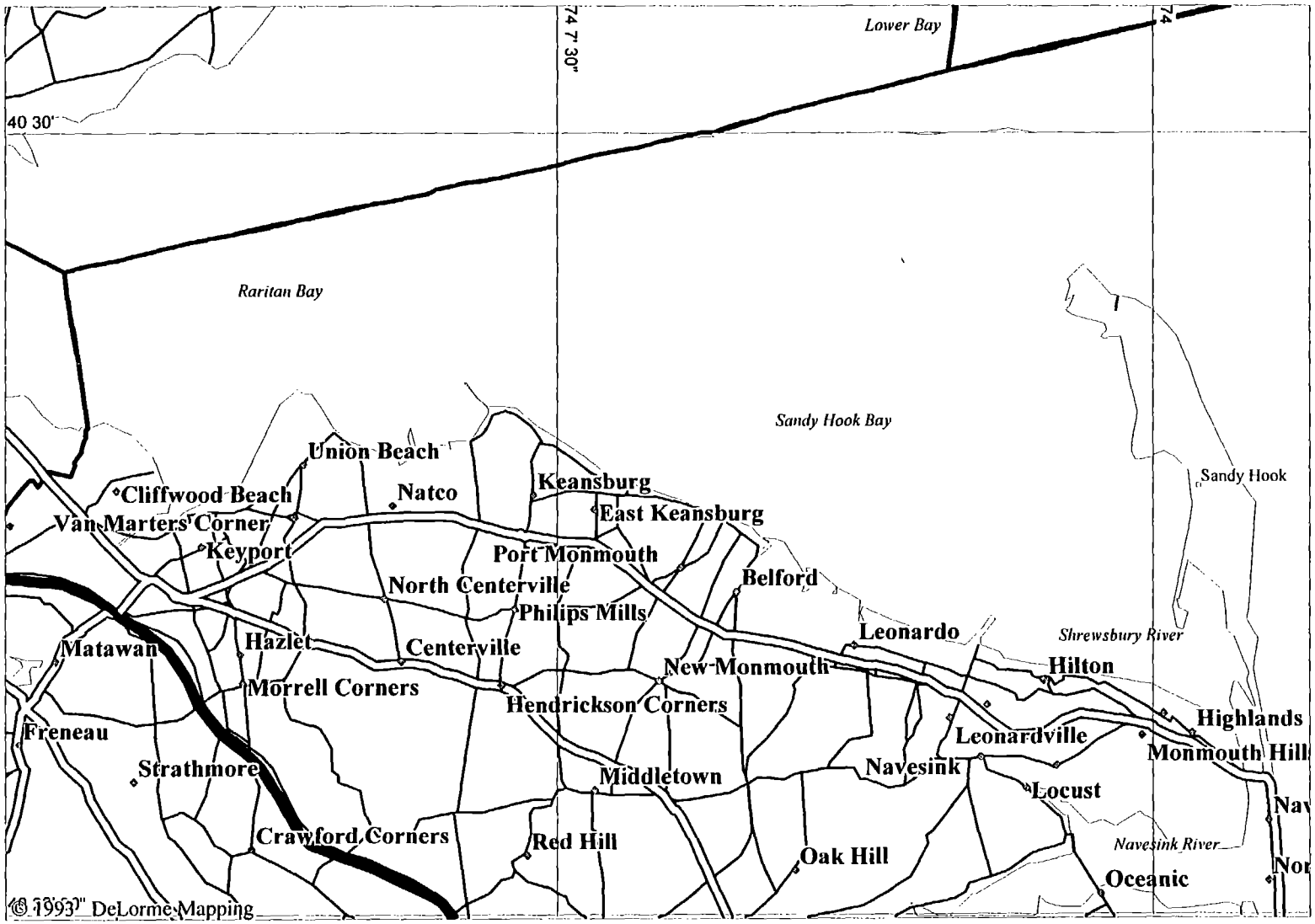
Lower Bay
74 7' 30"
74
40 30'
Raritan Bay
Sandy Hook Bay
Sandy Hook
Union Beach
Natco
Keansburg
East Keansburg
Cliffwood Beach
Van Marters Corner
Keyport
Port Monmouth
Belford
North Centerville
Philips Mills
Leonardo
Shrewsbury River
Hilton
Matawan
Hazlet
Centerville
New Monmouth
Morrell Corners
Hendrickson Corners
Highlands
Freneau
Leonardville
Monmouth Hill
Strathmore
Middletown
Navesink
Locust
Crawford Corners
Red Hill
Oak Hill
Navesink River
Oceanic
© 1993 DeLorme Mapping

NEW YORK- 1

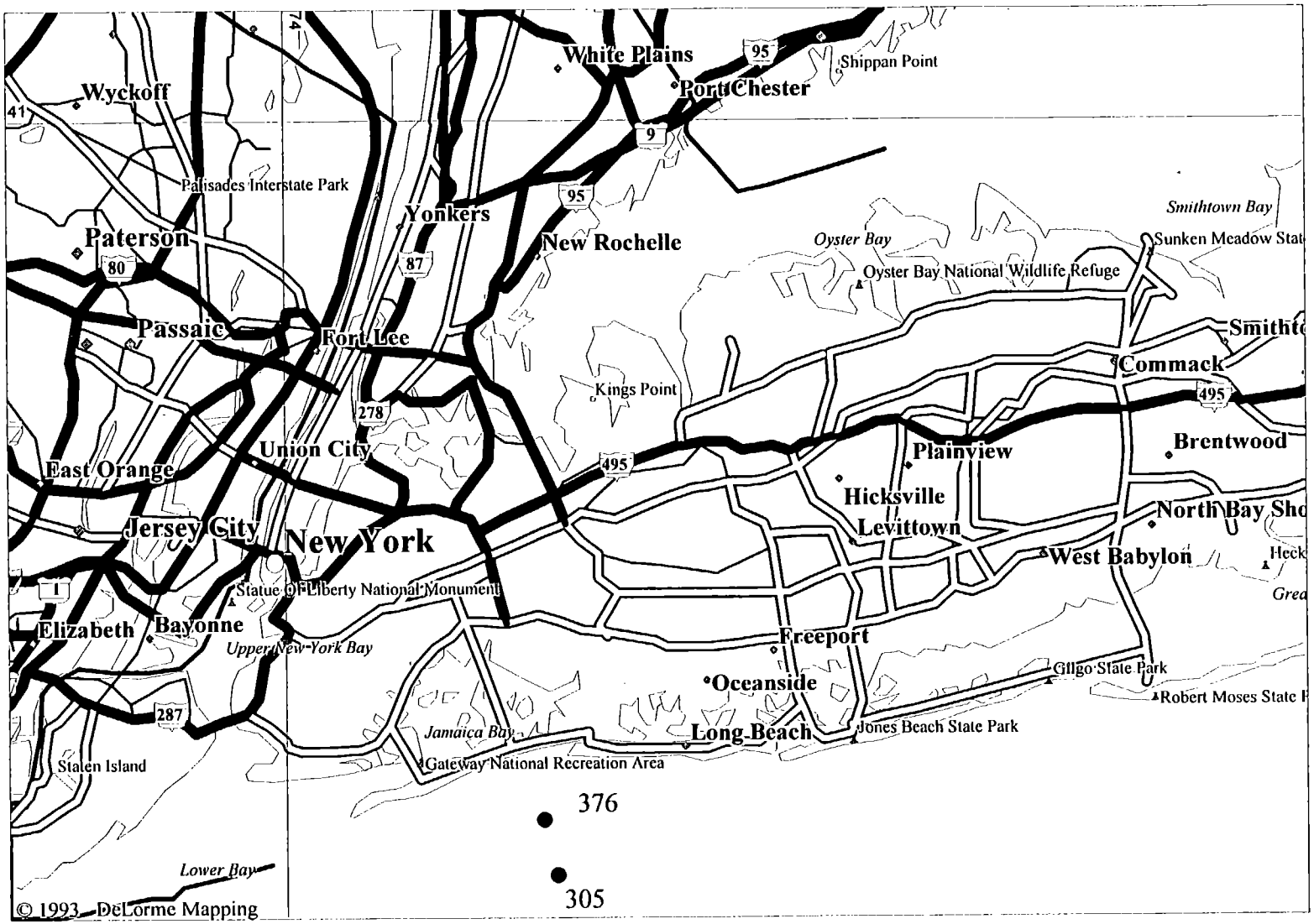
White Plains
Port Chester
Shippan Point
Wyckoff
Palisades Interstate Park
Yonkers
New Rochelle
Paterson
Passaic
Fort Lee
Oyster Bay
Oyster Bay National Wildlife Refuge
Smithtown Bay
Sunken Meadow Stat
Smithte
Commack
Kings Point
Brentwood
Plainview
Union City
East Orange
Hicksville
Levittown
North Bay Sho
Jersey City
New York
West Babylon
Statue of Liberty National Monument
Elizabeth
Bayonne
Upper New-York Bay
Freeport
Gilgo State Park
Robert Moses State P
Oceanside
Jamaica Bay
Long Beach
Jones Beach State Park
Staten Island
Gateway National Recreation Area
Lower Bay
© 1993 DeLorme Mapping
368
376
305

NEW YORK- 2

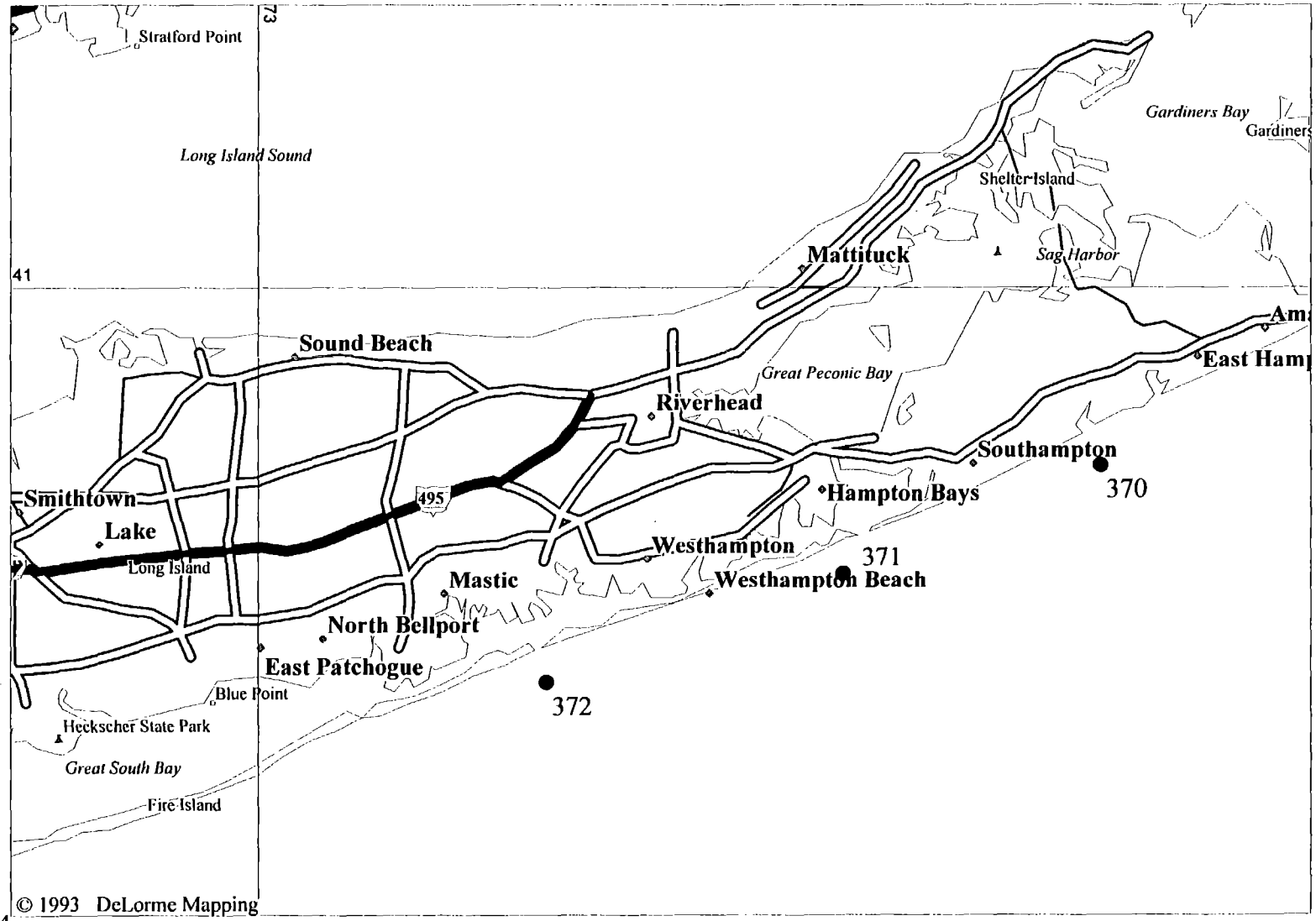
Stratford Point
Long Island Sound
73
41
Gardiners Bay
Gardiner
Shelter Island
Mattituck
Sag Harbor
Sound Beach
Great Peconic Bay
East Ham
Riverhead
Southampton
370
Smithtown
495
Hampton Bays
Lake
Long Island
Westhampton
371
Mastic
Westhampton Beach
North Bellport
East Patchogue
372
Blue Point
Heckscher State Park
Great South Bay
Fire Island
© 1993 DeLorme Mapping
374

CONNECTICUT- 1

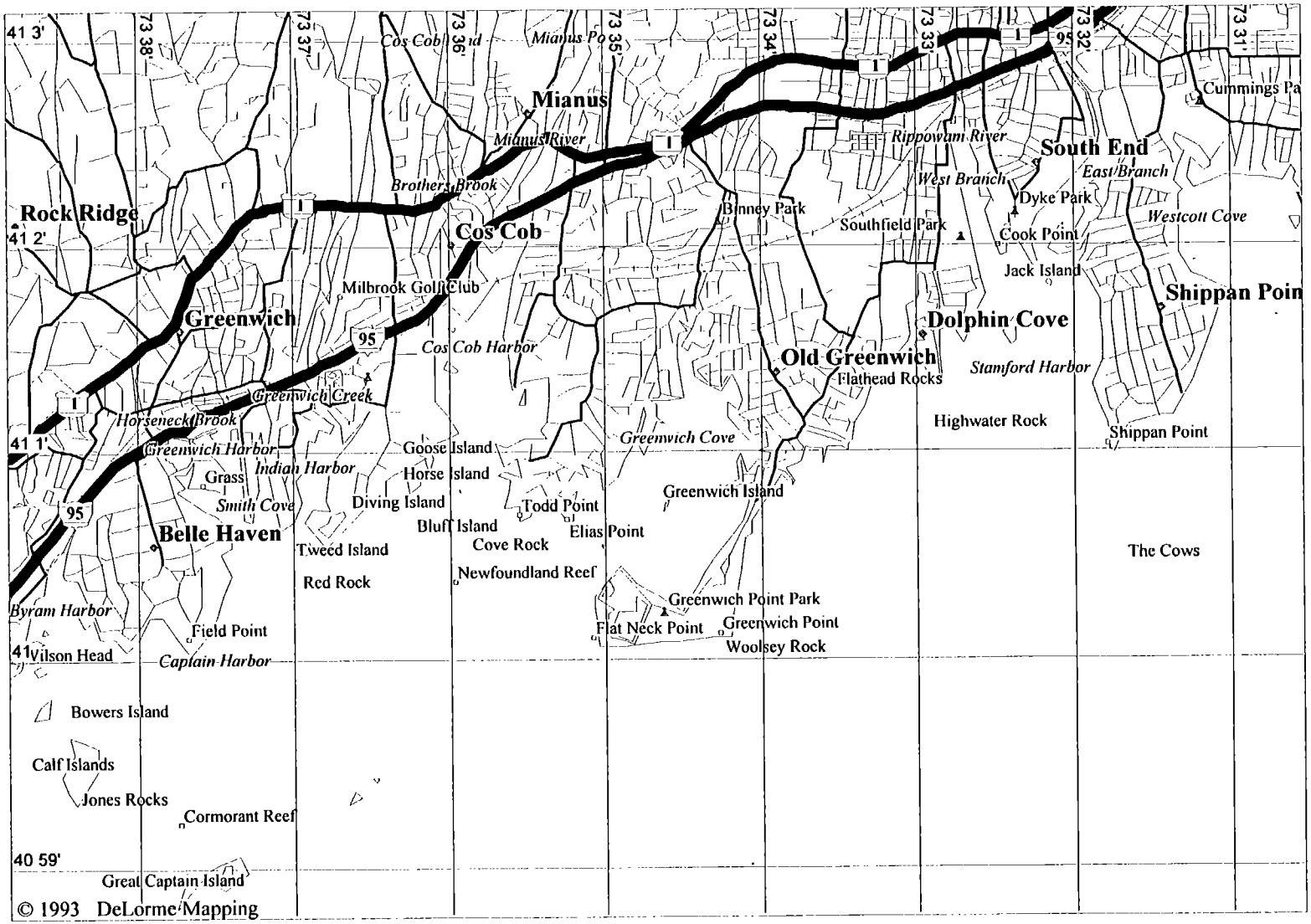

CONNECTICUT- 2

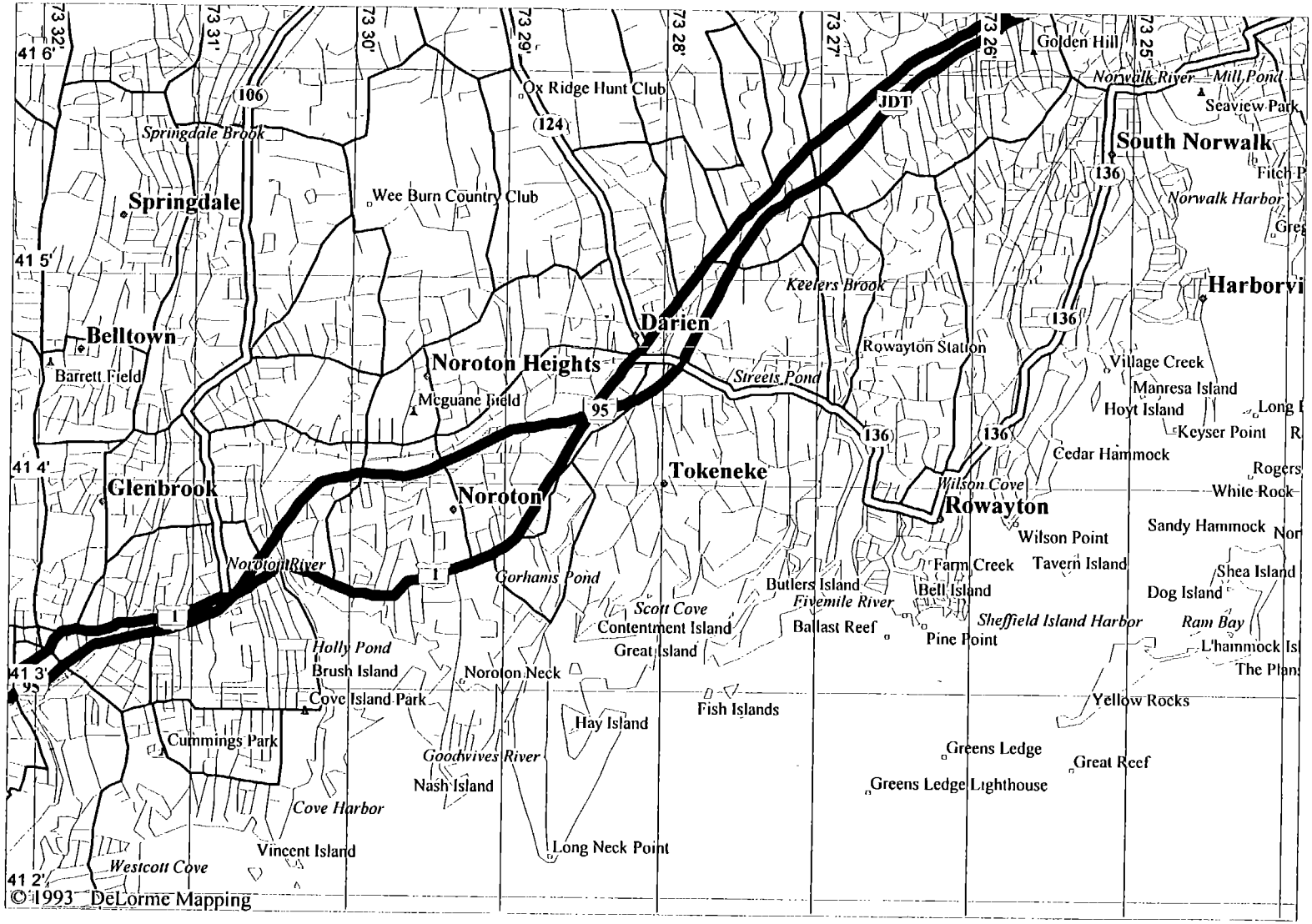

CONNECTICUT- 3

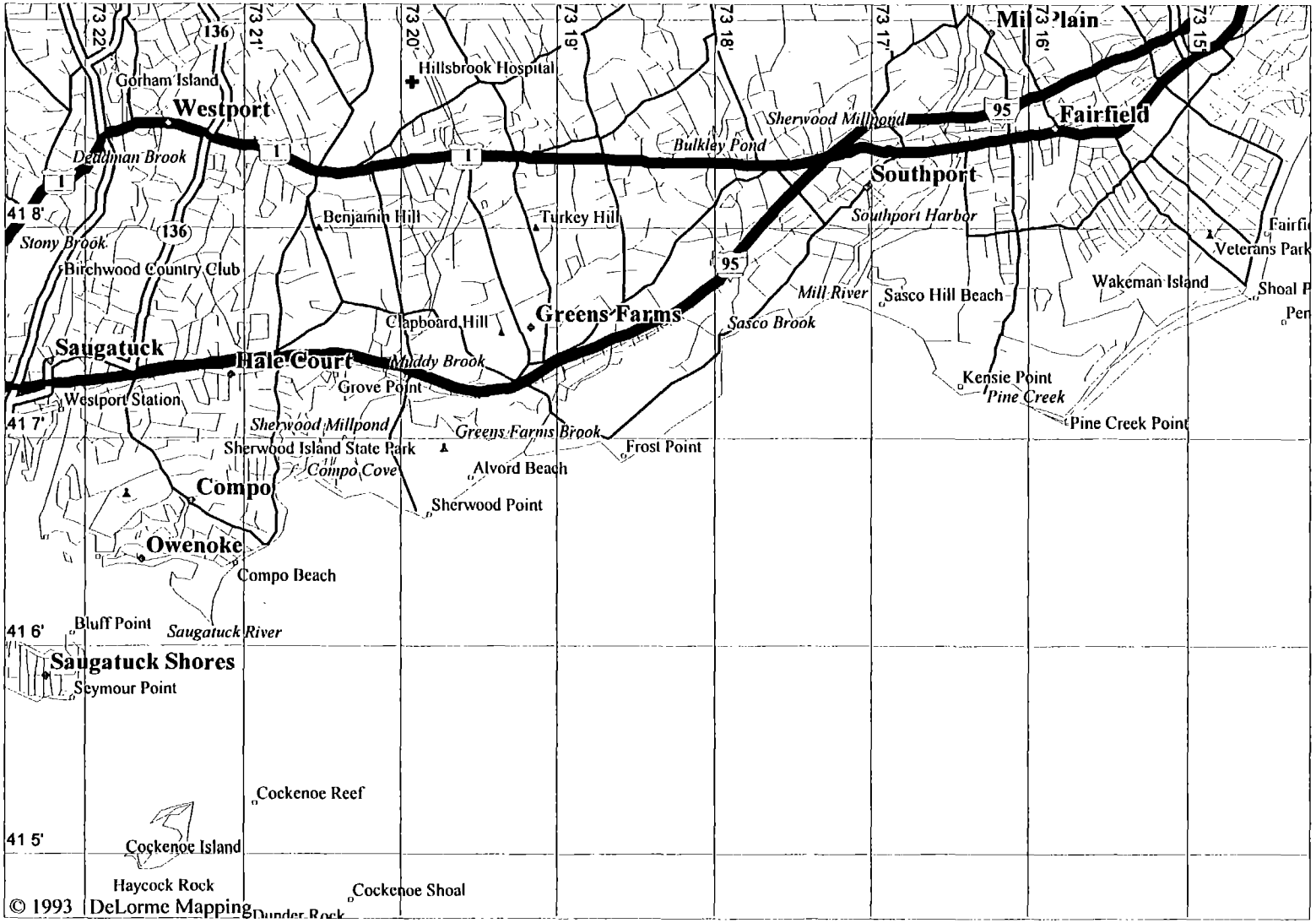

CONNECTICUT- 4

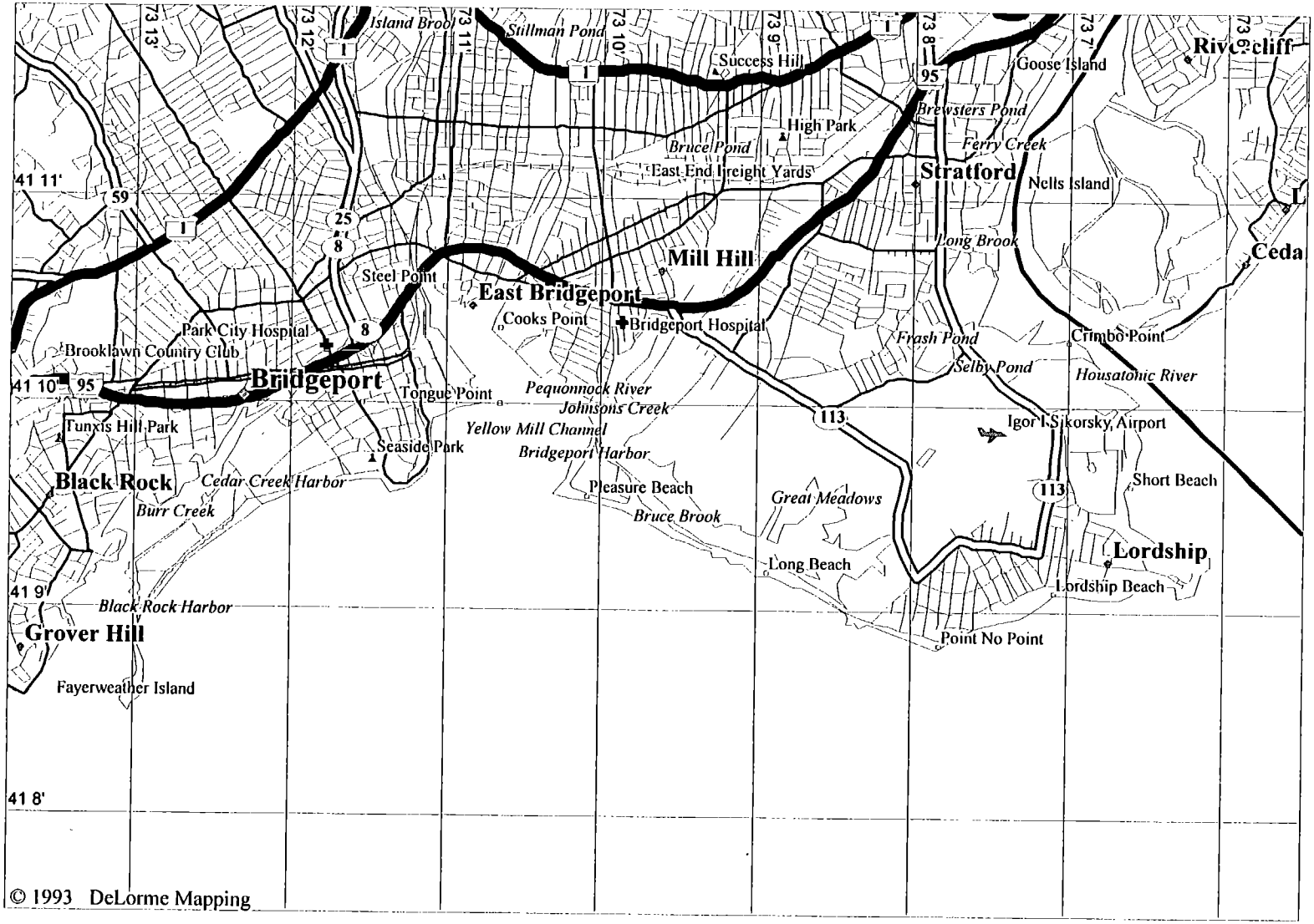

CONNECTICUT- 5

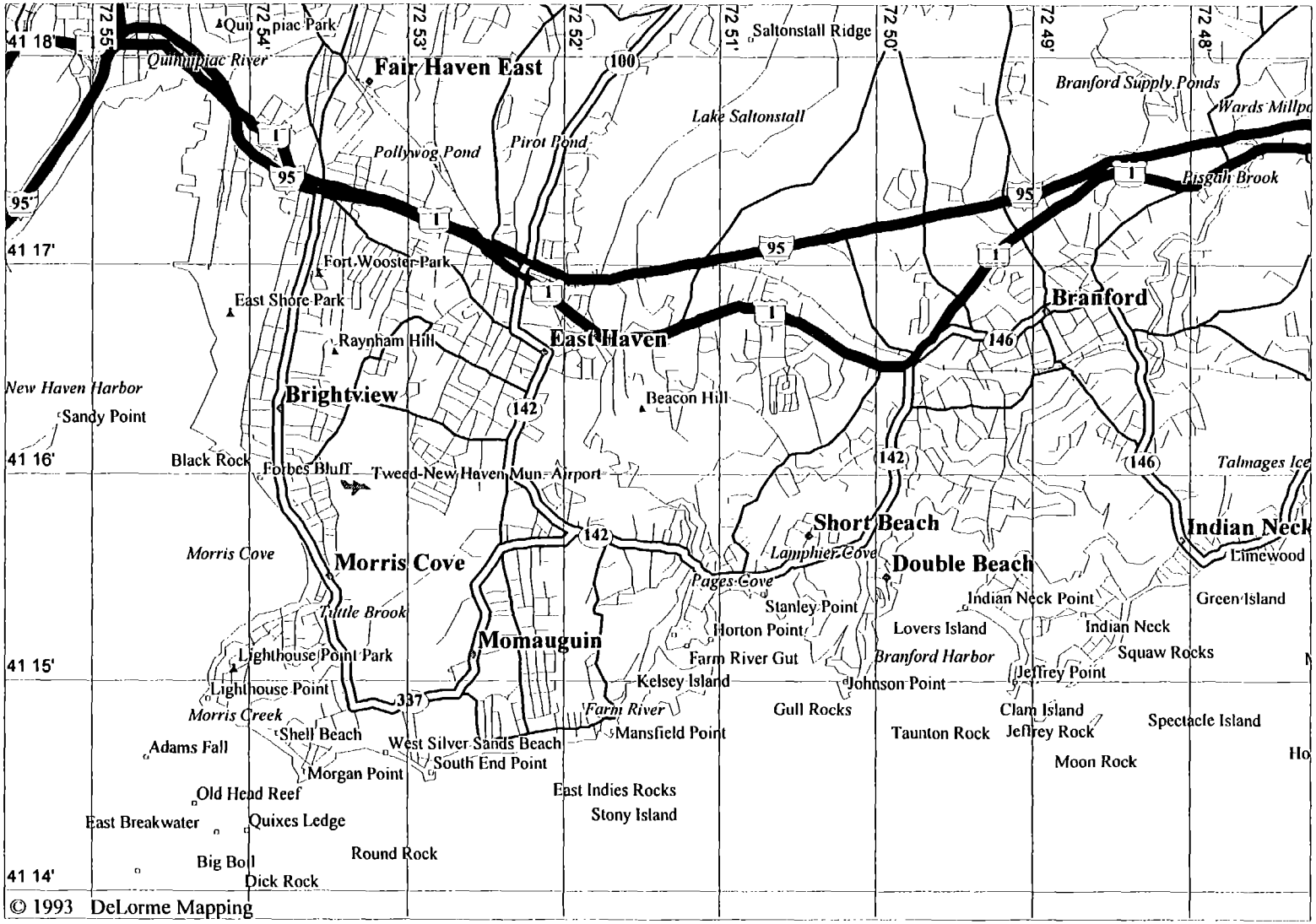

CONNECTICUT- 6

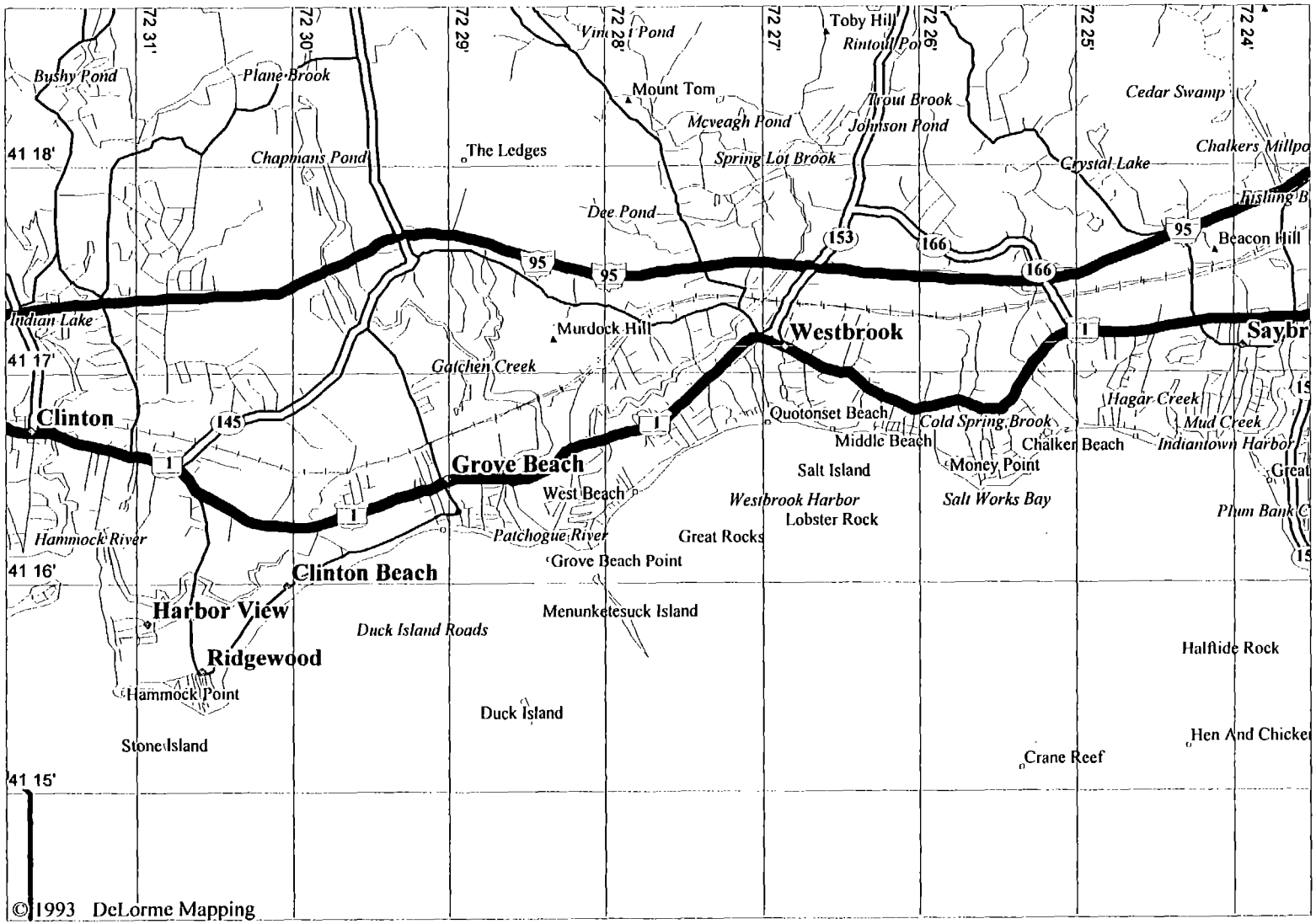

CONNECTICUT- 7

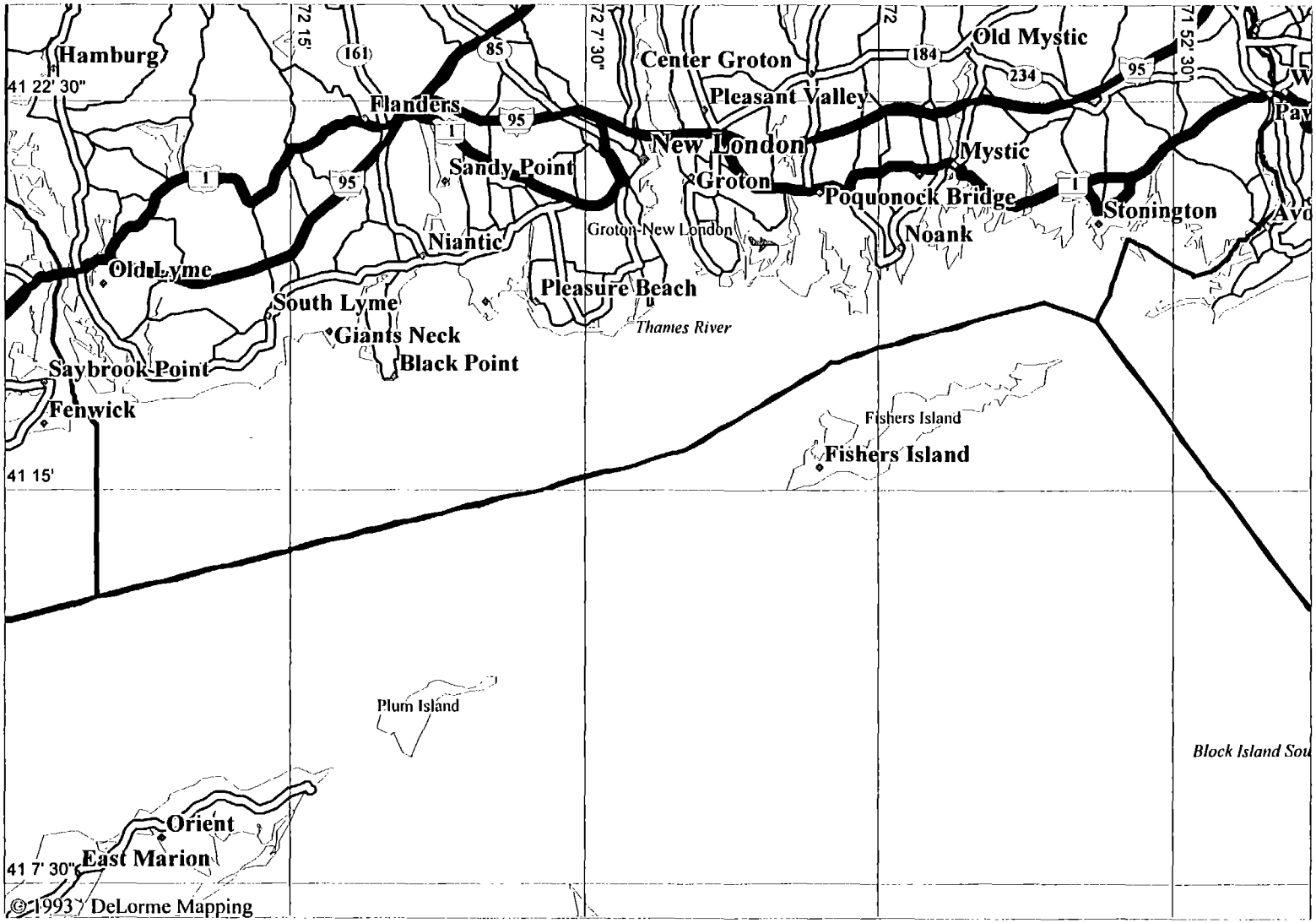

MAINE- 1

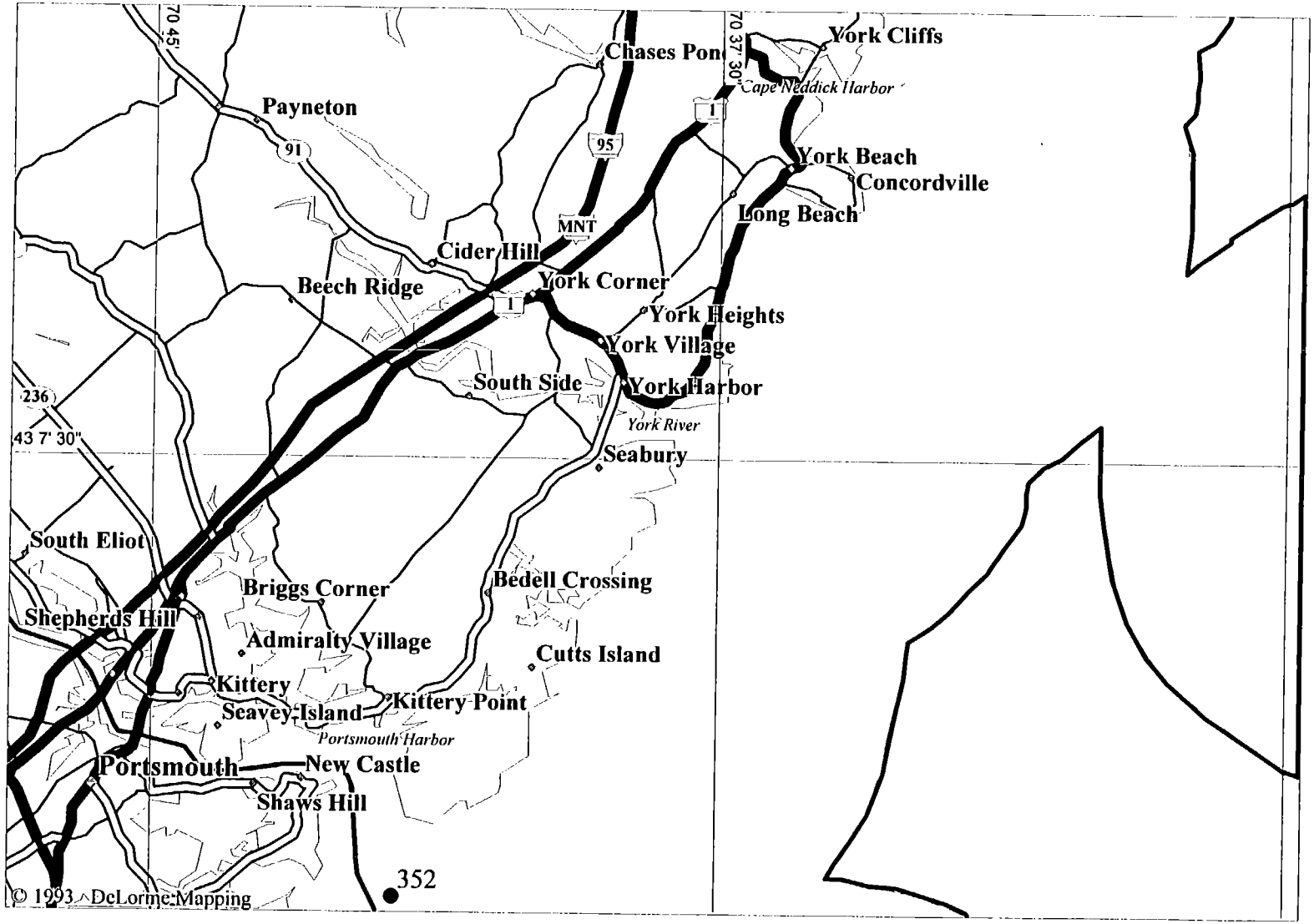
70 45'
70 37' 30"
43 7' 30"
Chases Pond
York Cliffs
Cape Neddick Harbor
Payneton
91
95
1
York Beach
Concordville
Long Beach
MNT
Cider Hill
Beech Ridge
York Corner
York Heights
York Village
South Side
York Harbor
York River
236
Seabury
South Eliot
Briggs Corner
Bedell Crossing
Shepherds Hill
Admiralty Village
Cutts Island
Kittery
Kittery Point
Seavey Island
Portsmouth Harbor
Portsmouth
New Castle
Shaws Hill
352
© 1993 DeLorme Mapping

MAINE- 2

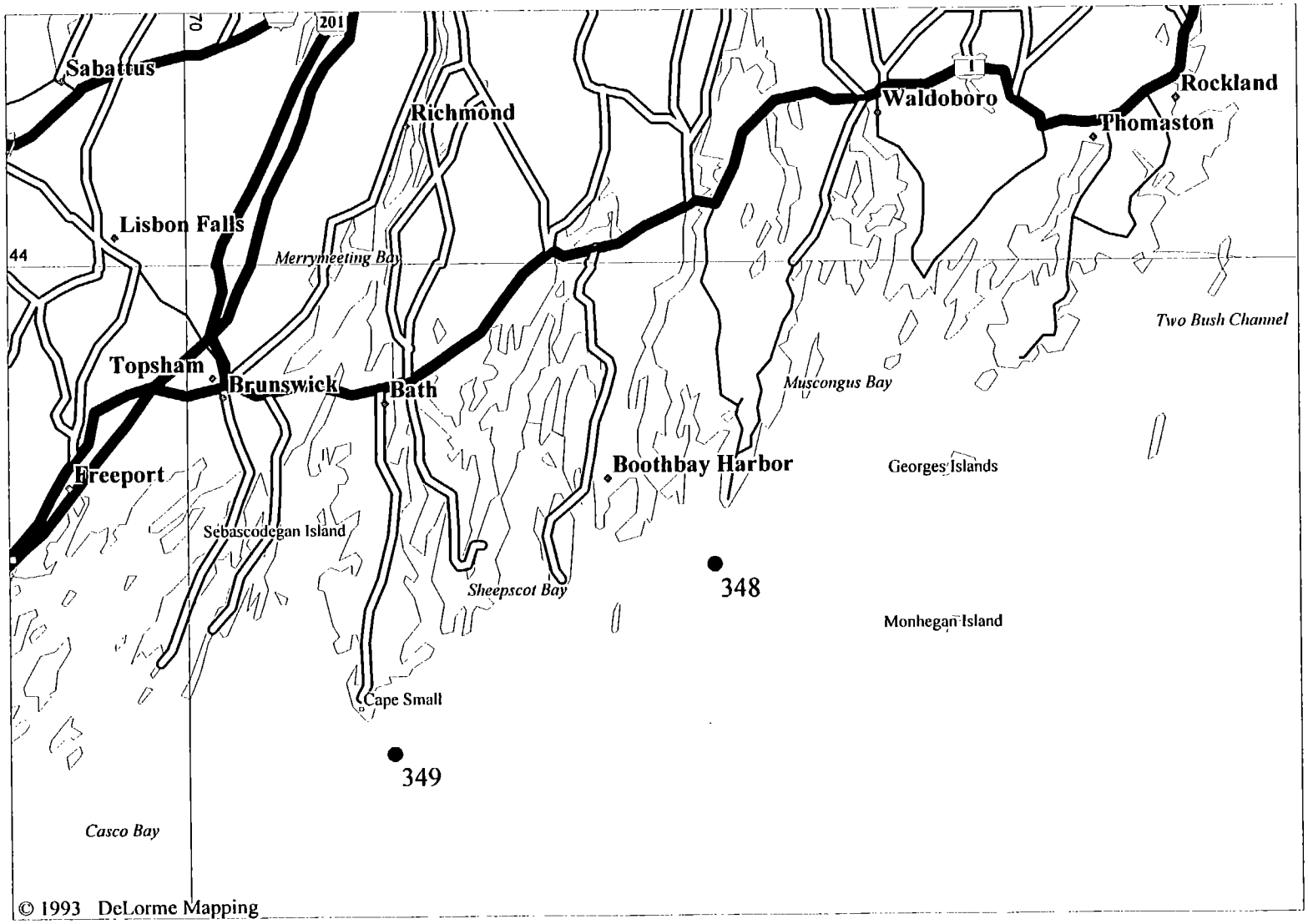
Sabattus
Richmond
Waldoboro
Rockland
Thomaston
Lisbon Falls
44
Merrymeeting Bay
Two Bush Channel
Topsham
Brunswick
Bath
Muscongus Bay
Boothbay Harbor
Georges Islands
Freeport
Sebascodegan Island
348
Sheepscot Bay
Monhegan Island
Cape Small
349
Casco Bay
© 1993 DeLorme Mapping

MAINE- 3

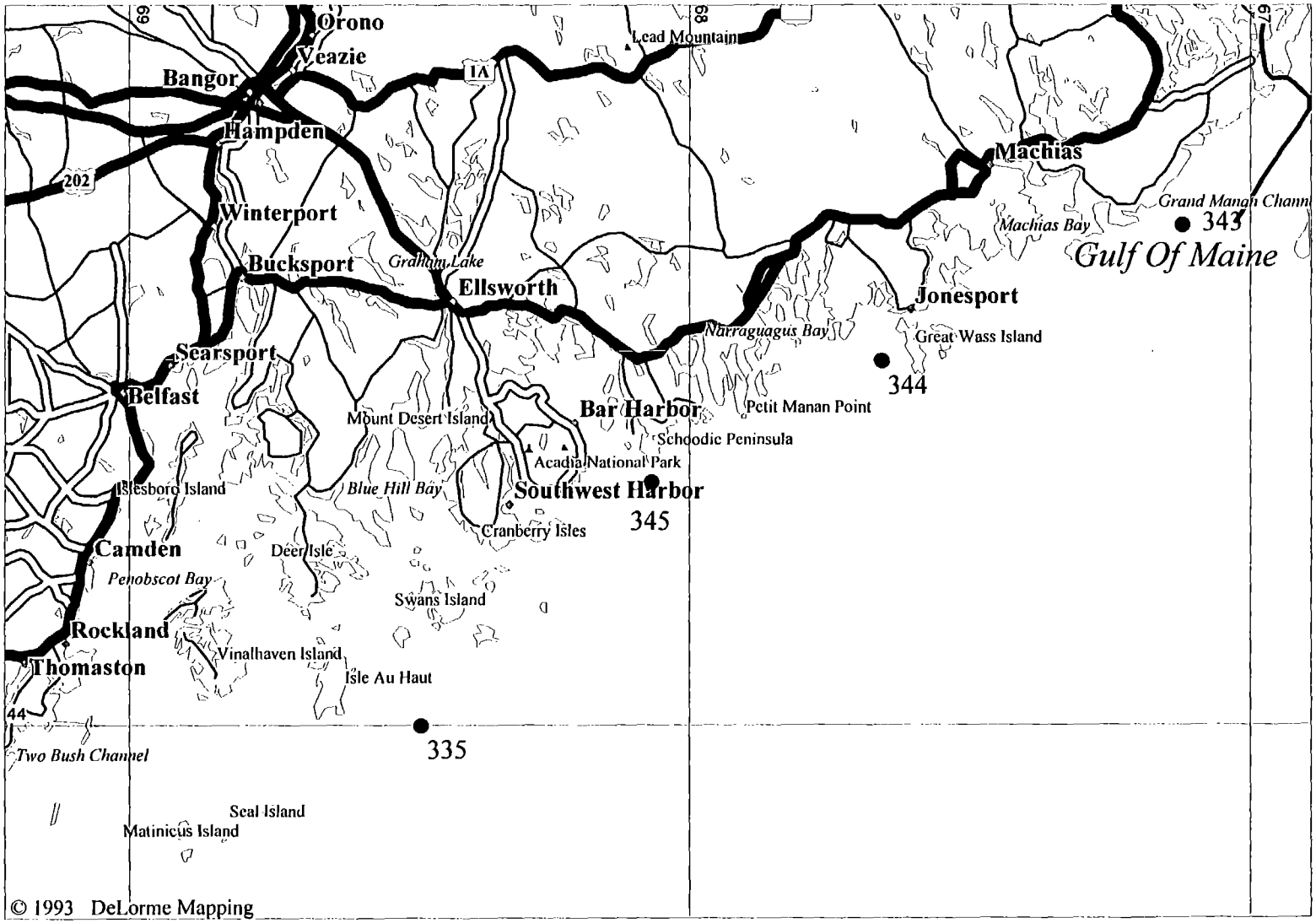
Orono
Veazie
Bangor
Hampden
202
Winterport
Bucksport
Graham Lake
Ellsworth
Searsport
Belfast
Islesboro Island
Camden
Penobscot Bay
Rockland
Thomaston
Mount Desert Island
Blue Hill Bay
Deer Isle
Swans Island
Vinalhaven Island
Isle Au Haut
Cranberry Isles
Bar Harbor
Acadia National Park
Southwest Harbor
345
Lead Mountain
1A
Machias
Machias Bay
Grand Manan Chann
343
Gulf Of Maine
Jonesport
Narraguagus Bay
Great Wass Island
344
Petit Manan Point
Schoodic Peninsula
44
Two Bush Channel
335
Seal Island
Matinicus Island
© 1993 DeLorme Mapping

APPENDIX C
Hurdat Events at Station 388

Appendix C - HURDAT Events at Station 388

Program

As mentioned above, the ADCIRC Gulf stations have not yet been identified. Once these stations will be available, a simple FORTRAN program, ADCIRC-F, could be used that reads the entire ADCIRC file and rewrites the data in a standard format (50 hours before and after the peak at 15 minutes interval), that could easily be read on a spreadsheet . The program is very straight forward. The user is prompted to enter the name of the ADCIRC file. Then, the program will automatically find out the number of storms , and then sort the data. The result is an ASCII file called ADC-"station #".txt. An example file,

ADC-388.txt is shown below. Surge values are in meters.

HURDAT events impacting ADCIRC station 388, off the Indian River

The following describes ADC-388.txt, the sorted version of the ADCIRC file for station 388, off the Indian River. The first control lines specify the ADCIRC station #, the total number of points, the interval of polling, the HURDAT storm number, the maximum surge and the time it occurs. This is done for each storm at the site of interest (Station 388 off the Indian River in this case). Then, the table figures the HURDAT storms numbers on the first line, and the surge values are listed in columns for 400 points (100 hours at 15 minutes interval). Only the first few time steps are printed in this example. The figure on the following page shows a graphic representation of this table.

A disc is available that contains the same information for all stations of interest in this study, along with the ADCIRC-F program.

WIS 388, 2064 points, 15.0 mn interval
hurdat # 112. surge= .76 M at point 657

WIS 388, 912 points, 15.0 mn interval
hurdat # 327. surge= .96 M at point 627

WIS 388, 1272 points, 15.0 mn interval
hurdat # 332. surge= 1.12 M at point 819

WIS 388, 1176 points, 15.0 mn interval
hurdat # 353. surge= 1.30 M at point 800

WIS 388, 1680 points, 15.0 mn interval
hurdat # 370. surge= .98 M at point 1026

WIS 388, 696 points, 15.0 mn interval
hurdat # 436. surge= 1.67 M at point 539

WIS 388, 1032 points, 15.0 mn interval
hurdat # 440. surge= .43 M at point 816

WIS 388, 1152 points, 15.0 mn interval

hurdat # 545. surge= 1.39 M at point 963

WIS 388, 1320 points, 15.0 mn interval
hurdat # 552. surge= .55 M at point 775

WIS 388, 1464 points, 15.0 mn interval
hurdat # 597. surge= .58 M at point 1093

WIS 388, 1296 points, 15.0 mn interval
hurdat # 657. surge= 1.13 M at point 823

WIS 388, 744 points, 15.0 mn interval
hurdat # 672. surge= .61 M at point 202

WIS 388, 840 points, 15.0 mn interval
hurdat # 702. surge= 1.02 M at point 745

WIS 388, 816 points, 15.0 mn interval
hurdat # 712. surge= .55 M at point 774

WIS 388, 1488 points, 15.0 mn interval
hurdat # 835. surge= 3.44 M at point 1058

112	327	332	353	370	436	440	545	552	597	657	672	702	712	835
.638	.069	.104	.473	.076	.319	-.015	.075	.110	.264	.112	.017	.075	-.088	.786
.640	.070	.103	.469	.077	.319	-.010	.073	.111	.262	.113	.021	.075	-.087	.787
.643	.072	.105	.464	.077	.320	-.005	.072	.110	.260	.114	.024	.074	-.087	.786
.645	.072	.105	.459	.078	.319	-.002	.072	.110	.259	.114	.026	.074	-.087	.789
.645	.073	.103	.453	.079	.315	.002	.070	.109	.257	.115	.029	.073	-.086	.791
.647	.075	.100	.448	.081	.312	.005	.069	.109	.256	.116	.032	.073	-.086	.790
.651	.075	.097	.442	.085	.308	.009	.068	.109	.255	.116	.036	.072	-.087	.789
.652	.076	.097	.437	.084	.305	.013	.065	.108	.253	.116	.040	.071	-.088	.789
.653	.076	.096	.432	.081	.302	.017	.063	.108	.252	.118	.044	.070	-.089	.791
.656	.075	.096	.427	.078	.298	.020	.061	.108	.250	.119	.049	.070	-.090	.790
.659	.077	.095	.422	.076	.294	.023	.059	.108	.249	.121	.053	.069	-.091	.788
.660	.078	.094	.416	.078	.292	.024	.057	.108	.248	.122	.057	.068	-.092	.787
.660	.079	.094	.411	.078	.291	.024	.055	.109	.246	.122	.061	.067	-.092	.785
.664	.081	.093	.405	.079	.291	.024	.054	.110	.245	.124	.064	.066	-.092	.782
.666	.081	.093	.399	.078	.292	.025	.052	.110	.244	.126	.068	.065	-.092	.780
.665	.082	.093	.393	.076	.288	.025	.050	.110	.244	.130	.071	.064	-.092	.780
.666	.083	.092	.388	.076	.284	.026	.048	.110	.243	.133	.074	.063	-.091	.778
.669	.083	.092	.382	.076	.283	.026	.046	.111	.242	.137	.076	.062	-.092	.774
.670	.084	.093	.377	.076	.280	.028	.044	.112	.241	.141	.079	.062	-.092	.772
.669	.083	.093	.371	.077	.276	.030	.042	.112	.240	.145	.081	.061	-.093	.771
.670	.086	.092	.365	.075	.275	.032	.041	.113	.239	.149	.084	.060	-.093	.769
.673	.088	.091	.359	.075	.271	.034	.040	.114	.237	.154	.088	.060	-.093	.769
.674	.088	.090	.353	.078	.270	.032	.039	.114	.236	.157	.092	.059	-.094	.765
.675	.090	.088	.348	.080	.271	.027	.039	.115	.235	.159	.097	.058	-.094	.762
.678	.092	.088	.343	.084	.269	.022	.039	.115	.234	.164	.101	.057	-.094	.761
.682	.094	.087	.338	.091	.267	.017	.038	.115	.233	.169	.105	.056	-.094	.759
.682	.097	.085	.334	.093	.263	.014	.036	.115	.233	.172	.109	.056	-.095	.758
.683	.096	.083	.329	.091	.255	.012	.036	.116	.233	.174	.111	.055	-.096	.755
.687	.093	.083	.324	.090	.252	.009	.035	.117	.233	.177	.114	.054	-.096	.752
.689	.096	.083	.320	.090	.250	.007	.034	.117	.232	.179	.117	.053	-.097	.749
.689	.096	.082	.316	.089	.244	.004	.033	.117	.231	.182	.121	.052	-.097	.748
.690	.101	.081	.311	.090	.242	.001	.032	.118	.231	.187	.124	.051	-.096	.748

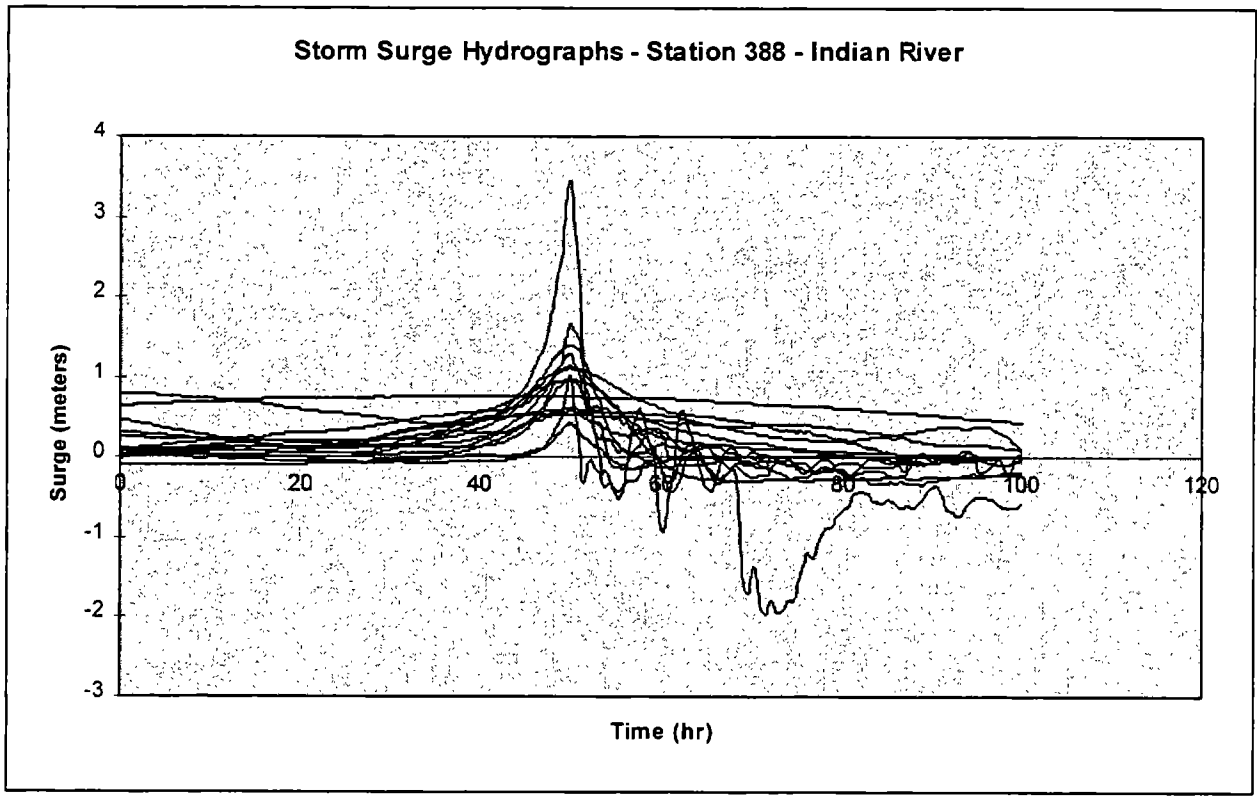

Figure C-1. Comparison of all tropical storms which have affected Indian River Inlet from ADCIRC station 388

APPENDIX D
EST Software

Appendix D - EST Software

After running all simulations of interest and preparing the EST input file (described in Chapter 3.), it is necessary to run two different FORTRAN programs in order to complete the EST procedure. The first program, EST208, is the core of the procedure, whereas the second program, RETUR208, sorts and presents the results so that they can be easily plotted.

EST208 only requires the input file to be named "*estinput.fim*" . Lines 228 through 253 define the parameters used in the program. As shown on the following listing, the program is currently set for an input file made of 60 storms (15 events * 4 tides), 7 storm parameters (defined in Chapter 4 as the tidal phase, the distance between the landfall point and the station, the peak surge value at the station, the angle of propagation, the minimum central pressure, the radius of maximum winds and the forward speed), one response vector (either flood or ebb peak velocity), the length of simulations is 208 years (twice the record period 104 years), and the procedure will run 100 simulations.

The parameter AVY = 0.1442 represents the average number of storms randomly simulated per year. Here, the value corresponds to 15 events/104 years. Previous values should be changed and the program compiled again if appropriate.

Table A. Listing of the EST208 parameters, lines 228 through 253

```
C     WRITTEN BY LEON BORGMAN, UNIVERSITY OF WYOMING
C  ****************************************************************
      PARAMETER  ( NTH   =  60 )  !   number of storms w response vectors
      PARAMETER  ( NTHD  =   1 )  !   storms w/o response vectors (min = 1)
      PARAMETER  ( NSTOT =  60 )  !  total number of storms
      PARAMETER  ( NSC   =   7 )  !  number of input vectors
      PARAMETER  ( NRES  =   1 )  !  number of response vectors
      PARAMETER  ( NYI   = 208 )  !  length of simulations (years)
       PARAMETER   ( NRUNS = 100 )   !  number of NYI simulations

PARAMETER (NTIMES=3)

C-------------------------------------------------------------
----------

PARAMETER ( NSTO5= 34 )
      PARAMETER ( IFLAG= 1)

C-------------------------------------------------------------
----------
      PARAMETER (NRV=1,NRVP1=2,ALPHA=0.5,TO=0.00001)
```

```
PARAMETER (NYIO5=40,NY=1)
PARAMETER (AVY=0.1442,NUMNAY=4)
PARAMETER (MAXNYI=35)
```

The return208 program is run after the EST208, and does not require any input. The final output file is freq208.dat. It consists of six columns, with the following data: the return period, the probability function, the mean velocity, the standard deviation, the minimum and the maximum velocities.

An example file of the first 20 years (out of 208) is shown below.

Table B. Result from the EST procedure: *freq208.dat*

RT	P	Vmean	Std.	Min	Max
1	.000	.000	.000	.000	.000
2	.500	.000	.000	.000	.000
3	.667	.000	.000	.000	.000
4	.750	.000	.000	.000	.000
5	.800	.028	.275	.000	2.766
6	.833	.562	1.227	.000	4.025
7	.857	1.819	1.774	.000	4.307
8	.875	3.135	1.395	.000	4.515
9	.889	3.784	.907	.000	4.666
10	.900	4.135	.550	.000	4.741
11	.909	4.281	.532	.000	4.920
12	.917	4.404	.522	.000	5.044
13	.923	4.523	.529	.000	5.128
14	.929	4.617	.515	.226	5.302
15	.933	4.731	.306	3.195	5.333
16	.938	4.803	.295	3.657	5.441
17	.941	4.879	.286	3.866	5.499
18	.944	4.952	.293	4.010	5.576
19	.947	5.019	.319	4.120	5.900
20	.950	5.086	.320	4.180	5.911

For example, the 80 percent confidence interval was obtained by adding or subtracting 1.28 times the standard deviation (column 4) to the mean velocity (column 3).

APPENDIX E
ADCIRC Storm Surge for Chesapeake Bay

APPENDIX E

ADCIRC Storm Surge for Chesapeake Bay

ADCIRC Model

Storm surge throughout Chesapeake Bay is estimated with the numerical model, ADCIRC (Advanced Circulation Model). ADCIRC was developed under the Dredging Research Program at the Waterways Experiment Station to simulate hydrodynamic circulation in coastal areas, along shelves, and within estuaries. ADCIRC solves the shallow-water equations in non-linear form, including nonlinear convective acceleration terms, finite amplitude terms, and bottom friction terms (in standard quadratic parametrized form). ADCIRC is a two-dimensional, depth-integrated model that yields free surface displacement and depth-averaged velocity. Circulation can be driven by tides, wind, pressure gradients, Coriolis forcing, and ocean currents.

The solution uses a generalized wave-continuity equation (GWCE) formulation with a finite element discretization in space and a finite difference method in time. Since the discrete GWCE is uncoupled from the discrete momentum equations, a sequential solution procedure can be used. A direct or iterative solver can be used for the GWCE matrix system, and mass lumping is implemented for the momentum equations. Even though the momentum equations system matrix is time dependent, it is easily solved since the matrix is diagonal (Westerink et al. 1994).

The ADCIRC code can use readily-available matrix solvers. Either a banded matrix solver from the LINPACK library (Dongarra et al. 1979) or a compact storage mode solver from the ITPACK 2D library (Kincaid et al. 1989) can be linked with the source code. The iterative solvers are less memory intensive, which should be considered for problems with large computational domains (Westerink et al. 1994).

The finite element grid used with the ADCIRC model includes Chesapeake Bay, the adjoining estuarine areas, river inflows, and the Atlantic Ocean. The ocean boundary of the grid extends off the continental shelf into the deep ocean. The grid is shown in **Figures E.1 and E.2**. Figure E.2 is a representation of the detail in the Chesapeake Bay area. The finite element grid was created using the software ACE/gredit (Turner and Baptista, 1993). The finite elements consist of three-node triangular elements. The resolution of the grid is somewhat coarse in the deep ocean areas of the domain, with an increasingly finer resolution as the domain progresses over the shelf and into the coastal region.

An advantage to using a model with a grid that extends beyond the continental shelf is the minimization of phase and amplitude errors in the computed tide. A linear tide signal can be used on the open boundary, which will include the nonlinearities of the tide as it propagates across the continental shelf. Additionally, the lateral boundaries are sufficiently far from the bay to minimize any errors that may exist at the open boundary from affecting the results at the area of interest.

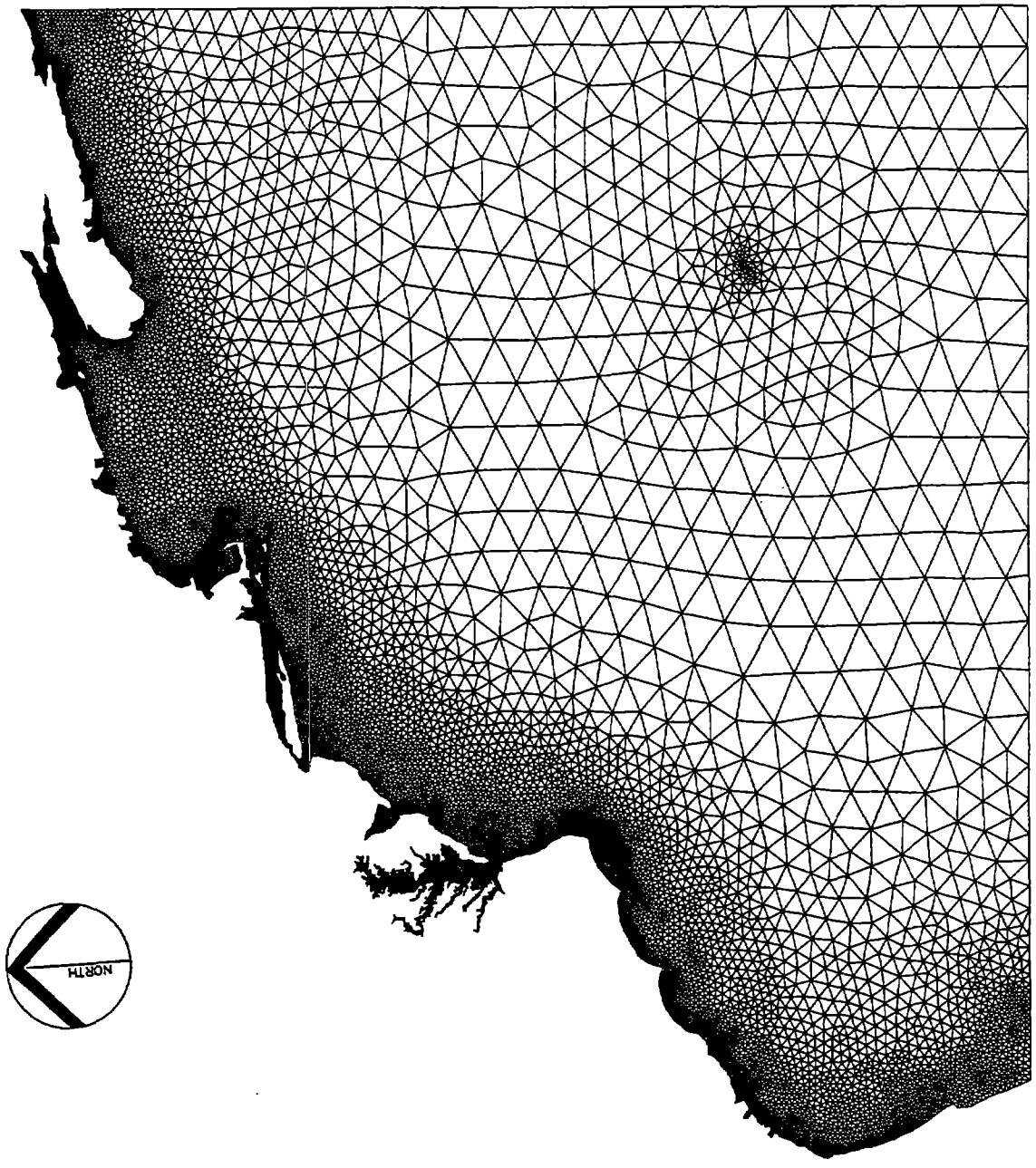

Figure E.1. Finite element grid of Atlantic Ocean and Chesapeake Bay.

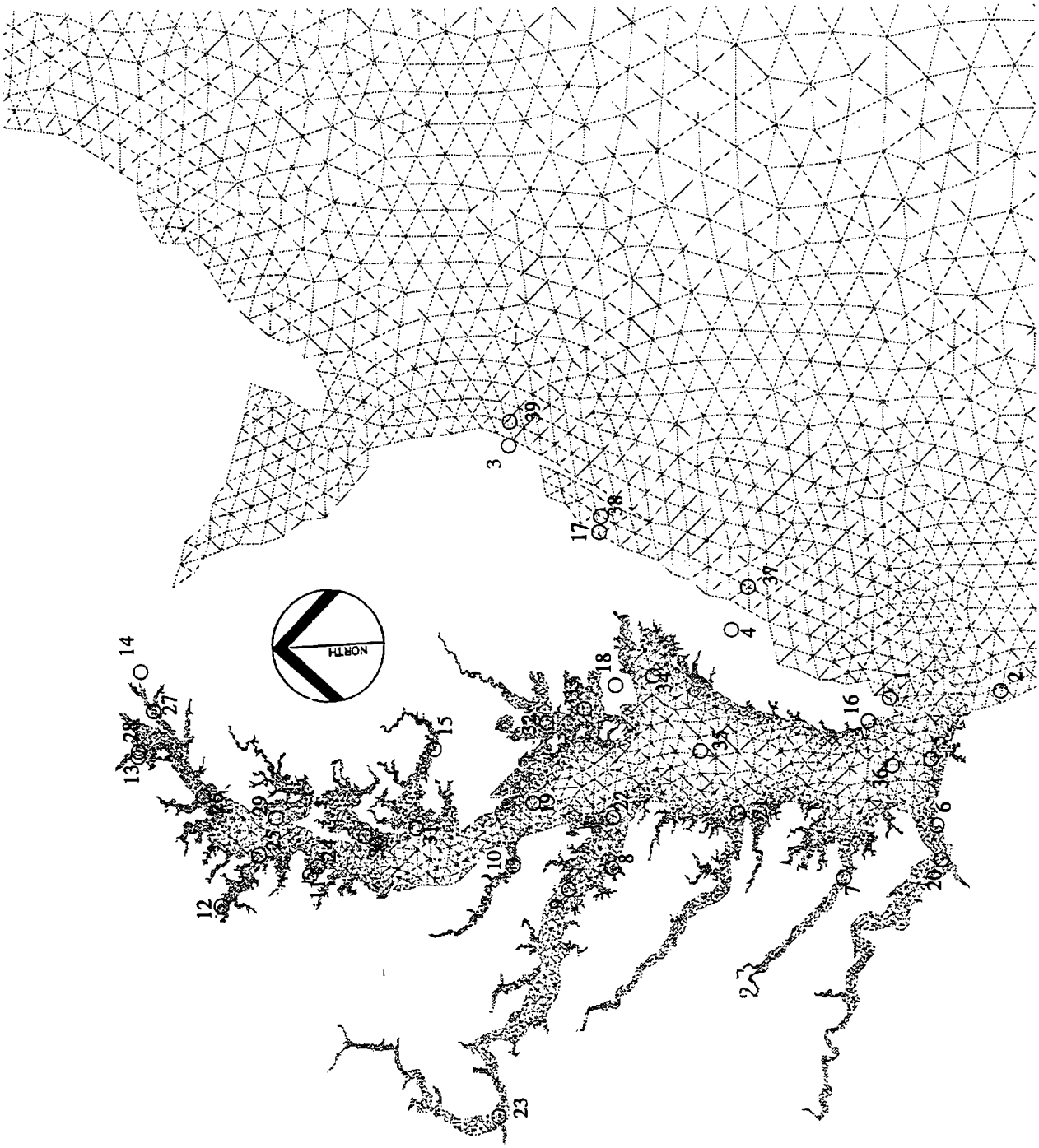

Figure E.2. Detail of Chesapeake Bay area of the finite element grid.

Application to Chesapeake Bay

The ADCIRC simulations of the storm set include tidal potential, river inflow, wind, and atmospheric pressure forcings. The tidal constituents with the largest amplitudes for the Chesapeake Bay area are included in the model runs. The river discharge rates are typical of rainstorm conditions. The National Hurricane Center's Hurricane Database (HURDAT) provides storm tracks and pressure distributions of historical storms in the Atlantic basin. The HURDAT includes storms from 1886 to the present. Thus all storms over a 110 year period were scanned to be included in the data set. The storms selected include all those of hurricane intensity as they passed within 1.5 degrees of the Bay. The selected storms are given in **Table E.1**. Information in HURDAT includes the latitude and longitude of the center of the storm, maximum wind speed, and pressure at the center of the storm.

Table E.1. Hurricane Events Affecting Chesapeake Bay.

Storm Number	Name	Dates of Occurrence
289	Not named	8/3/1928 – 8/12/1928
292	Not named	9/6/1928 – 9/20/1928
296	Not named	9/22/1929 – 10/4/1929
327	Not named	8/17/1933 – 8/26/1933
332	Not named	9/8/1933 – 9/21/1933
353	Not named	8/29/1935 – 9/10/1935
440	Not named	10/12/1944 – 10/23/1944
545	Connie	8/3/1955 – 8/15/1955
552	Ione	9/10/1955 – 9/24/1955
597	Donna	8/29/1960 – 9/14/1960
629	Cleo	8/20/1964 – 9/5/1964
657	Doria	9/8/1967 – 9/21/1967
672	Camille	8/14/1969 – 8/22/1969
702	Doria	8/20/1971 – 8/29/1971
835	Gloria	9/16/1985 – 10/2/1985

To include wind and atmospheric forcing in the ADCIRC model run, those parameters need to be provided at regular intervals for the duration of the storm. The planetary boundary layer (PBL) model by Cardone et al. (1992) was used to calculate the surface wind fields produced by the various storms as they translate over the computational domain.

The winds provided in HURDAT are the maximum sustained wind speeds over a one minute duration. They are insufficient to model the wind fields that are produced during a storm or hurricane. Due to this, the PBL model uses a series of storm parameters to compute the resulting wind field. The PBL model is a modification of Chow's (1971) vortex model. To define the storm as it progresses in time, the following parameters need to be provided: latitude and longitude of the eye, direction, forward speed, radius to maximum winds, central and peripheral pressures, and an estimate of the surface geostrophic wind speed and direction.

The location and motion of the hurricane is modeled as a stationary storm with a moving grid. The wind fields are computed on a rectangular, nested grid system of which the mesh of the grids is constant (within each grid system). The origin of each subgrid is located at the eye of the storm. The nested grid system enables an iterative process to the steady state solution. The PBL model provides the wind speed and direction (at 10 m) and pressure fields to run the model ADCIRC.

As a preliminary consideration, only storms that tracked within 1.5 degrees of Chesapeake Bay are examined. From that preliminary group, a smaller set of storms is assembled from those storms that produced winds of hurricane intensity at the entrance to Chesapeake Bay. Storms that had been downgraded to tropical storms were not considered since they would not affect the extreme distribution of storm surge heights at any point in the Bay. A series of ADCIRC runs using the conditions of the selected storms enables the simulation of the storm surges that result.

Calibration and Validation of Model

The ADCIRC model has been used to model the hydrodynamics of the Gulf of Mexico, the Atlantic Ocean, and the Pacific Ocean (among other ares). Mark and Scheffner (1993) utilized ADCIRC to provide a storm surge database for the Delaware coast. The finite element grid used for the database included the Atlantic Ocean and the Gulf of Mexico. (The finite element grid for the Chesapeake Bay runs included the same portion of the Atlantic Ocean, but not the Gulf of Mexico.) Calibration involved the tuning of bottom friction coefficient values to produce model-generated water elevations that agree with elevations recomposed from tidal constituents. Comparisons between the computed and recomposed elevations were made at Cape May, NJ and Ocean City, MD. The bottom friction value (0.003) found by Mark and Scheffner was used in the Chesapeake Bay model runs. Details of the calibration are given in Mark and Scheffner (1993).

The model was validated for Chesapeake Bay by performing a storm surge simulation using Hurricane Gloria. Model-generated elevation maxima were compared with historical tide gage data for stations in Chesapeake Bay and on the open Atlantic coast. The locations include Ocean City, MD (station 3), Lewisetta, VA (station 8), Solomon Island, MD (station 10), Annapolis, MD (station 11), Baltimore, MD (station 12), Cambridge, MD (station 15), and Kiptopeke, VA (station 16). Prototype values were obtained from the NOAA National Water Level Observation Network and shown in **Table E.2**.

Table E.2. Peak Elevations (m) for Storm 835 (Gloria).

Station	Description	Model (m)	Prototype (m)	D (m)
3	Ocean City, MD	2.39	1.76	+0.63
7	Gloucester, VA	1.49	0.82	+0.67
8	Lewisetta, VA	0.66	0.65	+0.01
10	Solomon Island, MD	0.42	0.57	-0.15
11	Annapolis, MD	0.46	0.45	+0.01
12	Baltimore, MD	0.64	0.51	+0.13
15	Cambridge, MD	0.48	0.61	-0.13
16	Kiptopeke, VA	1.84	1.30	+0.54

Historically, the upper Bay (Maryland) exhibits steeper tide hydrographs than the lower Bay (Virginia side). The model hydrographs are a result of the storm track directions and wind fields. For storms the cross the bay laterally, a steeper hydrograph in the Virginia limbs would be expected, mainly based on the resulting wind field. Also, a storm track that neared the mouth of the Bay and did not track near the upper Bay would similarly be expected to produce a more pronounced surge in the Virginia limbs.

In 1978, the Virginia Institute of Marine Science, VIMS, produced a similar report (Boon, 1978) for storm surge predictions in Chesapeake Bay for the Federal Emergency Management Agency, FEMA. Their approach was to develop the joint probabilities of historical storms and use those to develop a reasonable set of probable storms that were then modeled with a finite element model developed from the primitive equations. The finite element model developed by VIMS used approximately 800 elements to describe the entire Bay-Ocean system whereas the ADCIRC grid uses approximately 30,000 elements with much finer resolution in the Bay. The data used in this study included nearly twenty additional years of record (1997-1978) and one additional hurricane, Gloria, which was large enough to affect the statistical population from which the 100 and 500-year events are chosen. In summary, the ADCIRC and VIMS results are very comparable considering the different grid resolution and the different database.

Storm Surge Hydrographs

Results of all historical storms simulated with ADCIRC were retained at the stations shown in Figure E.2. The location of stations 1-19 were provided by the Maryland DOT. The remaining stations were added to provide more coverage and to replace some of the stations 1-19 which were in rivers or creeks too far from the main water body to be accurately displayed with the model grid. Those stations are indicated in Appendix A with the symbol NA for storm surge elevations.

All storm surge hydrographs are given on the companion CD-ROM. The storm surge values are without tide therefore to use the values properly, the tide must be added. For each station, the hydrographs are given along with a value of the duration, D, representing R/f. The value of the duration, given in hours, can be used with Equation 3.2 to calculate a synthetic hydrograph at a given station. The individual values of duration were obtained by fitting Equation 3.2 to the historical hydrographs computed by ADCIRC. The fitting was performed by eye and tended to conservatively match the backside of the larger storm surges.

References

Boon, J. D., C. S. Welch, H. S. Chen, R. J. Lukens, C. S. Fang and J. M. Zeigler, 1978. "A Storm Surge Model Study, vol. I storm surge height-frequency analysis and model prediction for Chesapeake Bay," Virginia Institute of Marine Science Special Report no. 189.

Cardone, V. J., Greenwood, C. V., and Greenwood, J. A., 1992. "Unified Program for the Specification of Hurricane Boundary Layer Winds over Surfaces of Specified Roughness," Contract Rep. CERC-92-1, U.S. Army Eng. Waterways Experiment Station, Vicksburg, Miss.

Chow, S., 1971. "A Study of the Wind Field in the Planetary Boundary Layer of a Moving Tropical Cyclone," Masters Thesis, New York Univ., New York.

Dongarra, J. J., Moler, C. B., Brunch, J. R., and Stewart, G. W., 1979. "LINPACK User's Guide," SIAM, Philadelphia, PA.

Kincaid, D. R., Oppe, T. C., and Young, D. M., 1989. "ITPACKV 2D User's Guide," Report CAN-232, Center for Numerical Analysis, The University of Texas at Austin.

Mark, D. J., and Scheffner, N. W., 1993. "Validation of a Continental-Scale Storm Surge Model for the Coast of Delaware," Proceedings of the Estuarine and Coastal Modeling Conference, ASCE, 1993.

Turner, P. J., and Baptista, A. M., 1993. "ACE/gredit User's Manual," v. xm2.00, Center for Coastal and Land-Margin Res., Oregon Graduate Inst. of Science and Tech., Ore.

Westerink, J. J., Luettich, R. A., and Scheffner, N. W., 1994. "ADCIRC: An Advanced Three-Dimensional Circulation Model for Shelves, Coasts, and Estuaries." Tech. Rep. DRP-92-6, U.S. Army Eng., Waterways Experiment Station, Vicksburg, Miss.

COST BREAKDOWN FOR PRINTING DOCUMENT

1.	Total printing cost	$2,164.80
2.	Number of documents printed	160
3.	Cost per unit	$13.53